Classification and mapping of tumour-infiltrating lymphocytes (TILs) in lung adenocarcinoma and lung squamous cell carcinoma

Inaugural dissertation

For obtaining the Degree of Doctor of Medicine of the faculty of medicine of the Justus-Liebig-University Gießen

Submitted by

Constantinos Hadjinicolaou

Gießen 2019

From the Institute of Pathology,

Justus-Liebig-University Gießen

Director: Prof. Dr. Stefan Gattenlöhner

Reviewer: Prof. Dr. Stefan Gattenlöhner

Reviewer: PD Dr. Savai

Day of disputation: 20.11.2020

Contents

Introduction

Lung cancer is the most common cause of cancer death worldwide and tobacco smoking is the leading cause. The risks in smokers increase with the duration of smoking and the number of cigarettes smoked daily and decline progressively following cessation (although never to the level among never-smokers). Mortality and incidence rates have generally been highest in high-income countries, particularly in the United States and in European countries, but are now declining, particularly in younger males and females. Lung cancer has long been more common in men than in women, but in many high-income countries, incidence rates in men and women have begun converging. Lung cancer does occur among never-smokers at estimated rates as low as 5-10 per 100 000 annually, but at higher rates in some populations based on relatively recent data from cohort studies. In contrast, the rates in smokers are as much as 20-30 times higher. Possible etiological factors for lung cancer among never-smokers include exposure to second-hand tobacco smoke, radon, various occupational agents, and emissions from indoor coal burning, but in most cases, a specific cause cannot be identified and the patterns and types of mutations differ from typical smoking-associated lung cancers. The overall lung cancer incidence rate (per 100 000 person-years, age-adjusted using the world standard) increased from 38.4 during 1977-1981 to peak at 43.5 during 1987-1991, and decreased to 33.6 during 2006-2010. The rates of the various histological types peaked at slightly different times. Among males, squamous cell carcinoma peaked in the late 1970s, small cell and large cell carcinomas in the mid-1980s, adenocarcinoma around 1990 and other specified carcinomas in the mid-1990s. Among females, the peaks were later - Namely in the late 1980s for squamous cell, small cell and large cell carcinomas; in the late 1990s for adenocarcinoma; and in the late 2000s for other specified carcinomas. Squamous cell and small cell carcinomas generally arise in the more proximal airways while adenocarcinomas originate in the peripheral airways. In the TNM classification of malignant tumours, staging is determined by assessment of the anatomical extent to three tumour components: the primary tumour (T), the lymph nodes (N), and the metastases (M). The t component has seven categories (Tx, T0, Tis, T1, T2, T3, and T4), defined by tumour size, tumour location, the involved structures, or the effects of tumour growth. The N component has five categories (NX, N0, N1, N2 and N3), defined by the absence or the presence and location of the involved nodes. The M component has two categories (M0 and M1),

defined by the absence or the presence and location of the metastases. (Travis et al., 2015)

Lung adenocarcinoma rank as the number one type of major lung cancer and it is located mostly peripheral in subpleural lung regions. (Fraire et al., 2010) They are malignant epithelial tumours with a presence of glandular differentiation. The tumour size ranges from 0,5 cm to larger than 10 cm. (Moran et al., 2010) The prognostic and predictive factors are based on the radiologic features, histopathological criteria and genetic factors. (Travis et al., 2015)

Squamous cell lung carcinoma is less common than adenocarcinoma and is more commonly associated with tobacco use. (Fraire et al., 2010) It is a malignant epithelial tumour showing keratinization and /or intercellular bridges that arise from bronchial epithelium. (Moran et al., 2010) They can reach large sizes obstructing the lumen of the airway and they may be located in the periphery of the lung, subpleural, or infiltrating the pleura with direct invasion onto the soft tissues of the chest. (Moran et al., 2010) Some of the most common symptoms of lung cancer include progressive shortness of breath, cough, chest pain/pressure, loss of voice and haemoptysis. Symptoms related to disseminated diseases include weight loss, abdominal pain due to the involvement of the liver, adrenals and pancreas and pain due to bone metastases. Whether signs and symptoms can be detected often depends on the extent of the disease and the site of metastases.

As a primary lesion, lung cancer usually manifests as a nodule, although more complex patterns for the primary lesion do occasionally exist. Chest CT provides much better detail than chest radiography in terms of tumour size, shape and location, as well as in terms of staging. Tumour spread may occur through the lymphatic or haematogenous route. Lymphatic spread gives rise to involvement of ipsilateral and contralateral hilar and mediastinal lymph nodes, whereas blood-borne metastases are most frequently found in the liver, bone, brain, adrenal glands and lungs. (Travis et al., 2015)

Tumour-infiltrating lymphocytes (TILs) have shown prognostic value in various kinds of cancers, and immune-checkpoint inhibitors have highlighted their potential in treating malignant melanoma and other cancer. (Hida et al., 2016) They are a specific histological feature of various cancers and are believed to reflect an individual immunological tumour response. The most frequently applied method to detect TILs is

the semiquantitative evaluation by light microscopy on Haematoxylin and Eosin (H&E)-stained slides. (Ingold et al., 2016) TILs have a prognostic relevance as many studies show. The number of TILs is not the only important paragon for the prognosis of a tumour patient. The location and the anatomical or histological structures that TILs infiltrate can also play an important role. A study about the prognostic significance of stromal and intraepithelial tumour-infiltrating lymphocytes in small intestinal adenocarcinoma showed that high stromal TILs density can be used as a prognostic indicator and high intraepithelial TILs count may provide a basis for the clinical use of targeted immunotherapy in Small Intestinal Adenocarcinoma patients. (Jun et al., 2019)

The Institute of Pathology of the University hospital Gießen, we receive two to five lung resections from patients with adenocarcinoma or squamous cell carcinoma every week. The aim of this thesis is to map the TILs and evaluate the relevance between the number of TILs in patients with lung adenocarcinoma or squamous carcinoma and other factors like stage of cancer, differentiation, age of patients etc.

The results of this study will help to better understand the immunological reaction of the human body against primary lung adenocarcinoma or squamous carcinoma.

Objective

1. Identification of patients diagnosed with primary lung adenocarcinoma or squamous carcinoma after surgery.
2. Identification of representative HE slides in the archive of the Pathology of the University of Gießen from patients with lung adenocarcinoma or squamous carcinoma and TILs.
3. Immunohistochemical subclassification of lymphocytes that infiltrate the tumour (CD20, CD3, CD4, CD8).
4. TILs mapping with digital photos directly from HE slides and immunohistochemical slides. Digital documentation of the infiltration patterns of -TILs from HE slides and comparison of the infiltrating patterns from every subtype (CD20, CD3, CD4, CD8).
5. Investigate the correlation between the infiltration form, number of TILs, and stage of tumour, age of patients or tumour differentiation.

The human lung

The human lung is one of the most important organs of the respiratory system. The main function of the lung is to exchange carbon dioxide in the Blood with oxygen in the inhaled air. The right lung consists of three lobes (Superior lobe, Middle lobe and Inferior lobe) and the left lung consists of two lobes (Superior lobe and Inferior lobe). At the lung hilum enters the pulmonary artery and veins. Trachea is the connection between larynx, pharynx and the lungs. The trachea enters the left and right lung (at hilum) with two primary bronchi, which then branch into three to the right and two lobar (secondary) bronchi to the left. The lobar bronchi then branch into segmental (tertiary) bronchi which continue to branch in smaller bronchi to bronchioles. At the end of this respiratory tree are the alveolar sacs where the gas exchange with the blood takes place. Both lungs are covered with the visceral pleura and the thorax inner wall with parietal pleura. The empty space between them (pleural cavity) contains the pleural fluid. The volume of the right lung is about 2-3 litres and can reach 5-8 litres at maximum inspiration. This volume corresponds a gas exchange surface of 70-140 m2. The left lung has 10-20% less volume because of the heart placement. (Paulsen et al., 2010)

Histologically, most of respiratory system's conducting portion is lined with respiratory epithelium. The respiratory epithelium consists of five major cell types (ciliated columnar cells, goblet cells, brush cells, small granule cells and basal cells). Terminal bronchioles and respiratory bronchioles are covered with simple cuboidal, ciliated and Clara cells. Clara cells or exocrine bronchiolar cells have many functions, including secretion of surfactant, detoxification of inhaled xenobiotic compounds, and mitosis for replacement of the other bronchiolar cell types. The surfactant material secreted by Clara cells and type II alveolar cells is an oily mixture of phospholipids and surfactant proteins which form a film that lowers the surface tension in alveoli. This helps prevent alveolar collapse at exhalation and allows alveoli to be inflated with less inspiratory force, easing the work of breathing. The alveolar sacs at the end of the respiratory tree are responsible for the spongy structure of the lungs. Type I alveolar cells or type I pneumonocytes line the alveolar surface and maintain the alveolar side of blood/air barrier, covering 95% of the alveolar surface. Gas exchange between air and blood occurs at a membranous barrier between each alveolus and the capillaries surrounding

it. Type II alveolar cells or type II pneumonocytes are cuboid cells often in group of two or three and they divide to replace their own population after injury and provide progenitor cells for type I cells. They also produce the pulmonary surfactant. (McGurk ,2013)
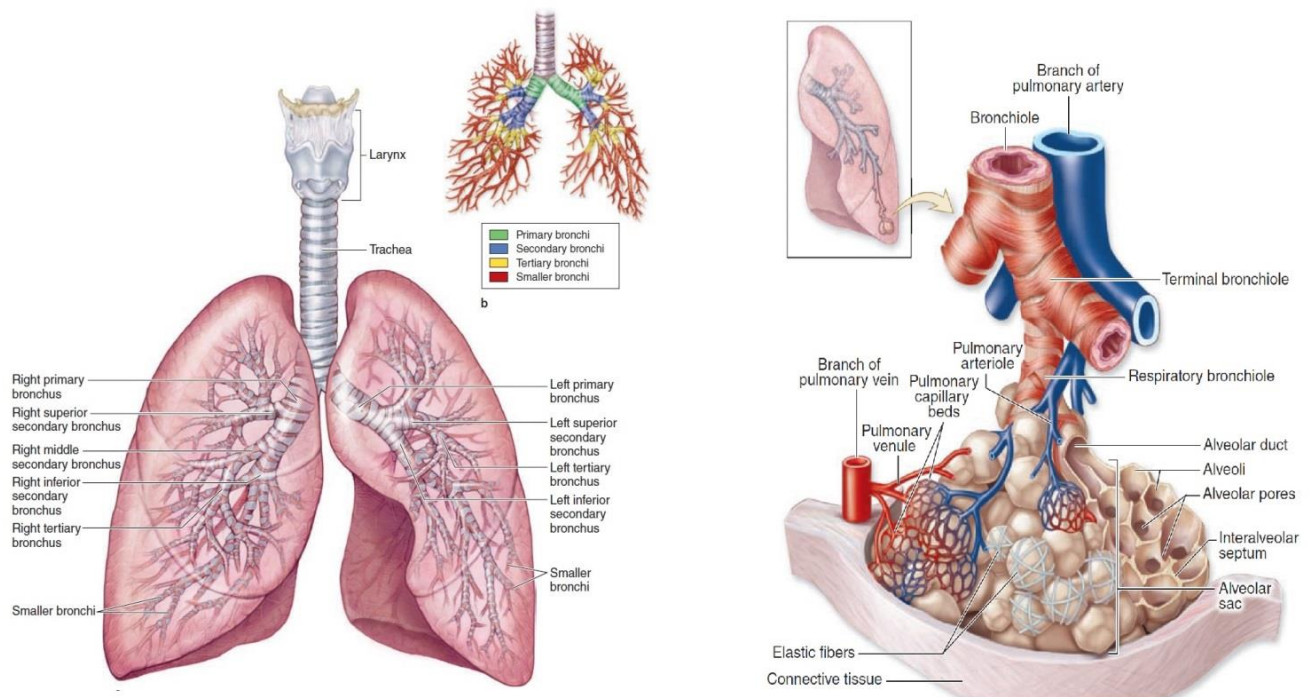

Figure 1 Bronchial tree, terminal bronchioles and alveoli

McGurk S 2013 Junqueira's Basic Histology Text and Atlas – 13th edition Mescher

| Region of Airway	Epithelium
Bronchioles	Respiratory
Terminal Bronchioles	Simple cuboidal, ciliated and Clara cells
Respiratory bronchioles with scattered alveoli	Simple cuboidal, ciliated and Clara cells
Alveolar ducts and sacs	Simple cuboidal between many alveoli
Alveoli	Types I and II alveolar cells (pneumocytes)
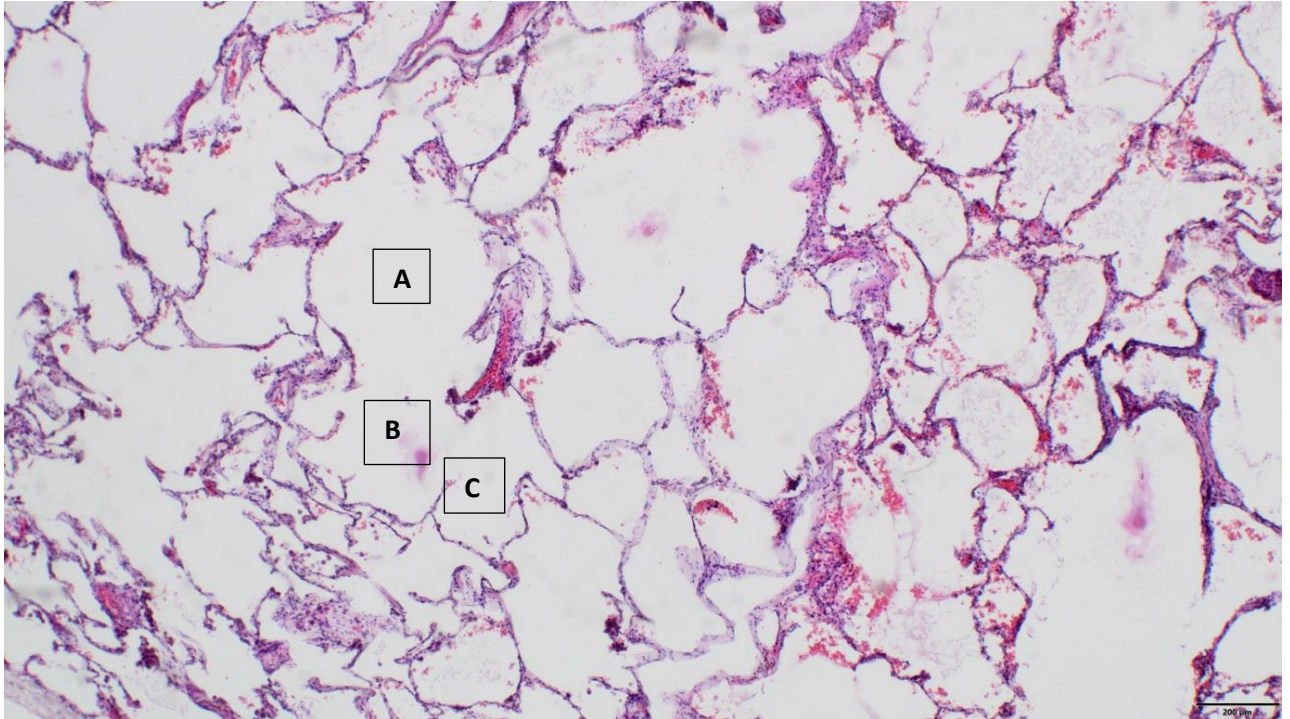
Figure 2 Alveolar ducts (A), alveolar sacs (B), individual alveoli (C)

The material used for this photo is from the Institute of Pathology of the University of Gießen archive. (Light microscope Olympus BX43, camera Olympus SC180)

Lung cancer

TNM classification of lung carcinomas

T – Primary tumour

TX Primary tumour cannot be assessed, or tumour proven by the presence of malignant cells in sputum or bronchial washings but not visualized by imaging or bronchoscopy
T0 No evidence of primary tumour
Tis Carcinoma in situ
T1 Tumour 3 cm or less in greatest dimension, surrounded by lung or visceral pleura, without bronchoscopic evidence of invasion is more proximal than the lobar bronchus, i.e, not in the main bronchus

T2 Tumour with any of the following features of size or extent: • More than 3 cm in greatest dimension • Involves main bronchus, 2 cm or more distal to the carina • Invades visceral pleura • Associated with atelectasis or obstructive pneumonitis that extends to the hilar region but does not involve the entire lung
T3 Tumour of any size that directly invades any of the following: Chest wall (including superior sulcus tumours), diaphragm, mediastinal pleura, parietal pericardium; or tumour in the main bronchus less than 2 cm distal to the carina1 but without involvement of the carina; or associated atelectasis or obstructive pneumonitis of the entire lung.
T4 Tumour of any size that invades any of the following: Mediastinum, heart, great vessels, trachea, oesophagus, vertebral body, carina; separate tumour nodule(s) in the same lobe; tumour with malignant pleural effusion.

N – Regional Lymph Nodes

NX Regional lymph nodes cannot be assessed
N0 No regional lymph node metastasis
N1 Metastasis in ipsilateral peribronchial and/or ipsilateral hilar lymph Nodes and intrapulmonary nodes, including involvement by direct extension
N2 Metastasis in ipsilateral mediastinal and/or subcarinal lymph node(s)
N3 Metastasis in contralateral mediastinal, contralateral hilar, ipsilateral or contralateral scalene, or supraclavicular lymph node(s)

M – Distant Metastasis

MX Distant metastasis cannot be assessed
M0 No distant metastasis

M1 Distant metastasis, includes separate tumour nodule(s) in a different lobe (ipsilateral or contralateral)

Lung cancer grading

Cancer grading is the division of a specific cancer into two or more prognostically relevant grades based on morphological appearance. A widely accepted grading system for lung cancer has not yet been established. (Travis et al., 2015)

In 2011, the IASLC, the American thoracic Society and the European Respiratory Society proposed a new classification for lung adenocarcinoma based on the presence and proportion of five histological patterns. The predominant histological subtype of a tumour has been shown to be associated with prognostic differences and this association may provide the basis for a simple architectural grading system with three grades: grade 1: lepidic predominant, grade 2: acinar or papillary predominant and grade 3: solid or micropapillary predominant. These grades correspond to well-, moderately and poorly differentiated tumours, respectively. Other grading schemes include two patterns, the highest-grade pattern, or nuclear features (such as mitotic count) in combination with an architectural approach (such as the predominant subtype). There is still insufficient data to determine how to grade carcinomas such as squamous cell carcinoma. Squamous cell carcinoma may be keratinizing or non-keratinizing. Keratinizing squamous cell carcinoma is recognized by the presence of keratinization, pearl formation and/or intercellular bridges. These features vary according to the degree of differentiation; they are prominent in better-differentiated tumours, where there is typically keratinization and are only focal or less prominent in less differentiated tumours. (Travis et al., 2015)

Lung adenocarcinoma

Invasive adenocarcinoma is a malignant epithelial tumour with glandular differentiation, mucin production, or pneumocyte marker expression. Adenocarcinomas show an acinar, papillary, micropapillary, lepidic or solid growth pattern. The tumours are classified according to either predominant pattern.

Smoking is the most important risk factor for lung adenocarcinoma. Lung adenocarcinoma can also develop in never-smokers, among whom they are the most frequent histological subtype. Other reported causal factors include exposure to second-hand tobacco smoke, radon and other ionizing radiation, asbestos and indoor air

pollution, as well as underlying chronic lung disease (e.g pulmonary fibrosis, chronic obstructive pulmonary disease etc.) There have been rare reports of families with an inherited genetic predisposition to lung cancer associated with germline EGFR mutation. Lung adenocarcinomas are staged and treated according to the standard TNM classification.

The most common localization of invasive adenocarcinoma is in the lung periphery. Macroscopically, most invasive adenocarcinomas appear as grey-white nodules with central scarring fibrosis associated with anthracotic pigmentation and pleural puckering. Invasive adenocarcinomas characteristically consist of a complex heterogeneous mixture of histological subtypes which often represent a morphological continuum rather than discrete compartments. Recording the percentages of histological subtypes makes it clear to the reader of a report whether a tumour has relatively even mixtures of several patterns or a clear single predominant pattern. The histological subtypes of adenocarcinomas are the lepidic adenocarcinoma, acinar adenocarcinoma, papillary adenocarcinoma, micropapillary adenocarcinoma and solid adenocarcinoma. The lepidic adenocarcinoma consists of bland pneumocytic cells growing along the surface of alveolar walls, similar to the morphology defined in the sections on minimally invasive adenocarcinoma and adenocarcinoma in situ. The acinar adenocarcinoma shows a majority component of glands which are round to oval-shaped with a central luminal space surrounded by tumour cells. The papillary adenocarcinoma shows a major component of a growth of glandular cells along central fibrovascular cores. Micropapillary adenocarcinoma has tumour cells as its main component, which grow in papillary tufts forming florets that lack fibrovascular cores. The tumour cells are usually small and cuboidal with variable nuclear atypia. The solid adenocarcinoma shows a major component of polygonal tumour cells forming sheets that lack recognizable patterns of adenocarcinoma.

The most important immunohistochemically markers/stains for lung adenocarcinomas are: TTF-1 (usually present), CK 7, CK20, CEA, thyreoglobulin (helps to exclude metastatic thyroid carcinoma), Ber-EP4 (primarily used to differentiate from mesothelioma). (W.Böcker et al., 2008) (Rekhtman et al., 2011)

Squamous cell carcinoma and large cell neuroendocrine carcinoma present the most frequent problems in differential diagnosis. Solid adenocarcinomas and poorly differentiated tumours may be correctly diagnosed using immunohistochemistry for TTF1 and a squamous marker such as p40 or p63.

The most clinically relevant mutations for lung adenocarcinoma are EGFR and ALK. KRAS mutations are reported most often in tumours with a solid pattern and can be present in tumours producing extracellular mucin.

Like other subtypes of lung cancer, TNM classification and performance status significantly influence treatment choice and strongly predict survival. Never-smoking status and female sex are favourable prognostic factors, independent from the stage of the disease. (Travis et al., 2015)
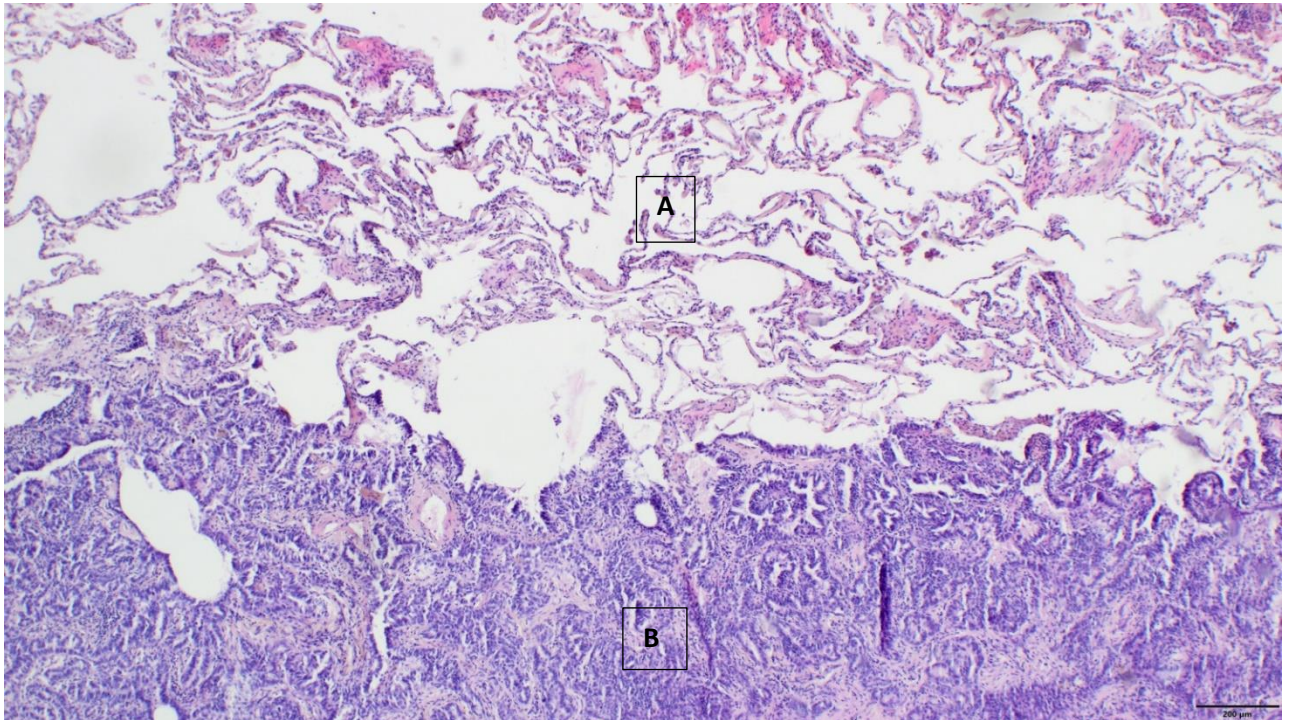

Figure 3 Borders of a lung adenocarcinoma at the normal lung tissue. The upper half of the photo shows the normal lung (A) and the lower half the lung adenocarcinoma (B).

The material used for this photo is from the archive of the Institute of Pathology of the University of Gießen. (Light microscope Olympus BX43, camera Olympus SC180)

Squamous cell carcinoma

Squamous cell carcinoma is a malignant epithelial tumour that either shows keratinization and/or intercellular bridges, or is a morphologically undifferentiated non-small cell carcinoma. Squamous cell carcinoma depends on the amount of smoking duration, starting age and tar level as well as on the fraction smoked. Also, many occupational agents and exposures have been associated with lung cancer. Arsenic exposure has been reported to have greater association with squamous cell carcinoma.

Regardless of which subtype of squamous cell carcinoma is present (keratinizing or non-keratinizing) the signs and symptoms are the same. Distant metastases are common. Both keratinizing and non-keratinizing squamous cell carcinomas usually arise in a main or lobar bronchus.

Macroscopically, the tumours are grey and frequently soft and friable. The tumours may grow to a large size and cavitate due to central necrosis. They may oculate the bronchial lumen, resulting in stasis of bronchial secretions, atelectasis, bronchial dilation, obstructive lipoid pneumonia and infective bronchopneumonia.

Well-differentiated squamous cell carcinomas show obvious keratinization, manifesting as dense refractile cytoplasm with red, orange, yellow, or light blue colour in Papanicolaou staining. The nuclei of well-differentiated squamous cell carcinoma typically have dark, non-transparent chromatin, without obvious nuclear detail and without prominent nucleoli. Spindle cell shapes are common. Extensive necrosis and inflammation are also common. Poorly differentiated squamous cell carcinoma shows no cytoplasmic keratinization, the nuclei may have open chromatin with prominent nucleoli. Immunostaining is needed by poorly differentiated squamous cell carcinomas to distinguish them from adenocarcinomas.

Histologically, keratinizing squamous cell carcinoma shows keratinization, pearl formation and/or intercellular bridges. These features are prominent in better differentiated tumours. In non-keratinizing squamous cell carcinoma, immunohistochemistry is required to distinguish tumours from large cell carcinoma with a null phenotype. (Travis et al., 2015)

Most squamous cell carcinomas express immunohistochemical CK 5/6, p63, p40, CEA and very few express TTF-1 or CK7. (Travis et al., 2015) (Rekhtman et al., 2011)

Differential diagnosis occurs mainly in poorly differentiated non-small cell tumours or small biopsy specimens with limited tumour tissue showing no morphological features of squamous cell differentiation. In very well-differentiated central airway squamous carcinoma with papillary features, distinction from papilloma can be difficult, requiring demonstration of invasion. Metastases from urothelial carcinoma are more often GATA3, uroplakin 3 and CK20 positive. Distinguishing primary lung squamous cell carcinoma from a metastasis in patients with prior history of squamous cell carcinoma

at other sites, such as the head and neck, oesophagus, or cervix, can be challenging. This may require comparing the TP53 mutation/p53 immunostaining status between the lung and prior tumour of other sites, loss of heterozygosity involving microsatellite markers or HPV testing and p16 immunohistochemistry.

Squamous cell carcinomas are characterized by alterations of gene copy number, including gain/amplification of chromosome 3q (SOX2, TP63), 7p (EGFR) and 8p (FGFR1), as well as frequent deletion of chromosome 9p (CD-KN2A), which occurs in 72% of cases. Common gene mutations include TP53, (the most frequent), CDKN2A, PTEN, PIK3CA, KEAP1, MLL2, HLA-A, NFE2L2, NOTCH1 and RB1. With only rare exceptions, pure squamous cell carcinomas, as diagnosed in resection specimens, do not harbour EGFR and KRAS mutations.

The prognosis is mainly dependent on the patient's performance score and the clinical/tumour stage, with highest stages having the worst prognosis.
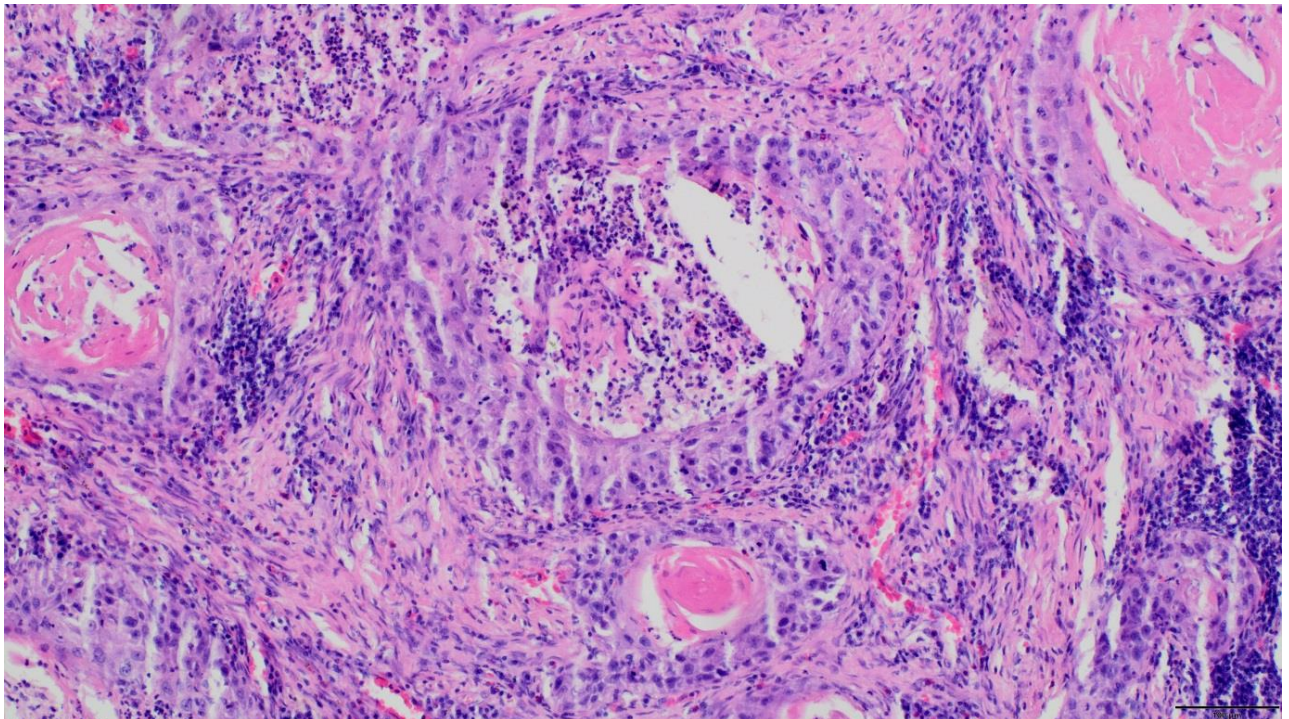
Figure 4 Squamous cell lung carcinoma (keratinized)

The material used for this photo is from the archive of the Institute of Pathology of the University of Gießen. (Light microscope Olympus BX43, camera Olympus SC180)

Therapy

Lung cancer of stage I and II have the highest cure rate with primary measures. For lung cancer from stage III, there is a multimodal therapy concept. An operation is helpful if a complete resection of the cancer can be achieved. (Preiß et al., 2017)

Stage dependent standard therapy:

IA Resection. If the tumour is inoperable then radiosurgery / stereotactic radiotherapy
IB Resection (possibly with adjuvant chemotherapy)
IIA/B Resection and adjuvant chemotherapy
IIIA Resection and adjuvant chemotherapy; induction chemotherapy and resection and radiotherapy; simultaneous inductions – radiochemotherapy and resection
IIIB simultaneous radiochemotherapy; sequential chemotherapy and radiotherapy
IV palliative system – therapy (chemotherapy or targeted therapy)

Adjuvant chemotherapy -4 cycles

1 Cisplatin	80mg/m2	Inf.(30`)	day 1
Vinorelbin	30mg/m2	Inf.(6-10´)	day 1,8,15,22; repeat day 29

2 Cisplatin	50mg/m2	Inf.(30`)	day 1, 8
Vinorelbin	25-30mg/m2	Inf.(6-10´)	day 1,8,15,22; repeat day 29

Radiochemotherapy

1 Cisplatin	80mg/m2	Inf.(60`)	day 1

Vinorelbin	15mg/m2	Inf.(6-10´)	day 1,8,15; repeat day 29

2 Carboplatin	AUC 2	Inf.(30`)	weekly
Pacitaxel	50mg/m2	Inf.(60´)	weekly

EGFR – Tyrosinkinase inhibitors

Gefitinib	250 mg	p.o	1 x daily
Erlotinib	150 mg	p.o	1x daily
Afatinib	40 mg	p.o	1x daily

(Preiß, Honecker, Claßen, 2017)

Tumour-infiltrating lymphocytes (TILs)

The tumour-infiltrating lymphocytes are the immune reaction of our immune system to a tumour. They are white blood cells that left the blood system with the aim of controlling tumour growth and progression and, if possible, eliminating the tumour cells. The observation of lymphocytes and mononuclear cells associated with human cancer was first noted more than a century ago, and these infiltrates were considered to be the causa of the disease. The concept of an immunologic response to malignant tumours in patients was probably first proposed by Paul Ehrlich in 1907 and later expanded in 1909. The term "tumour-infiltrating lymphocytes" (TILs) was first used in the work of Wallace H. Clark, Jr. In the detailed study of malignant melanomas that was spearheaded by Dr. Clark, the anatomic levels of invasion were proposed. A biopsy revealed a nodule of metastatic melanoma diffusely infiltrated by lymphocytes as observed by Dr. Clark described this response as "tumour-infiltrating lymphocytes." It was the first time that this description of TILs was applied to this type of host response in melanoma. (Mihm et al., 2015)

The underlying principle of any immunotherapeutic strategy is the capability of the immune system to differentiate tumours from normal tissue and, once the tumour has been recognised as non-self, to trigger an immune response. Isolation of tumour-infiltrating lymphocytes (TILs) from a tumour specimen followed by stimulation in an in vitro system has demonstrated the ability of TILs to lyse tumour cells in a manner specific to the tumour cell population. Together, the presence of an immune cell infiltrate and the demonstration of tumour-specific cell killing by cells isolated from the infiltrate strongly suggest the existence of an antigen specific antitumour immune response. On the other hand the existence of an antigen-specific antitumour immune response has been confirmed by the identification of a growing number of immunogenic tumour-associated antigens (TAAs) across a broad range of cancers. (Berger et al., 2005)

On the other hand, evidence began to accumulate in the late 1990s that the infiltration of neoplastic tissues by cells of the immune system serves, perhaps counterintuitively, to promote tumour progression. The counterintuitive existence of both tumour-promoting and tumour-antagonizing immune cells can be rationalized by invoking the diverse roles of the immune system: On the one hand, the immune system specifically detects and targets infectious agents with the adaptive immune response, which is supported by cells of the innate immune system. On the other hand, the innate immune system is involved in wound healing as well as clearing dead cells and cellular debris. These specialised tasks are accomplished by distinct subclasses of inflammatory cells, namely a class of conventional macrophages and neutrophils (engaged in supporting adaptive immunity), and subclasses of ''alternatively activated'' macrophages, neutrophils, and myeloid progenitors that are engaged in wound healing and tissue housecleaning. The latter subtypes of immune cells are one of the major sources of the angiogenic, epithelial, and stromal growth factors and matrix-remodelling enzymes that are needed for wound healing, and it is these cells that are recruited and subverted to support neoplastic progression. Similarly, subclasses of B and T lymphocytes may facilitate the recruitment, activation, and persistence of such wound-healing and tumour-promoting macrophages and neutrophils. Of course, other subclasses of B and T lymphocytes and innate immune cell types can cause demonstrable tumour-killing responses. (Hanahan et al., 2011)
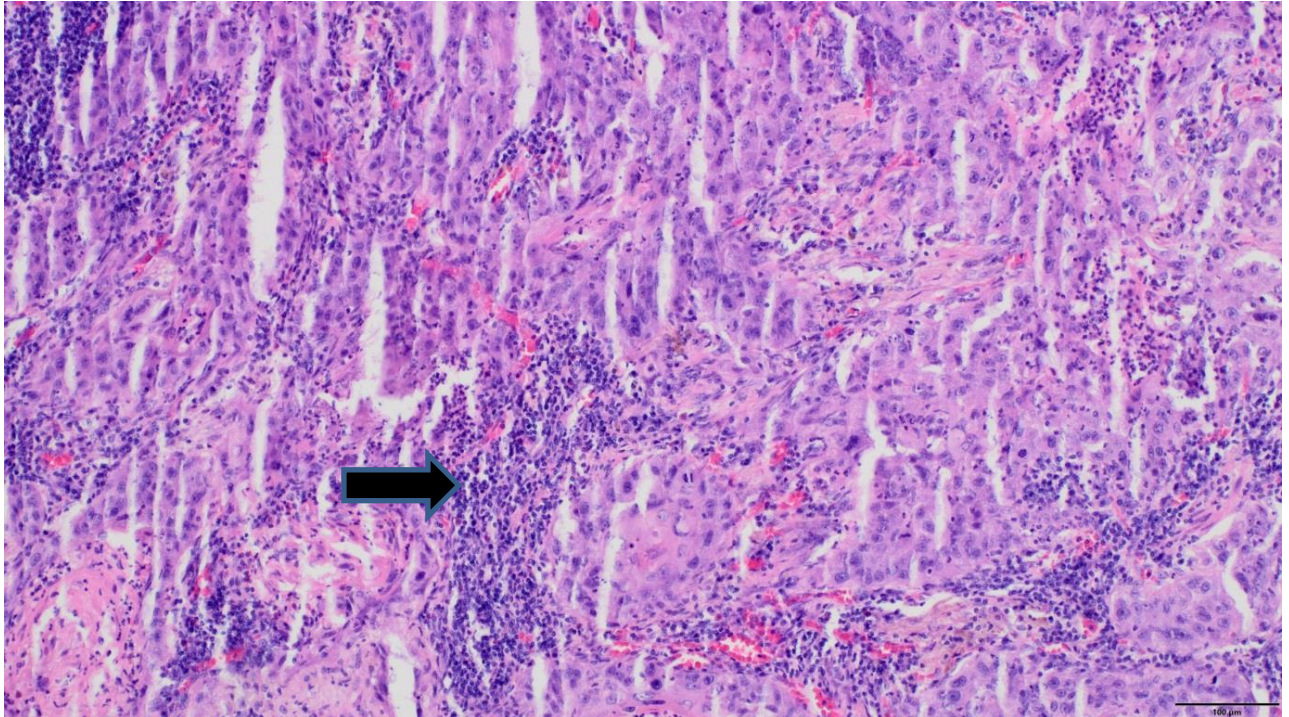
Figure 5 Tumour-infiltrating lymphocytes (arrow) in a squamous cell lung carcinoma

The material used for this photo is from the archive of the Institute of Pathology of the University of Gießen. (Light microscope Olympus BX43, camera Olympus SC180)

The immune escape mechanism of a tumour

Within the context of antitumour immunity, the emergence of a tumour is a failure of the immune system on two fronts. In a first step, a tumour must avoid the initial mechanisms of immune surveillance. Immune surveillance is based on the hypothesis that circulating APCs and T-cells will encounter, distinguish as non-self, and destroy cells expressing mutated proteins before the establishment of a tumour. A key step in this process is the ability of the APC to recognize the cell-expressing mutant protein as a threat and thereby be activated to present the antigen with the co-stimulatory signals that lead to T-cell activation. A failure by the APC to recognize the mutant protein as a threat leads to antigen presentation without the necessary co-stimulation. This has the potential to lead to T-cell tolerance and could form the basis for the establishment of a tumour. The second failure of the immune system is the generation of an ineffective response during tumour growth, continuing to produce antigenic mutations, creates an environment full of inflammatory signals by disrupting the local environment. The immune escape mechanism can be summarized in two categories: failure of antigen

presentation (downward regulation of MHC expression, elimination of immunogenic antigens by tumour, antigen expression level insufficient to generate a response to heterogeneity of antigens across tumour cell population) and failure of the immune response (lack of necessary costimulatory signals, T-cell tolerance/anergy toward tumour antigen, active immunosuppression via secreted or cell surface factors). (Berger et al., 2005)

Targeted information about the immune system

One of the major functions of the immune system is the ability to distinguish the „same" from „foreign". The immune system normally does not develop immune responses against self-antigens because the clones of the self-reacting leukocytes are destroyed or inactivated in primary lymphoid organs, especially during their development. T - cells recognize antigens via T cell receptor (TcR), which are presented on the infected cell surface in combination with the MHC (Major Histocompatibility Complex). This phenomenon is known as MHC restriction or education. The MHC restriction is achieved by the positive and negative selection of T-cells during the development and differentiation in thymus. The T-cells which do not have TcR receptor or TcR, which do not recognise the same MHC molecules or TcR with very high power for connection to the same MHC molecules, are destroyed before their maturation (positive selection). During the development and differentiation of T-cells in the thymus gland approximately 95% of cells produced are shed before maturation. The T-cells which have TcR moderate binding force with the same MHC molecules are selected to multiply, differentiate and mature (positive selection). Autoreactive T-cells can escape negative selection. These cells become inactive (clonal anergy) in peripheral lymphoid organs or are ignored by the immune system (clonal ignorance). The Self-reacting B-cells are destroyed or inactivated in a similar way in the bone marrow or peripheral lymph organs. (Νίκη Ι.Αγνάντη et al., 2005)

MHC (Major Histocompatibility Complex)

There are two types of MHC, the MHC class I and the MHC class II, also known as human leukocyte antigen (HLA) genes. (Serhan et al., 2010) (William B. et al., 2009) All nucleated cells express major histocompatibility complex MHC class I. The MHC I present peptides derived from the cell itself and from intracellular pathogens, such as

viruses. If a cell is uninfected, the antigens presented on the cell surface will not be recognized by cytotoxic T-cells. However, if the presenting cell is infected or cancerous, the T-cell will target it for death. B-cells use the BCR to recognize pathogenic molecules which bind pathogens directly. In contrast, T-cells rely on other, more innate, antigen- presenting cells (APCs) to break down pathogenic proteins into peptides, which are then presented to the TCR by the major histocompatibility complex (MHC). MHC class II molecules are generally found on the surface of professional APCs and typically present antigen from extracellular pathogens. (Serhan et al., 2010) APCs, particularly dendritic cells, ingest pathogens and associated antigens and travel from the site of an infection (for example) to lymph nodes where they encounter dense collections of T-cells and B-cells. APCs process antigens and present them combined with MHC class II. T-cells that bind these peptide-MHC complexes are activated to proliferate and they then produce cytokines that further direct immune responses. This process leads to clonal amplification of pathogen-specific T-cells. Specialized APCs, called follicular dendritic cells (FDCs), do not process antigens into fragments, but carry larger fragments and even entire pathogens on their cell surface where they can be presented to B-cells, which are then clonally amplified as well. B-cells can also process antigen and present it to T-cells in the context of MHC class II. T-cells recognizing this antigen can then provide signals to B-cells leading to maturation of the antibody response, including isotype switching and somatic hypermutation. The activation of lymphocytes requires two signals: (i) antigen binding, which signals through the antigen receptor, and (ii) a second signal provided by another cell. For T-cells, this second signal is provided by APCs. For B-cells, the second signal is usually provided by activated T-cells. If lymphocytes receive signalling only through the antigen receptor without co-stimulation, the lymphocyte either becomes anergic (immunologically inactive) or dies via apoptosis. (William B. et al., 2009)
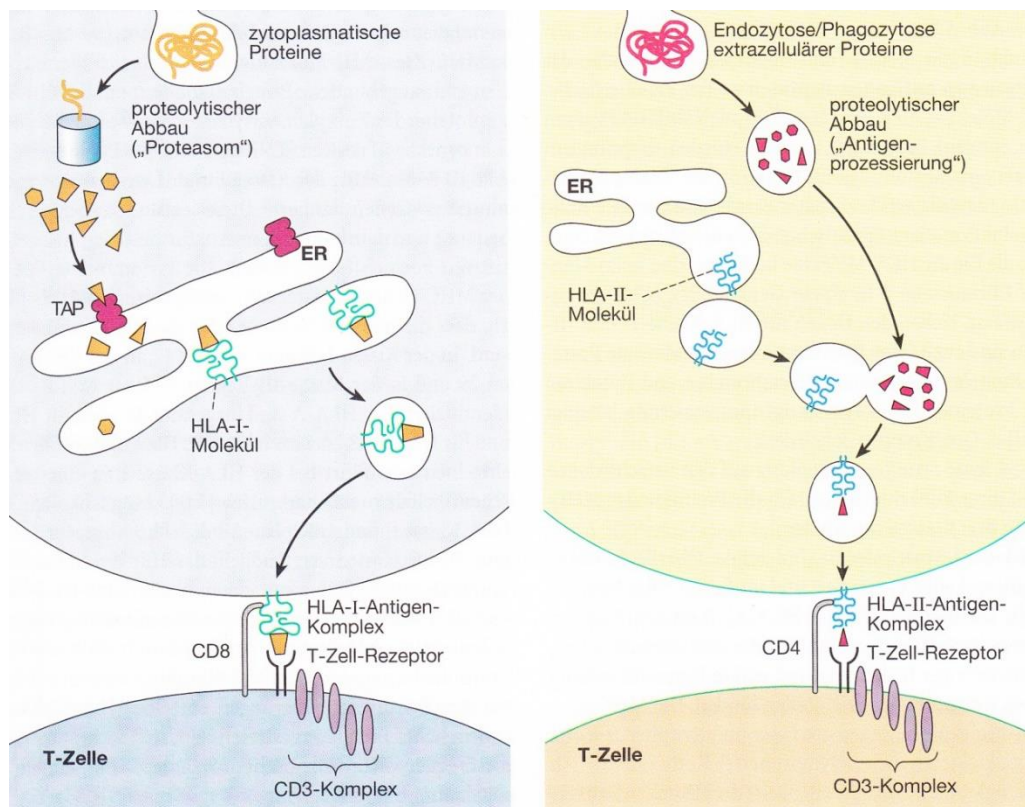
Figure 6 MHC I Antigen complex and MHC II Antigen complex

W.Böcker, H.Denk, Ph. U. Heitz, H. Moch (2008)"Pathologie" ELSEVIER

SURFACE INDICATORS leukocytes (CD - antigens)

Leucocytes express a large number of molecules (markers) on their surface, which (at least most) can be immunologically detected by using specific single-stranded antibodies. (Νίκη Ι.Αγνάντη et al., 2005) One of the most significant advancements in the immunophenotyping analysis of cell-surface antigens/markers is the development of highly specific monoclonal antibodies. Individual monoclonal antibodies are produced by cloned antibody-secreting cells and specifically recognize the antigen that was used in immunization for the antibody production. (Hecker et al., 2009) For the classification of surface markers of leukocyte there is a specific classification system, which is known as CD system (Cluster Designation). (Νίκη Ι.Αγνάντη et al., 2005) Each surface molecule that is recognized by antibodies, is assigned an individual CD number. Using the CD system, it is possible to identify cells by the presence or absence of particular surface molecules. Cells are usually defined using a "+" or a "−" symbol to indicate whether they express or lack the CD molecules. The CD system has been expanded and

is widely used in all types of cells. (Hecker et al., 2009) With immunological detection of CD molecules it is possible to identify different populations and subpopulations of white blood cells, their differentiation stage and their functional status. (Νίκη Ι.Αγνάντη et al., 2005)

SURFACE INDICATORS that were used in the Project

<u>CD3</u>: it shows a membranous or cytoplasmatic positivity. CD3 is a pan-T-cell marker.

<u>CD4</u>: it shows a membranous positivity. CD4 marks the helper T-cells and monocytes.

<u>CD8</u>: it shows a membranous positivity. CD8 marks the Cytotoxic and suppressor T-cells and NK – like T–cells.

<u>CD20</u>: it shows a membranous or cytoplasmatic positivity. CD 20 is a pan–B-cell marker.(Rekhtman et al., 2011)

PD-1 and its ligands

Programmed cell death-1 (PD-1) is a member of the CD28 superfamily that delivers negative signals upon interaction with its two ligands, PD-L1 or PD-L2 (Jin et al., 2011) and among them, PD-L1 is responsible for tumour immune modulation. The binding affinity of PD-1 with PD-L1 is three times greater than the affinity between PD-1 for PD-L2. (Alsaab et al., 2017) Subsequent studies show that PD-1-PD-L interaction regulates the induction and maintenance of peripheral tolerance and protects tissues from autoimmune attacks. PD-1 and its ligands are also involved in attenuating infectious immunity and tumour immunity, as well as facilitating chronic infection and tumour progression. The biological significance of PD-1 and its ligand suggests the therapeutic potential of manipulation of PD-1 pathway against various human diseases. (Jin et al., 2011)

The PD-1 and PD-L1 is a receptor-ligand system and in tumour microenvironment, they are attached to each other, resulting in a blockade of anti-tumour immune responses. PD-1/PD-L1 inhibitors pharmacologically prevent the PD-1/PD-L1 interaction, thus facilitating a positive immune response to kill the tumour. PD-1 and PD-L1 targeting is an efficient way to maintain the function of effector T-cells. Monoclonal antibodies (mAbs) are a class of drugs called checkpoint inhibitors that inhibit the interaction of PD-1 and PD-L1 and overcome the disadvantages of conventional anticancer therapy. Indeed, immune checkpoint inhibitors have emerged as a frontline treatment for

multiple cancers, such as metastatic melanoma, non-small cell lung cancer (NSCLC), renal cell carcinoma (RCCs), and bladder or urothelial cancer. They are presently being assessed in numerous other cancer types, including breast cancer, head and neck cancer, and some advanced solid and haematological malignancies. The loss of immunologic control has been confirmed as one of the emerging hallmarks of cancer and in 1996, Leach et al. proposed an immune checkpoint blockade. This is an advanced strategy of cancer management. In 2011, the first immune checkpoint inhibitor (ipilimumab as an anti-CTLA-4 antibody) was approved by the FDA for the treatment of melanoma that created a footstep in immunotherapy cancer treatment. Targeting both PD-1 and PD-L1, the immune checkpoint inhibitors agents could reactivate cytotoxic T-cells to work against cancer cells. When the T-cell receptor (TCR) distinguishes antigens in the presence of a major histocompatibility complex (MHC), the immune checkpoint molecule modulates signalling of co-stimulatory factors such as CD28 to amplify the signal, whereas co-inhibitory molecules suppress it. It has been found that PD-1 is expressed on a variety of immune cells, such as monocytes, T-cells, B-cells, dendritic cells, and tumour-infiltrating lymphocytes (TILs). However, PDL-1 is expressed in tumour cells and antigen presenting cells (APCs), and the engagement of PD-L1 with PD-1 of T-cell creates T-cell dysfunction, exhaustion, neutralization, and interleukin-10 (IL-10) production in a tumour mass. Therefore, the function of a tumour overexpressing PD-L1 is to protect itself from cytotoxic T-cell (CD8+) mediated cell killing. Due to exhaustion of CD8+ T-cells, tumour cells become very aggressive and secrete several pro-inflammatory cytokines, such as tumour necrosis factor alpha (TNF-α), interleukin-2 (IL-2), and interferon gamma (IFN-γ). (Alsaab et al., 2017)

The objective of this project

The tumour-infiltrating lymphocytes are the reaction of our immune system to a tumour and are often associated with a favourable prognosis. They can also predict a response to chemotherapy in many cancer types. Tumour-infiltrating lymphocyte therapy for example has consistently shown very good clinical responses in selected patients with metastatic melanoma and is increasingly applied to treat other solid tumours, including head and neck squamous cell carcinoma, cervical cancer, breast cancer, and lung cancer. (Radvanyi, 2015) Therefore, the goal of this study is to determine the type, infiltrating pattern and number of tumour-infiltrating lymphocytes in lung squamous cell carcinoma and adenocarcinoma. Furthermore, the goal of this study is to determine the expression

of PD-1 surface protein of tumour-infiltrating lymphocytes and to show which type of lymphocytes predominate in this immune response. The goal is furthermore to investigate if there is a correlation between tumour-infiltrating lymphocytes and the age of a patient, TNM classification or differentiation of the tumour.

In this study, two types of lung cancers were examined, the squamous cell carcinoma and adenocarcinoma of the lung (the two most common lung cancers). The samples are from 40 patients with squamous cell carcinoma or adenocarcinoma. They are post-surgical histological material from patients with lung adenocarcinoma and squamous cell carcinoma from the archive of the institute of Pathology of the University of Gießen. These samples were stained immunohistochemically (in the Institute of Pathology of the University of Gießen) with antigens for CD3, CD4, CD8 and CD20 to show the subpopulation of TILs (the T-helper lymphocytes, Natural killer lymphocytes and B-lymphocytes).

Materials and methods

Patient samples

For this study, 40 lung cancer samples from 40 different patients were examined. The material comes from the archive of the Institute of Pathology of the University of Gießen. These samples come from patients that were surgically operated at University of Gießen between the years 2013 – 2017. The probes were fixated in formalin and in long-term storage paraffin blocks, archived in the Institute of Pathology of the University of Gießen. In total, 22 patients with lung adenocarcinoma and 18 patients with squamous cell carcinoma were examined. For the sample collection and its further use, there is a positive verdict by the Ethic-Commission of the University of Gießen.

Inclusion criteria

For this study, patients with primary lung adenocarcinoma and primary squamous carcinoma were used from the archive of the Institute of Pathology of the University of Gießen. Age limit did not present a criterion.

Exclusion criteria

One of the most important exclusion criteria was patients with lung metastasis. The goal was to find patients with primary lung cancer. Determining whether a patient has a lung metastasis or a primary lung carcinoma was done in the primary diagnostic using

immunohistochemistry and when needed molecular pathology as well; diagnostic procedures were not the responsibility of the author.

Another exclusion criterion was patients with lung infections and carcinoma. Patients with lung cancer often have lung infections (for example, pneumonia) resulting in a mixed population of lymphocytes and neutrophil granulocytes. Patients with lung infections were excluded as the aim of this study was to examine only immune reaction (TILs) to lung cancer.

The two most common lung cancers are lung adenocarcinoma and lung squamous carcinoma. Therefore, patients with these two types of lung cancer were investigated and other lung cancers were, excluded.

Timeframe

The collection of the data from the archive and the processing / counting for this study took place between December 2016 and February 2018.

Equipment

Equipment	Modell	Manufacturer, company headquarters
Lightmicroscope	Leica DM IL	Leica, Wetzlar
Lightmicroscope	Olympus BX43	Olympus
Microtom	SM2000R	Leica, Wetzlar
Camera	Olympus SC180	Olympus
Stainer	Bond Max	Leica, Wetzlar

Material	Manufacturer, company headquarters

Slides, super frost	R. Langenbrinck, Emmendingen
Cover slips (24 x 26 mm)	R. Langenbrinck, Emmendingen

Chemicals, reagents and Enzymes

Substance	Manufacture, company headquarters
Hämatoxylin	Dako, Glostrup, Germany
Citrate buffer	Leica, Wetzlar
Bond wash solution	Leica, Wetzlar
Mixed DAB refine	Leica, Wetzlar
Post Primary	Leica, Wetzlar
Deionized Water	
Alcohol	

Antibody

Name	Manufacture	Dilution	Reference	Application
CD3	Dako	1/50	117254	EDTA
CD8	Dako	1/100	117103	EDTA
CD4	Dako	1/50	117310	EDTA
CD20	Dako	1/500	110755	EDTA
PD1		1/50		Citrate

Methods

Identifying potential patients and material

Using the digital patient file program of the Institute of Pathology of the University of Gießen, it was possible to identify suitable patients for this study according to our exclusion and inclusion criteria. With the help of the digital patient program, it was possible to find all the relevant information and most importantly the histopathological diagnosis for each patient. The histology slides and tissue blocks from each patient that were used for this study are stored in the archive of the Institute of Pathology of the University of Gießen. The selected patients had to fill the following criteria:

a) Patients with primary adenocarcinoma or squamous cell carcinoma
b) The histopathological report does not mention an infection

Choosing suitable patients and material:

After selecting all patients and obtaining their HE / tissue slides, a light microscopic analysis of every slide was done. The selected patients had to meet the following criteria:

a) The material includes sufficient (tumour tissue)
b) The material is in good quality and able to be assessed
c) There are no signs of secondary inflammation due to infection

After selecting the final patients who fulfilled all our criteria, the relevant tissue blocks of each patient were located in the archive of Institute of Pathology of the University of Gießen. Finally, new slides were stained from one block from each patient with CD3, CD4, CD8, CD20 and PD-1.

Charting the tumour infiltrating lymphocytes:

The histological examination of the stained slides (CD3, CD4, CD8 and CD20) from each patient showed that there are two different infiltrating patterns of TILs.

The first is an irregular / diffuse infiltrating pattern in the cancer stroma. This pattern consists of CD3, CD4 and CD8 lymphocytes. CD20 B-lymphocytes do not show a significant number of irregular patterns.

The second infiltrating pattern shows a concentration of lymphocytes in small clusters / herds in the form of small lymph follicles. In this pattern, the majority of the concentrated lymphocytes were B- lymphocytes.

The charting of these two patterns was done with the help of digital photography (Light microscope Olympus BX43, camera Olympus SC180)

Counting tumour-infiltrating lymphocytes:

Based on the two patterns of TILs (diffuse and lymph follicle – like pattern) two different strategic approaches were for counting lymphocytes. While many digital programs are able to automatically count cells for this study the counting of lymphocytes was done manually. Thus, the tumour-infiltrating lymphocytes were counted with light microscopy, directly from the slide, counting each one lymphocyte. Although this method is time consuming is in the opinion of the author also very accurate.

All the TILs found in the lymph follicle pattern (of all stains: CD3, CD4, CD8 and CD20) of every patient were counted individually.
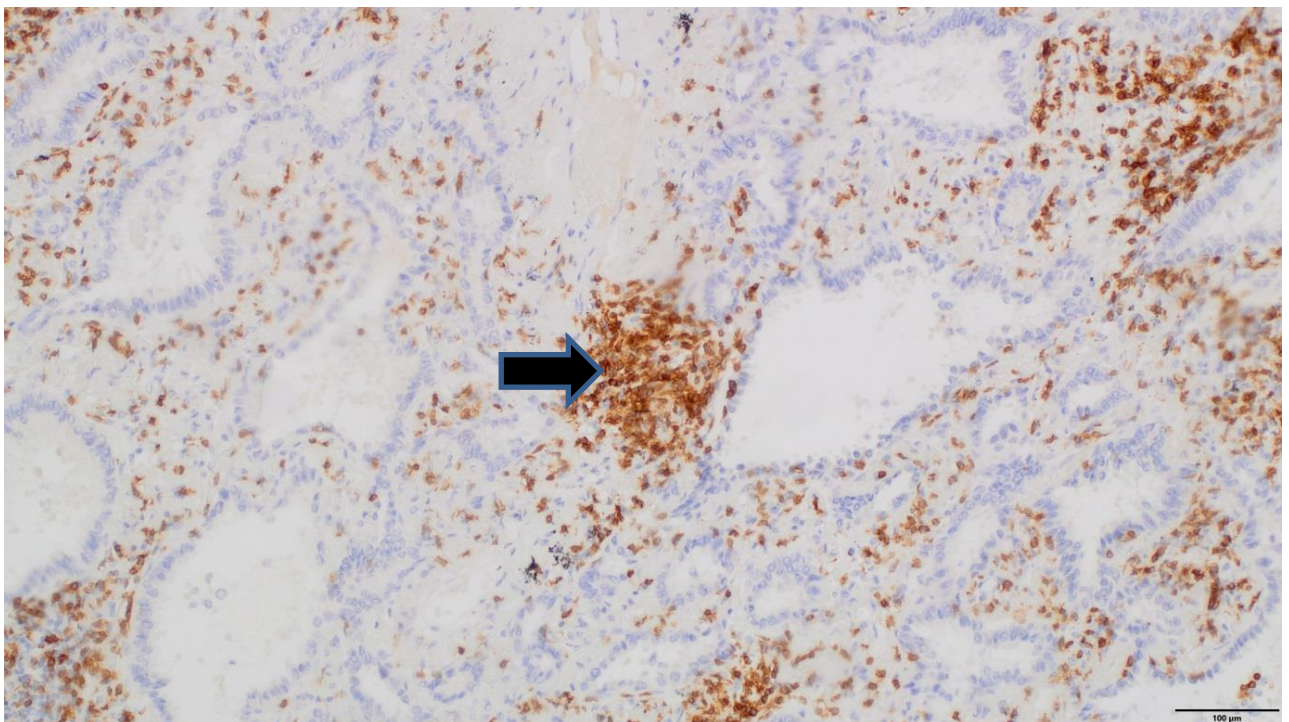
Figure 7 CD3 stain of tumour infiltrating lymphocytes found in lymph follicle pattern (arrow) in an adenocarcinoma of the lung.

The material used for this photo is from the archive of the Institute of Pathology of the University of Gießen. (Light microscope Olympus BX43, camera Olympus SC180)
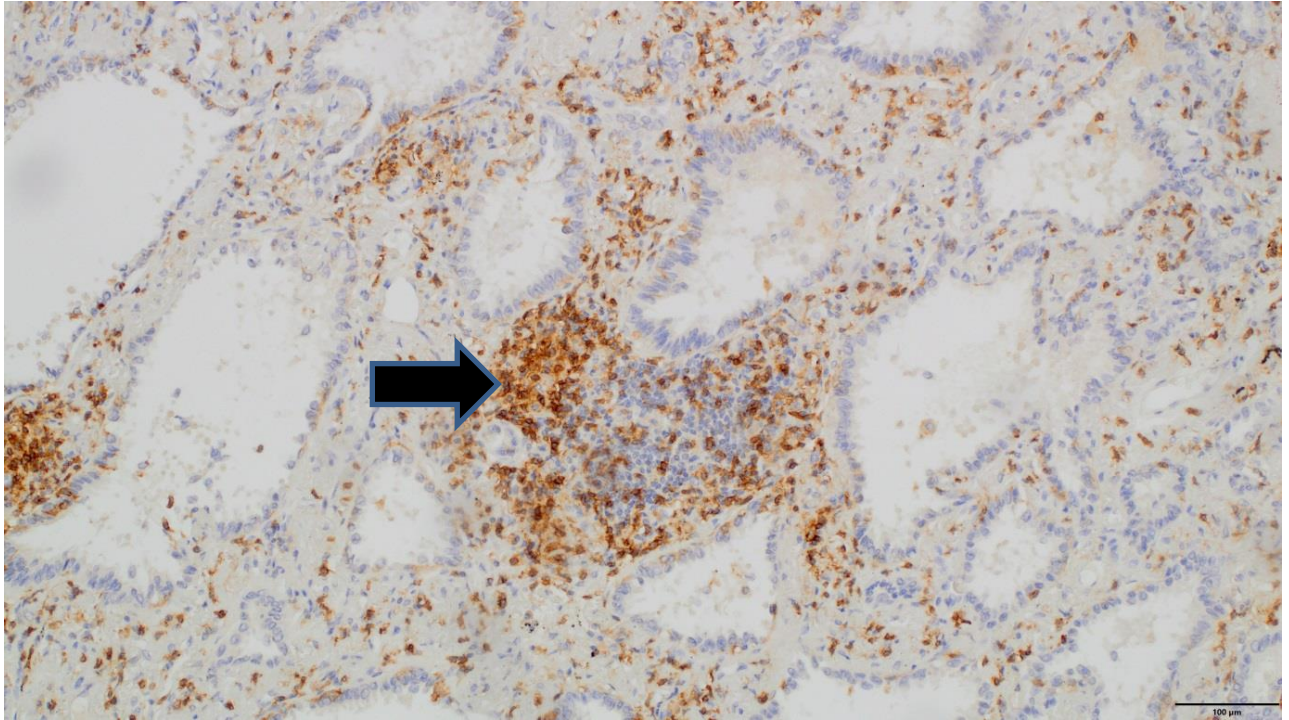
Figure 8 CD4 stain of tumour infiltrating lymphocytes found in lymph follicle pattern (arrow) in an adenocarcinoma of the lung

The material used for this photo is from the archive of the Institute of Pathology of the University of Gießen. (Light microscope Olympus BX43, camera Olympus SC180)
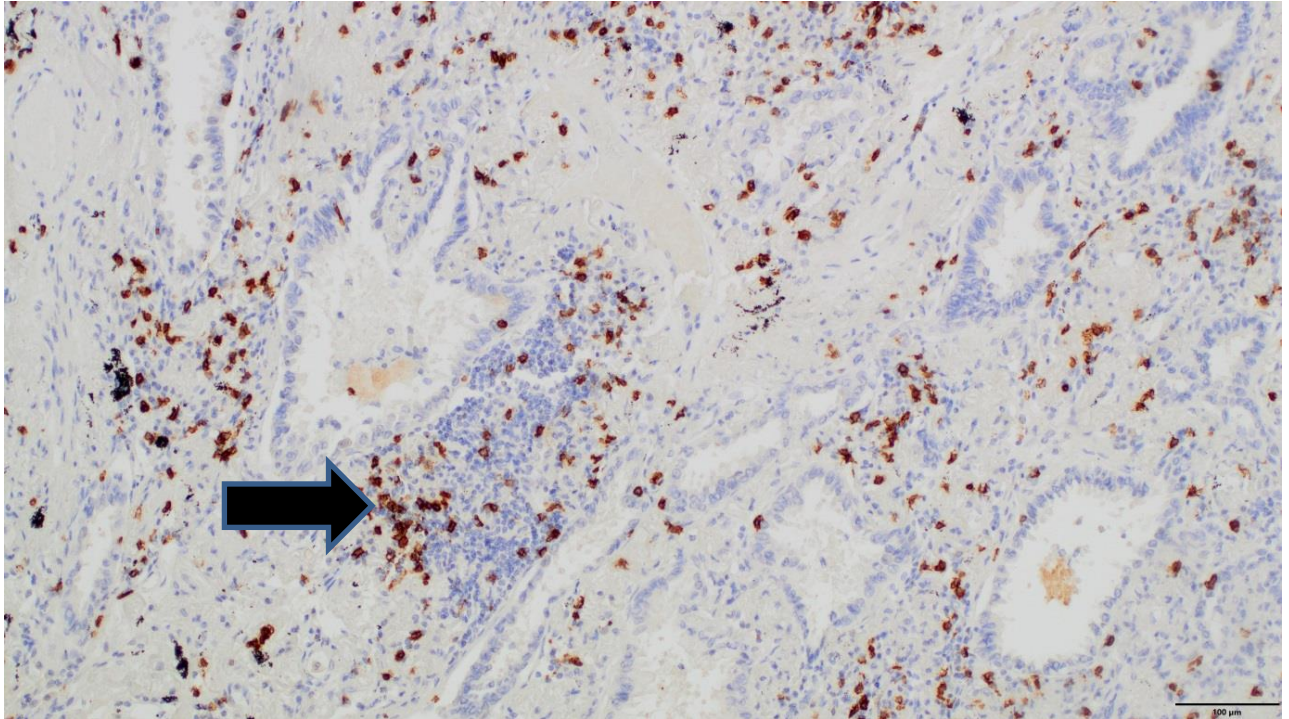
Figure 9 CD8 stain of tumour infiltrating lymphocytes found in lymph follicle pattern (arrow) in an adenocarcinoma of the lung.

The material used for this photo is from the archive of the Institute of Pathology of the University of Gießen. (Light microscope Olympus BX43, camera Olympus SC180)
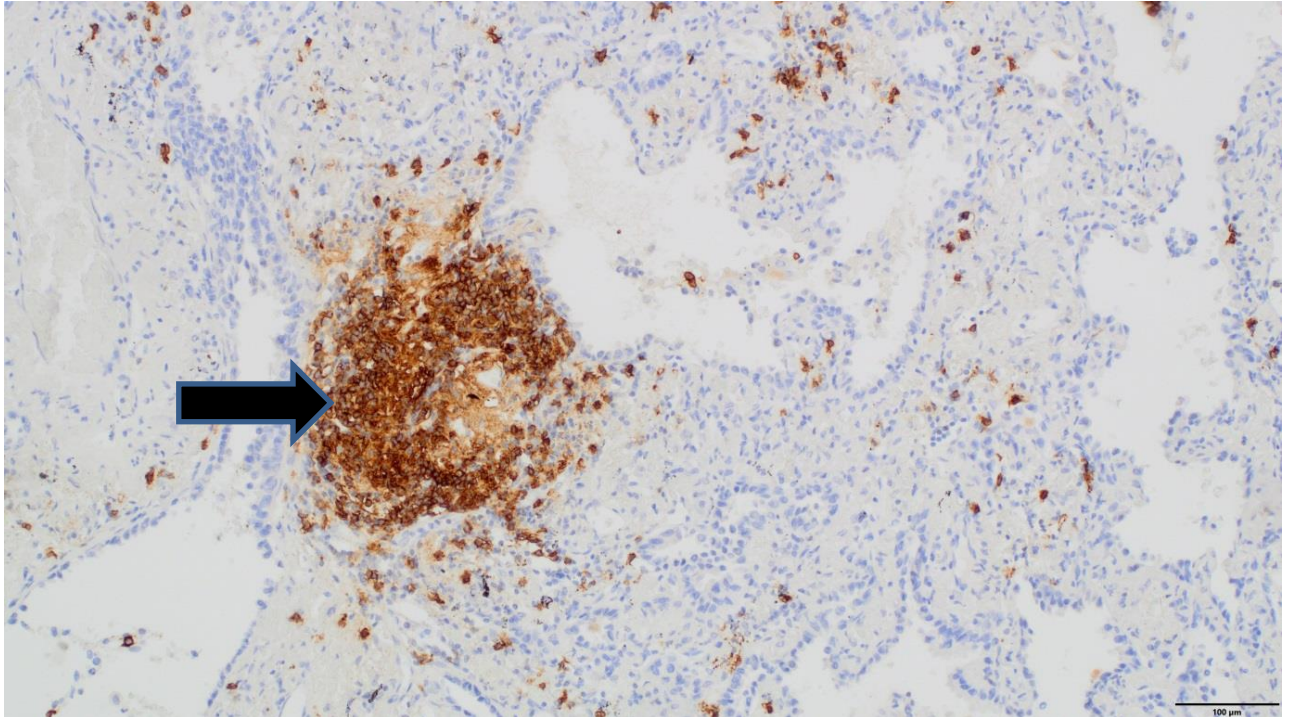
Figure 10 CD20 stain of tumour infiltrating lymphocytes found in lymph follicle pattern (arrow) in an adenocarcinoma of the lung.

The material used for this photo is from the archive of the Institute of Pathology of the University of Gießen. (Light microscope Olympus BX43, camera Olympus SC180)

Furthermore, the TILs of the diffuse pattern were not counted one by one in the whole area of the tumour tissue because their dispersal infiltration in the tumour tissue makes it impossible to count them manually / with light microscopy. For this measurement, a square millimetre in three different tumour tissue regions according to the observed distribution of diffuse TILs (one region with relatively high density, one region with a relatively medium density and one region with relatively low density of TILs) was marked in every slide (CD3, CD4, CD8 and CD20) and the stained TILs in these square millimetres were then counted. The average of the three numbers found is considered as the average number of diffuse TILs per square millimetre in the tumour tissue.
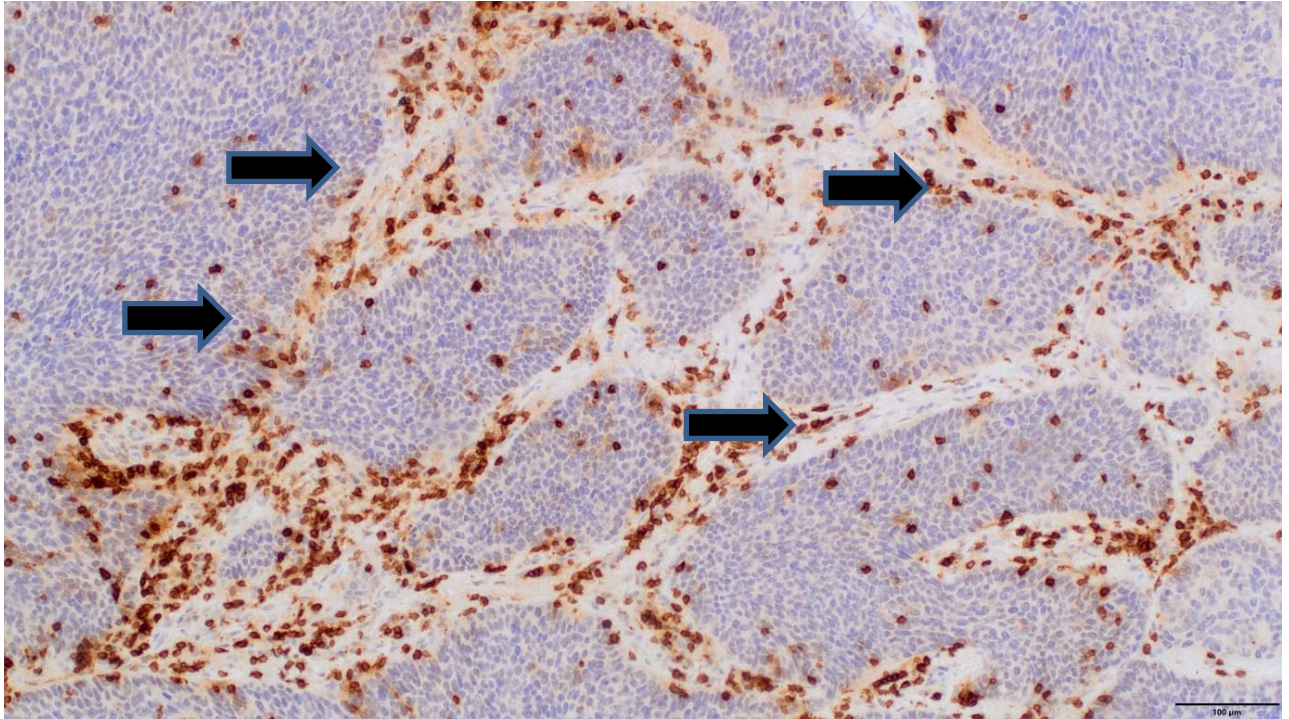
Figure 11 CD3 stain of tumour infiltrating lymphocytes in a diffuse pattern (arrows) in a squamous carcinoma

The material used for this photo is from the archive of the Institute of Pathology of the University of Gießen. (Light microscope Olympus BX43, camera Olympus SC180)
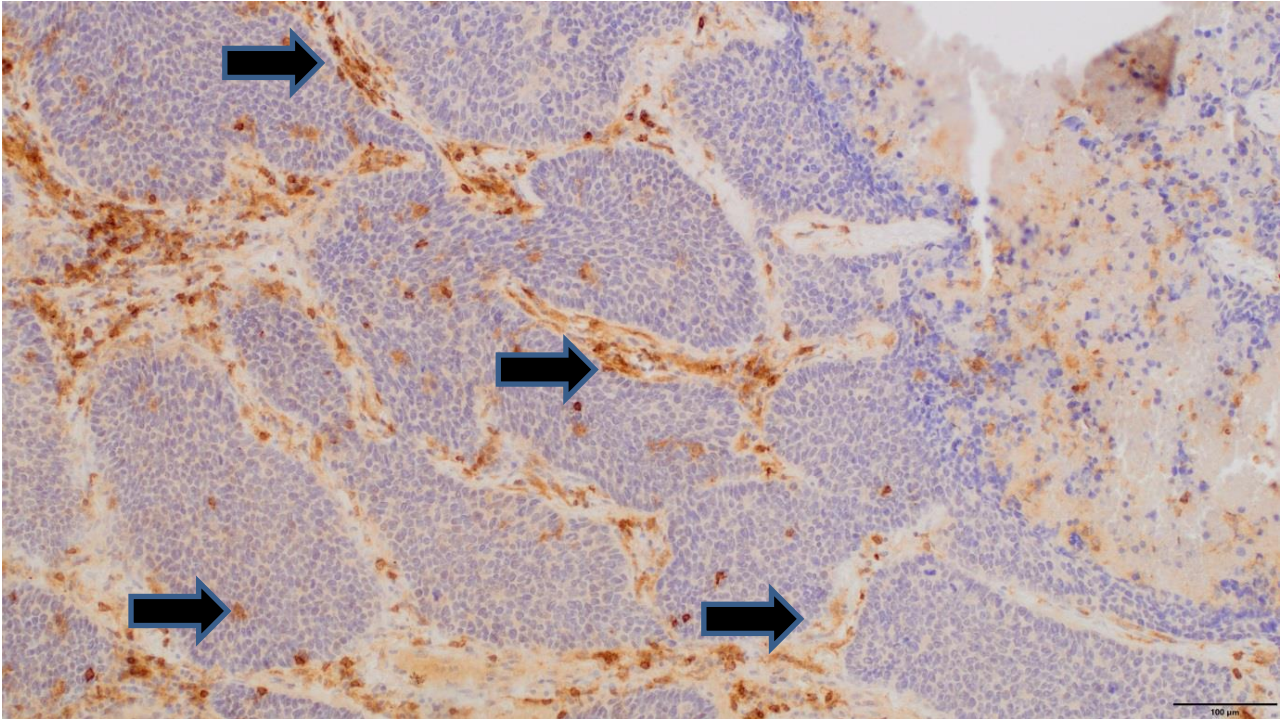
Figure 12 CD4 stain of tumour infiltrating lymphocytes in a diffuse pattern (arrows) in a squamous carcinoma.

The material used for this photo is from the archive of the Institute of Pathology of the University of Gießen. (Light microscope Olympus BX43, camera Olympus SC180)
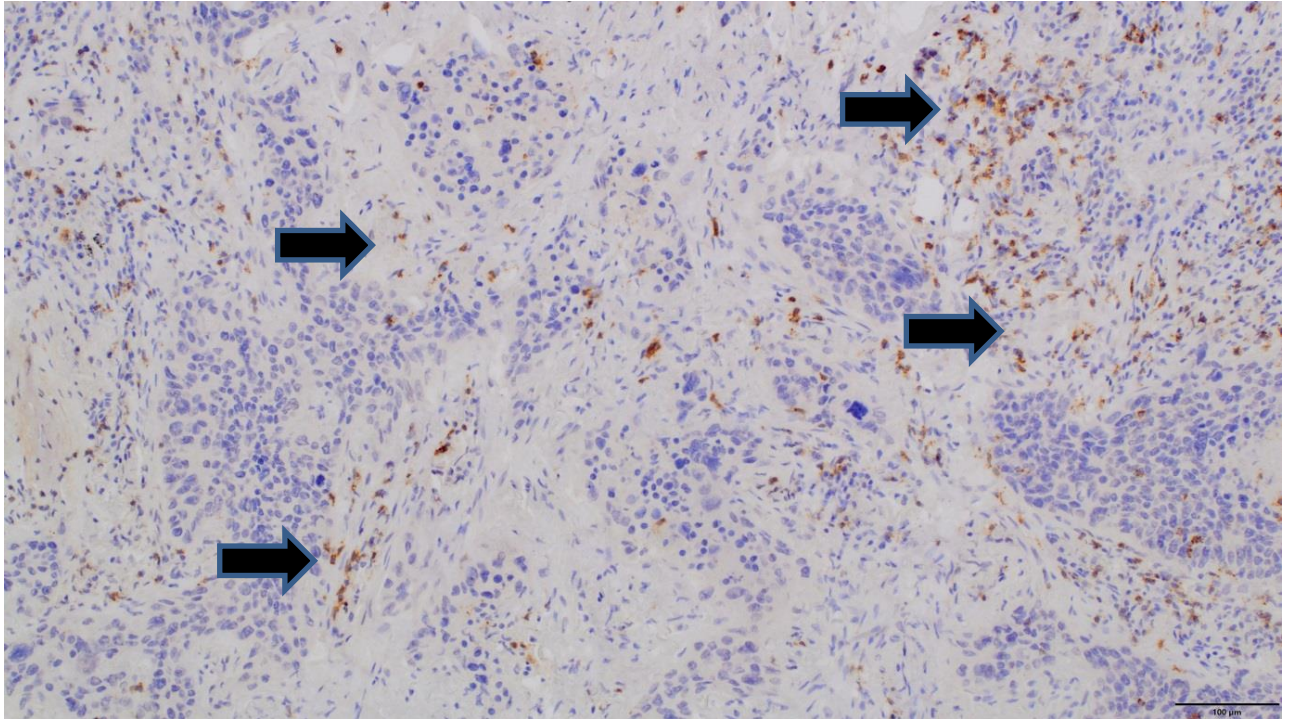
Figure 13 CD8 stain of tumour infiltrating lymphocytes in a diffuse pattern (arrows) in a squamous carcinoma.

The material used for this photo is from the archive of the Institute of Pathology of the University of Gießen. (Light microscope Olympus BX43, camera Olympus SC180)
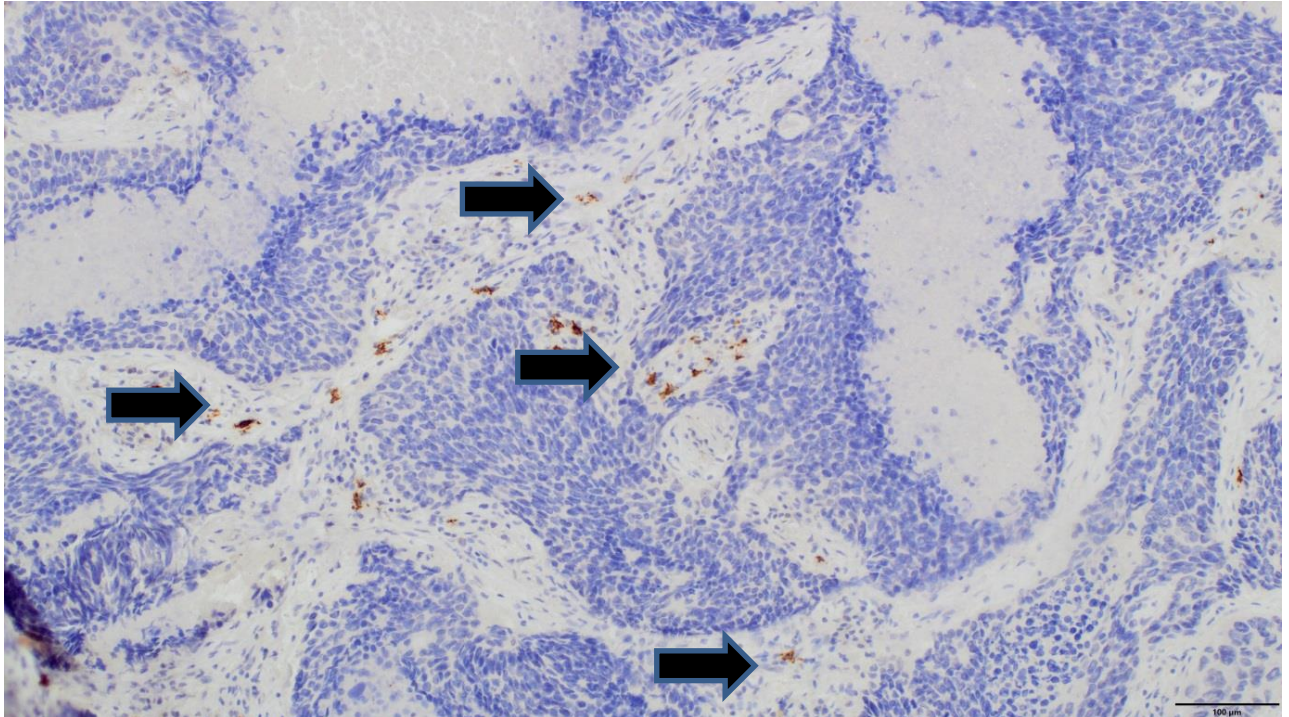
Figure 14 CD8 stain of tumour infiltrating lymphocytes in a diffuse pattern (arrows) in a squamous carcinoma.

The material used for this photo is from the archive of the Institute of Pathology of the University of Gießen. (Light microscope Olympus BX43, camera Olympus SC180)

Statistic

The data collection and the presentation, such as the evaluation of the data, was done with Microsoft Excel Version 2010.

To compare the groups, a Mann-Whitney nonparametric test was applied (GraphPad PRISM).

A p-value of <0.05 was considered statistically significant.

Subsequently, the correlation coefficient with r after Pearson was calculated.

Results

The aim of this study is to map and classify the tumour-infiltrating lymphocytes from patients with squamous carcinoma or adenocarcinoma of the lung and to find a correlation between all the data that will be collected. In the following section, the results of this study will be analysed.

Characteristics of the patients included in the study

Number of patients	n=40
Age (Average)	67
Number of patients with squamous lung carcinoma	18
Number of patients with lung adenocarcinoma	22
Number of patients with pT1 stage	22
Number of patients with pT2 stage	14
Number of patients with pT3 stage	3
Number of patients with pT4 stage	1
Number of patients with differentiation grade 1	1
Number of patients with differentiation grade 2	28
Number of patients with differentiation grade 3	11

CD3 diffuse infiltrating lymphocytes:

The average number of CD3 diffuse tumour-infiltrating lymphocytes in one square millimetre from all 40 patients, regardless of type of cancer, will be shown on the next box plot.
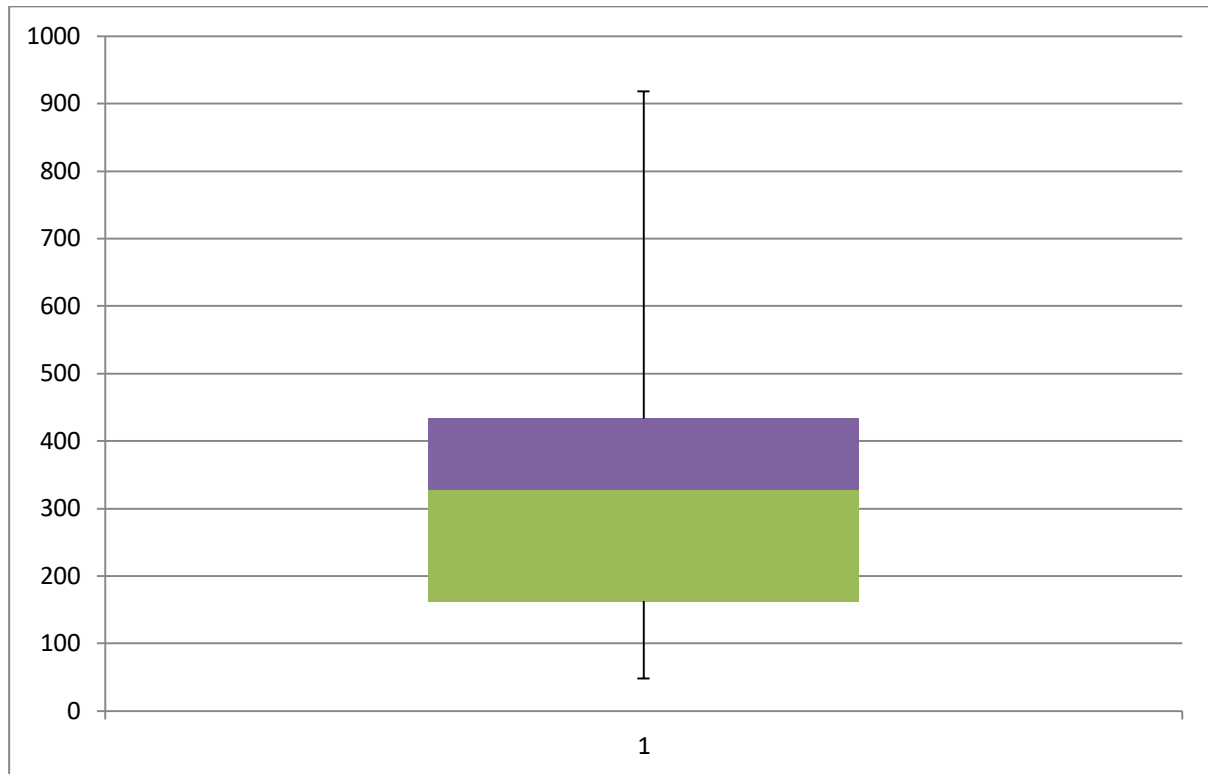
The minimum average number of diffuse tumour-infiltrating CD3 lymphocytes in one square millimetre was 48 and the maximum 918. The middle value was 328 lymphocytes. The number of CD3 diffuse tumour-infiltrating lymphocytes varies more in the fourth quartile.

In the following graph, the average number of CD3 diffuse tumour-infiltrating lymphocytes in one square millimetre can be found on the X-axis, and the differentiation grade of the carcinomas (adenocarcinomas and squamous lung carcinomas together) is shown on the Y-axis. Each blue point represents a patient.

Average numbers of CD3 diffuse infiltrating lymphocytes in one square millimetre
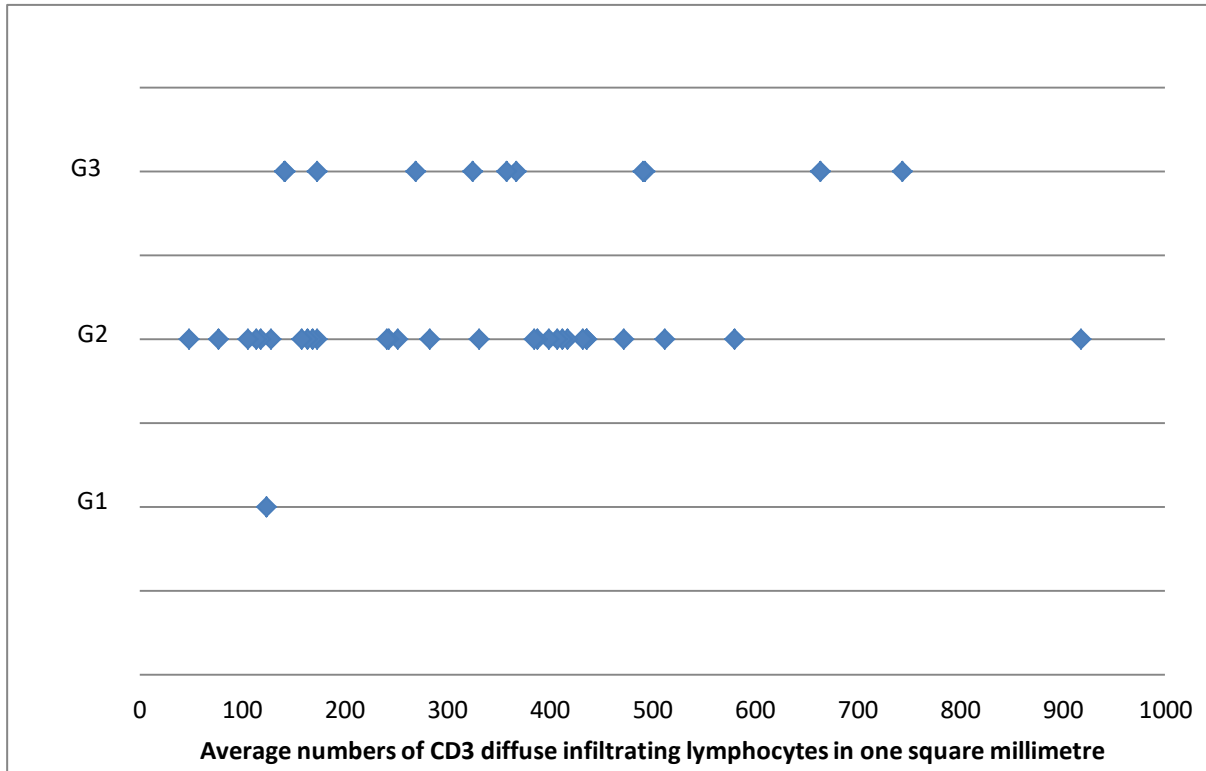
As seen above, there is no correlation between the differentiation grade of the carcinomas and the average number of CD3 diffuse tumour-infiltrating lymphocytes in one square millimetre. The correlation coefficient (r) is 0.02 showing that there is no linear relation.

In the following graph, the average number of CD3 diffuse tumour-infiltrating lymphocytes in one square millimetre can be found on the X-axis, and the T-grading of lung cancers (adenocarcinomas and squamous lung carcinomas together) is shown on the Y-axis. Each blue point represents a patient.
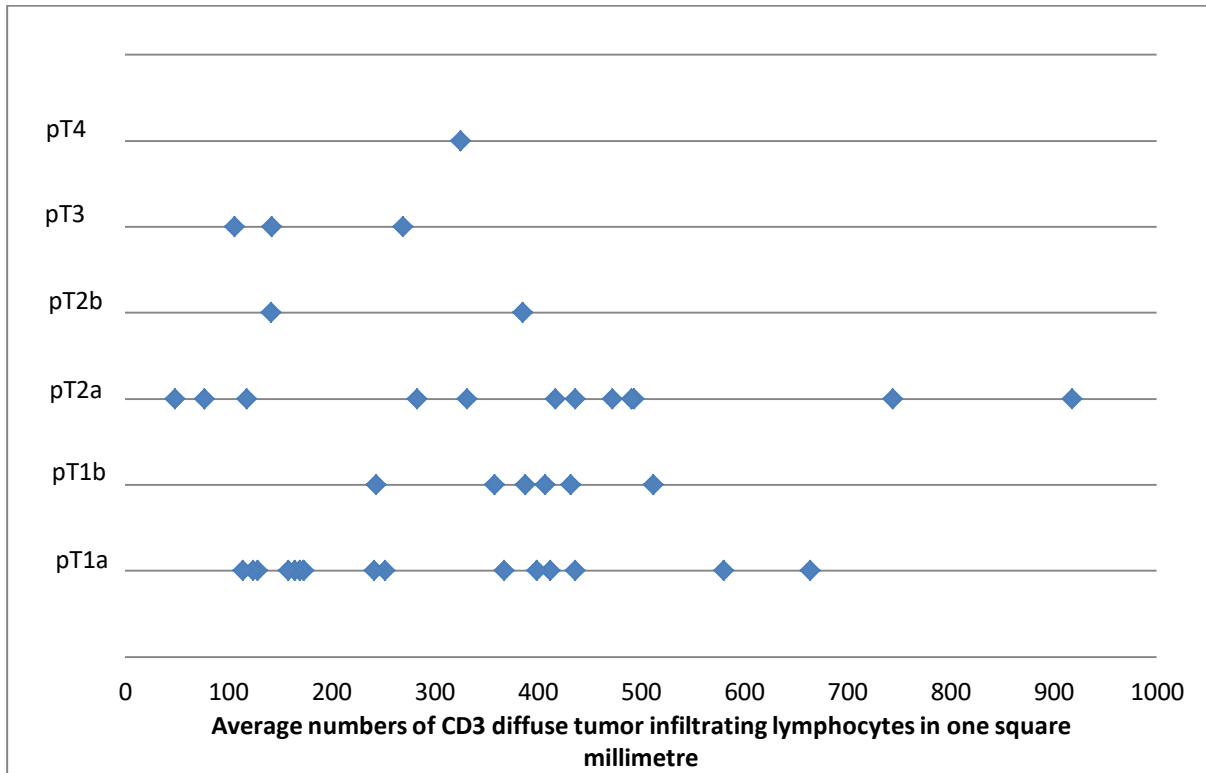
As seen above, there is no correlation between the T-grading of carcinomas and the average number of CD3 diffuse tumour-infiltrating lymphocytes. The correlation coefficient (r) is 0.007 showing that there is no linear relation.

In this last graph, the average number of CD3 diffuse tumour-infiltrating lymphocytes in one square millimetre is shown on the X-axis and the age of the patients is located on the Y-axis. Each blue point represents a patient.
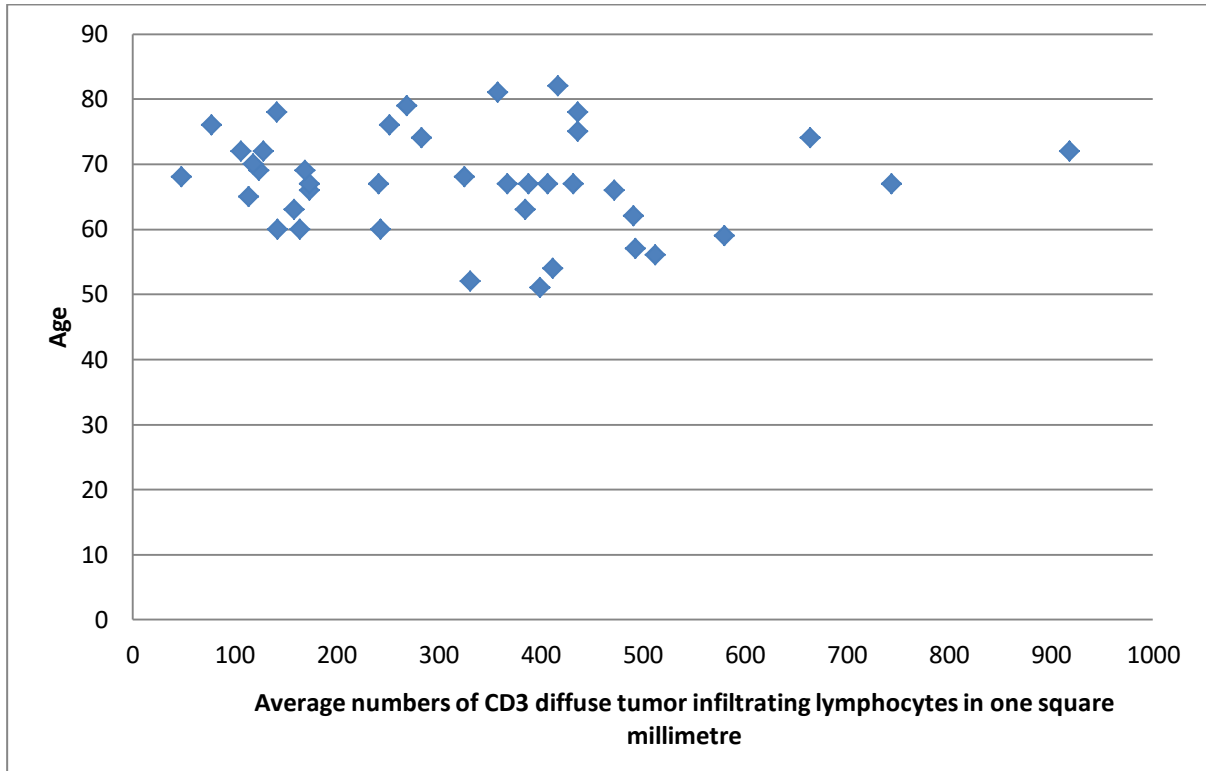
As seen above, there is no correlation between patient age and the average number of CD3 diffuse tumour-infiltrating lymphocytes in one square millimetre. The correlation coefficient (r) is -0.093 showing that there is no linear relation.

<u>CD3 lymphocytes in herds</u>

The number of CD3 tumour infiltrating lymphocytes counted in all herds from each of the 40 patients regardless of type of cancer is shown on the next box plot.
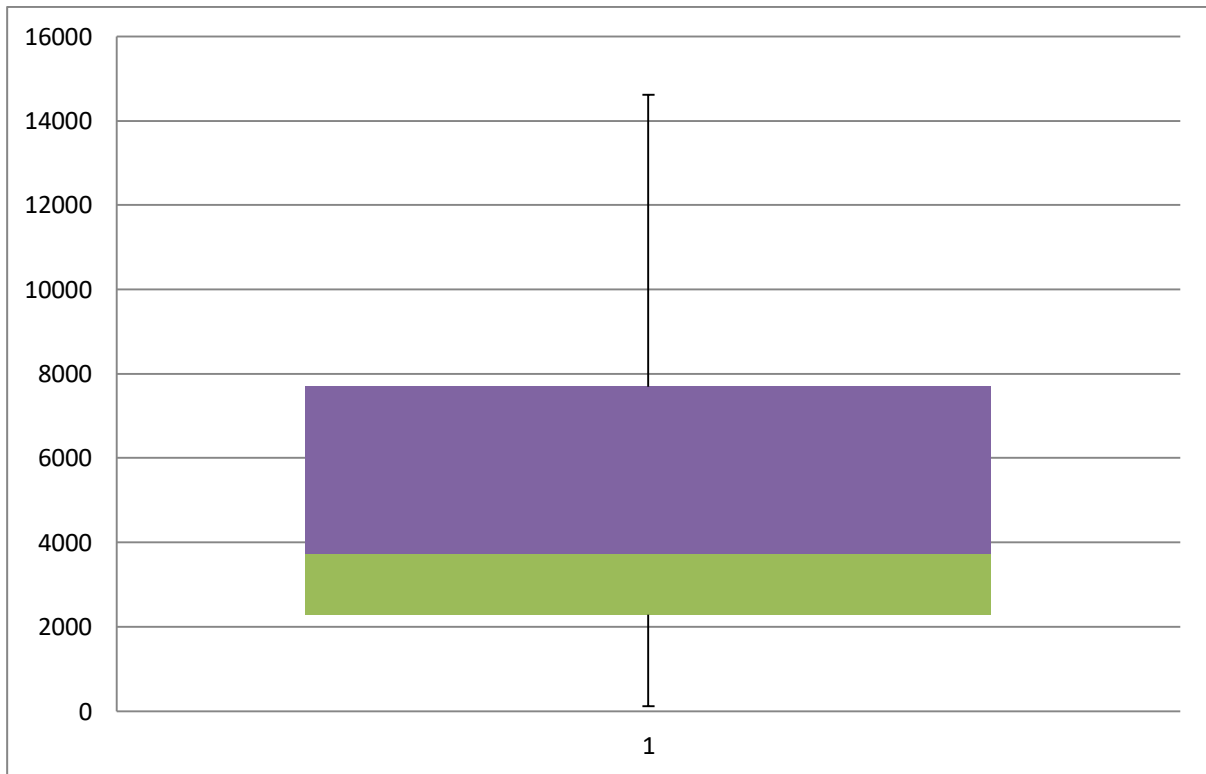
The minimum number of CD3 tumour infiltrating lymphocytes was 124, the maximum 14,622. The middle value was 3,741 lymphocytes.

In the following graph, the numbers of CD3 tumour-infiltrating lymphocytes counted from all herds from each patient are located on the X-axis, and the differentiation grade of the carcinomas (adenocarcinomas and squamous lung carcinomas together) on the Y-axis. Each blue point represents a patient.
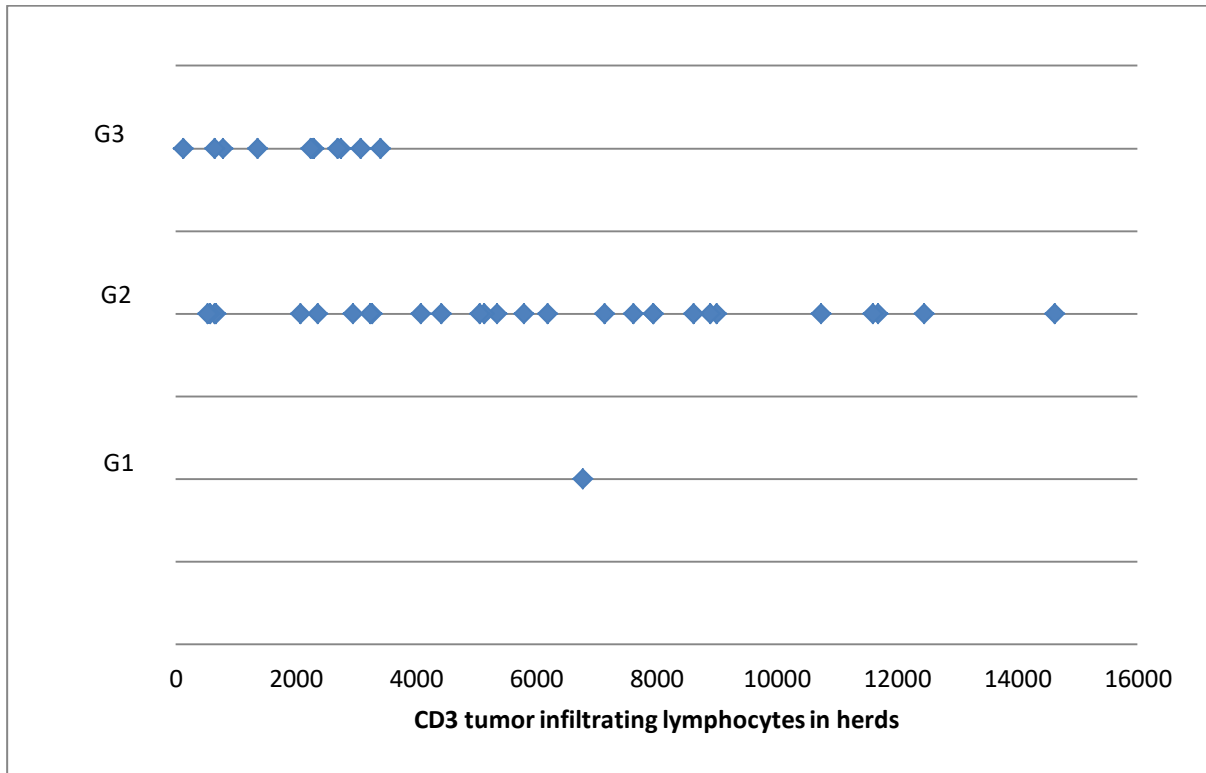
The graph shows that poorly differentiated carcinomas (G3) tend to have less CD3 lymphocytes in herds than G2 carcinomas. This result is statistically significant (p=0. 0012).

The next box plot shows the difference of CD3 lymphocytes counted from all herds from each patient between G2 and G3 lung carcinomas (adenocarcinomas and squamous lung carcinomas together).
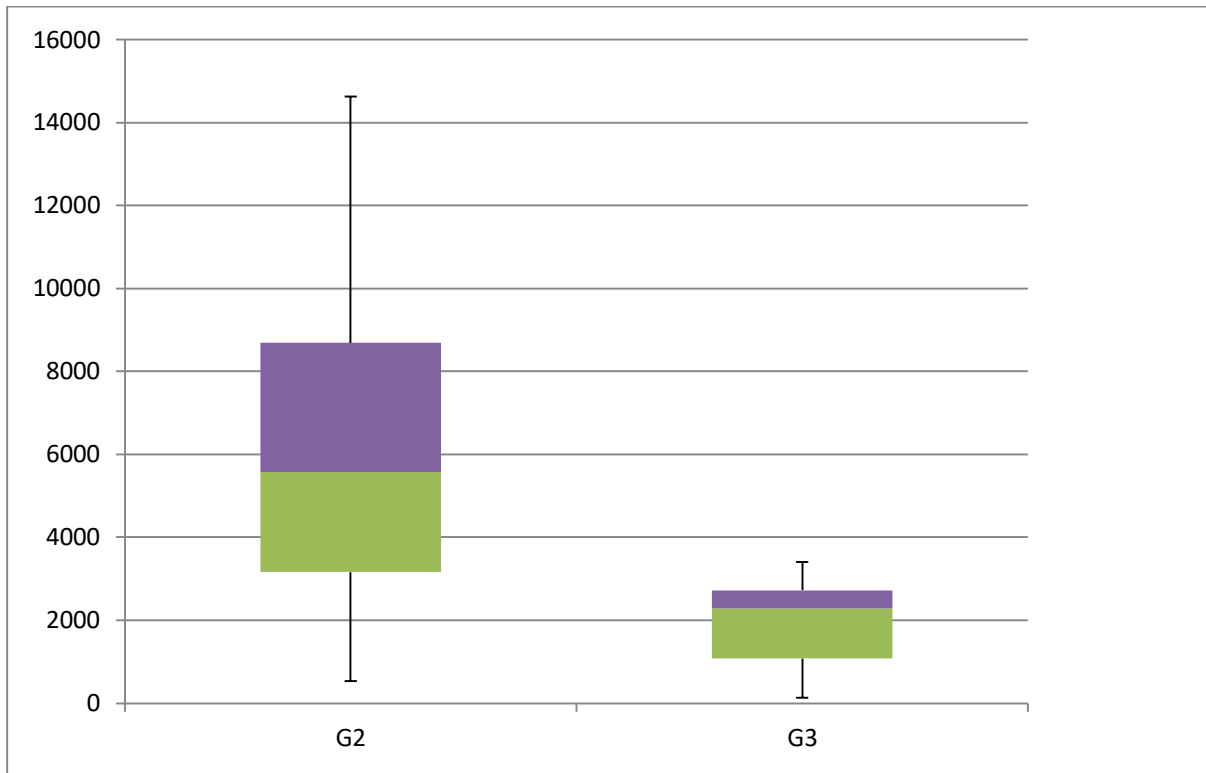
The G2 lung cancers show a minimum number of CD3 lymphocytes (in herds) of 532 and a maximum number of 14,622. On the other side, the G3 lung cancers show a minimum number of CD3 lymphocytes of 124 and a maximum of 3,402. In comparison, it can be seen in this box plot that the range of lymphocytes of G3 lung cancers almost coincides with the first quartile of the G2 lung cancers.

The following box plot shows a further analysis of CD3 lymphocytes counted in all herds from each patient between G2 and G3 lung carcinomas, separating them in two categories, squamous lung carcinomas and lung adenocarcinomas.
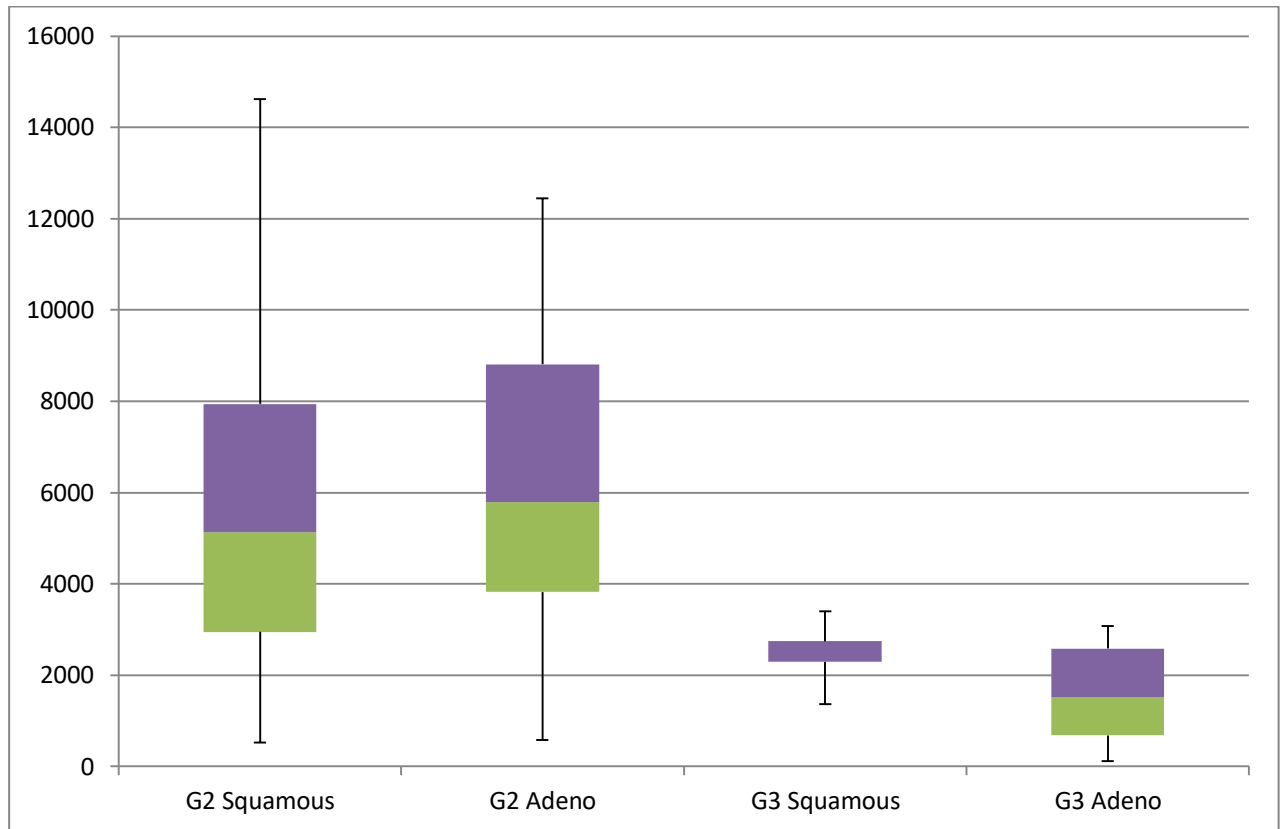
The patients with G2 squamous lung cancers have the most of CD3 lymphocytes in herds, showing a range between 531 and 14,622 lymphocytes. On the contrary, the patients with G3 lung adenocarcinomas have the least CD3 lymphocytes in herds, with a range between 124 and 3,072 lymphocytes.

On the following graph, the CD3 tumour-infiltrating lymphocytes counted in all herds from each patient are located on the X-axis, and the T-grading of the lung cancers on the Y-axis. Each blue point represents a patient.
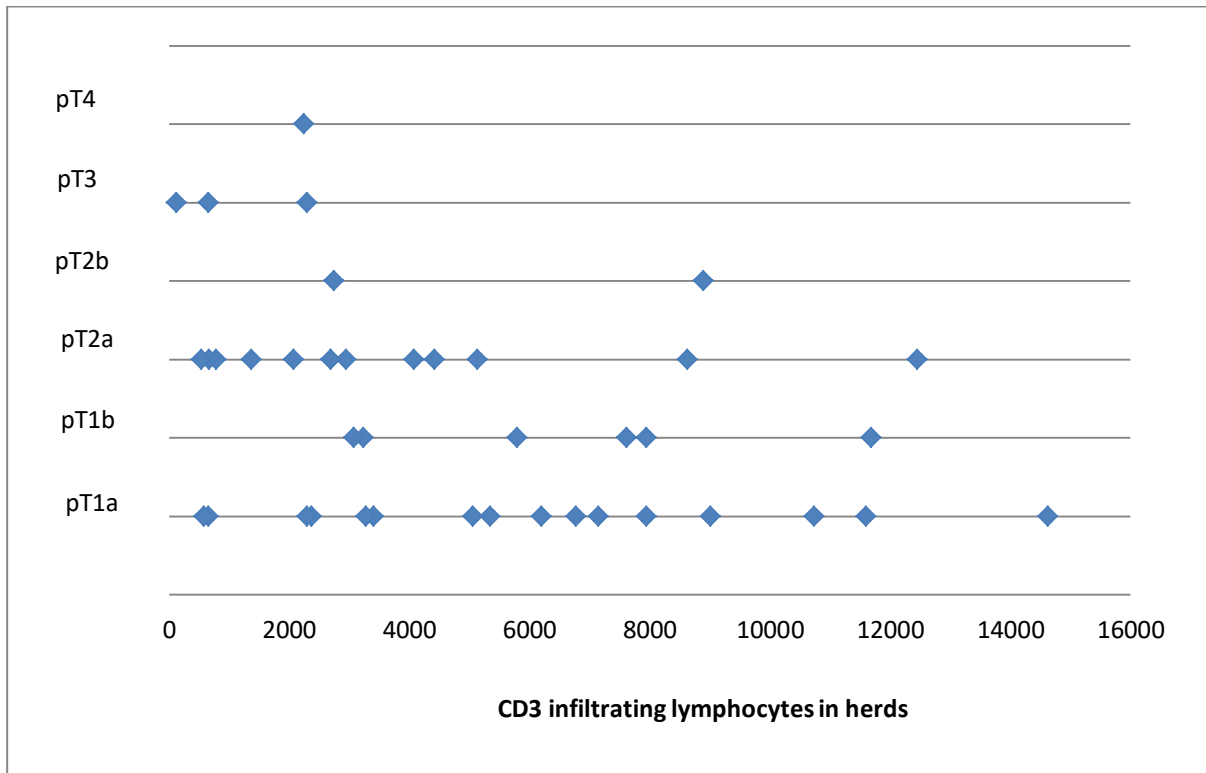
As seen above, there is no correlation between the T-grading of carcinomas and the CD3 infiltrating lymphocytes in herds. The correlation coefficient (r) is -0.36238 showing that there is no linear relation.

On the last graph, the CD3 infiltrating lymphocytes counted from all herds from each patient are located on X-axis and the age of the patients on the Y-axis. Each blue point represents a patient.
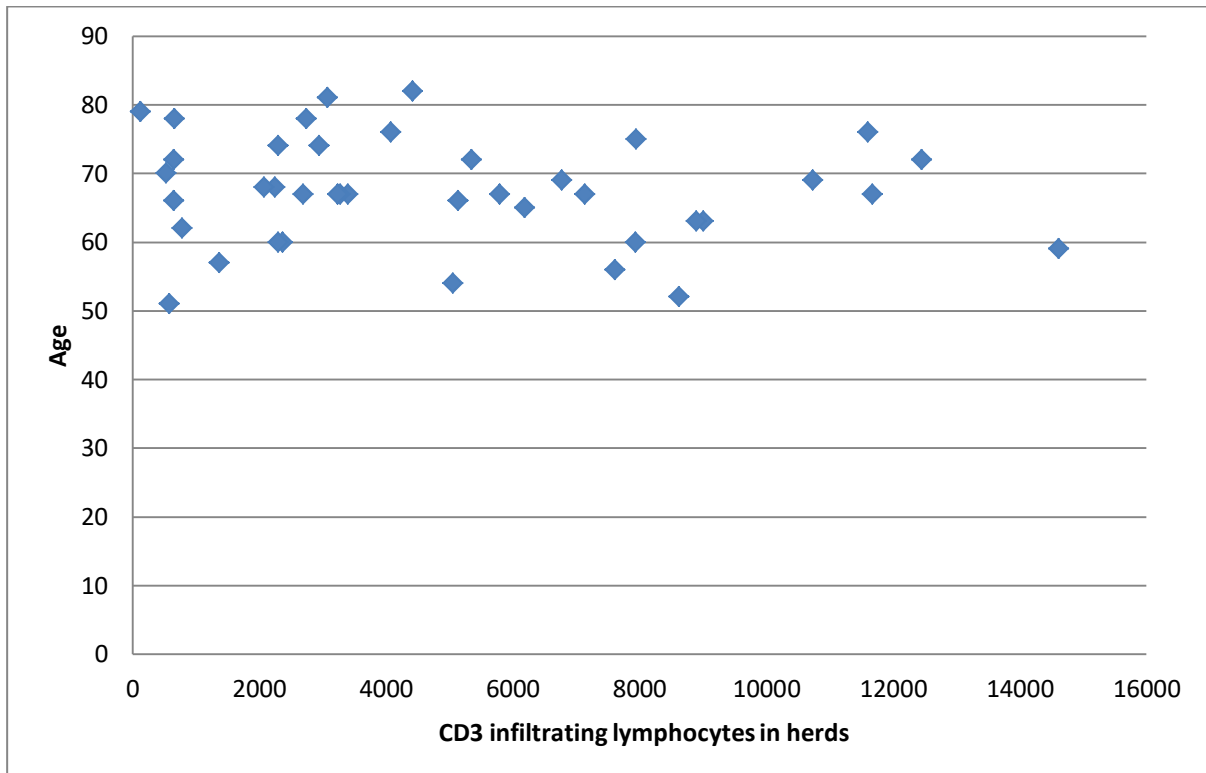
As seen above, there is no correlation between patient age and the CD3 infiltrating lymphocytes in herds. The correlation coefficient (r) is -0.136260224 showing that there is no linear relation.

CD4 diffuse infiltrating lymphocytes:

The next box plot shows the average number of diffuse tumour-infiltrating CD4 lymphocytes in one square millimetre from each of the 40 patients, regardless of type of cancer.
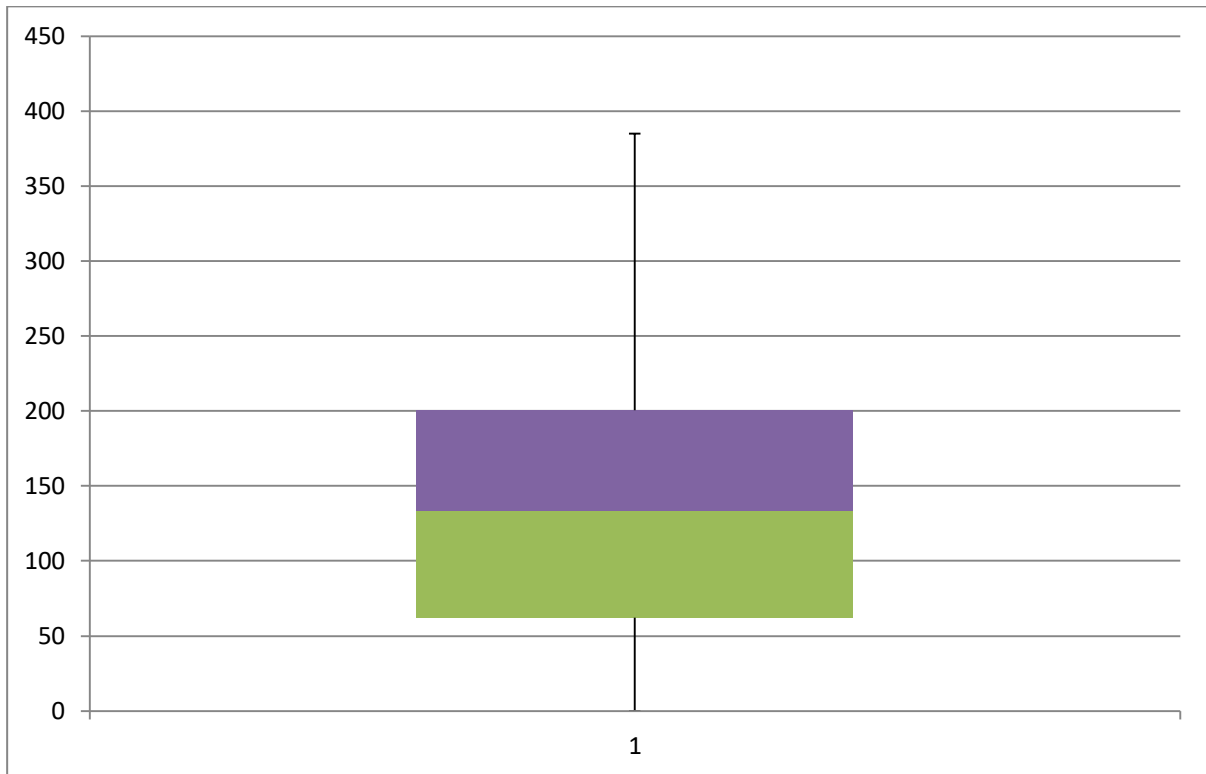

The minimum average number of CD4 tumour-infiltrating lymphocytes in one square millimetre was 0 and the maximum 385. The middle value was 133 lymphocytes.

On the following graph, the average numbers of CD4 diffuse tumour-infiltrating lymphocytes in one square millimetre are located on the X-axis, and the differentiation grade of the carcinomas (adenocarcinomas and squamous lung carcinomas together) on the Y-axis. Each blue point represents a patient.


Average number of CD4 diffuse infiltrating lymphocytes in one square millimetre
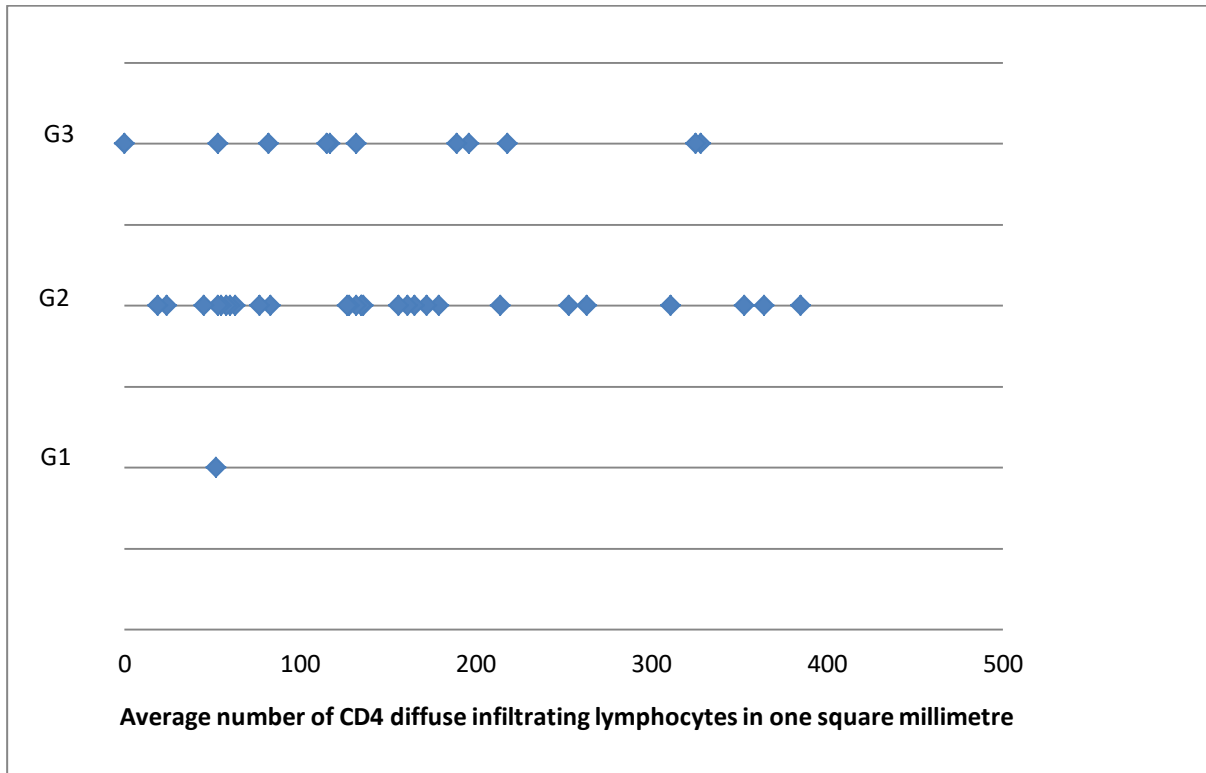
As seen above, there is no correlation between the differentiation grade of the carcinomas and the average number of CD4 diffuse tumour-infiltrating lymphocytes in one square millimetre.

On the following graph, the average numbers of CD4 diffuse tumour-infiltrating lymphocytes in one square millimetre are shown on the X-axis and the T-grading of lung cancers on the Y-axis. Each blue point represents a patient.
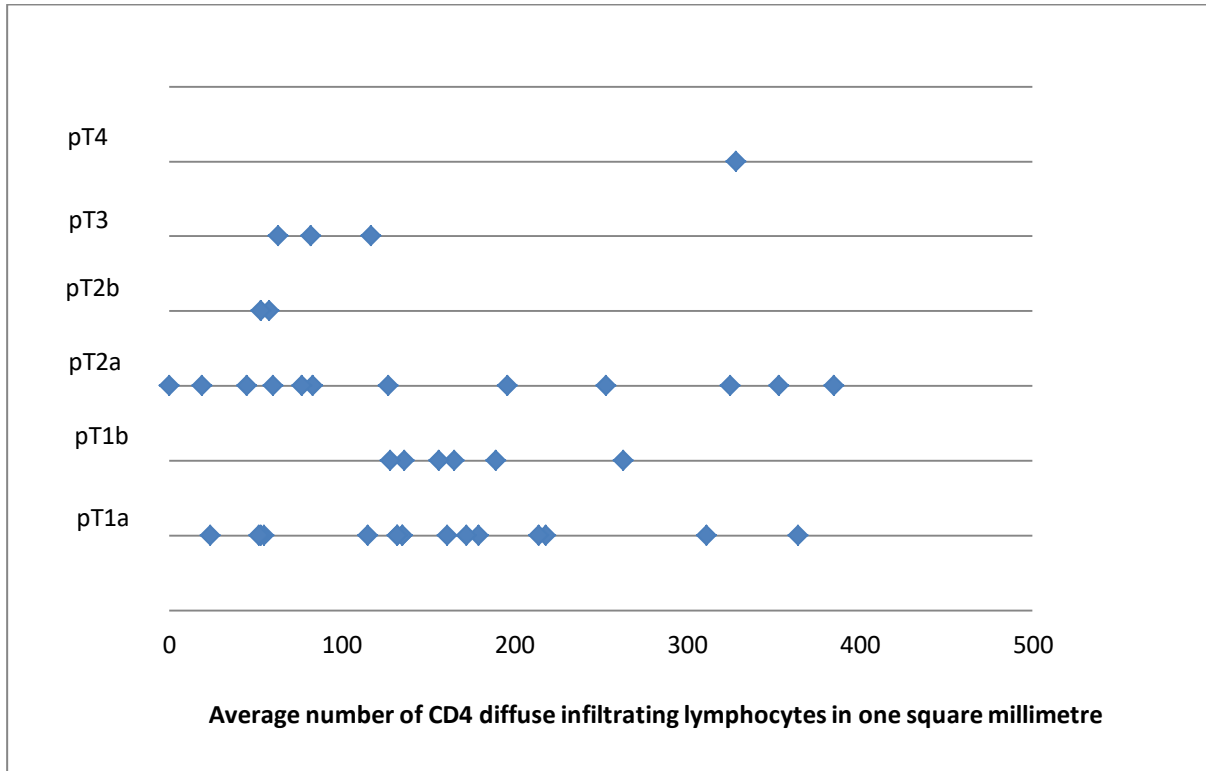
As seen above, there is no correlation between the T-grading of carcinomas and the average number of CD4 diffuse tumour-infiltrating lymphocytes in one square millimetre. The correlation coefficient (r) is -0.035 showing that there is no linear relation.

On the last graph, the average numbers of CD4 diffuse tumour-infiltrating lymphocytes in one square millimetre are located on the X-axis and the age of the patients on the Y-axis. Every blue point represents a patient.
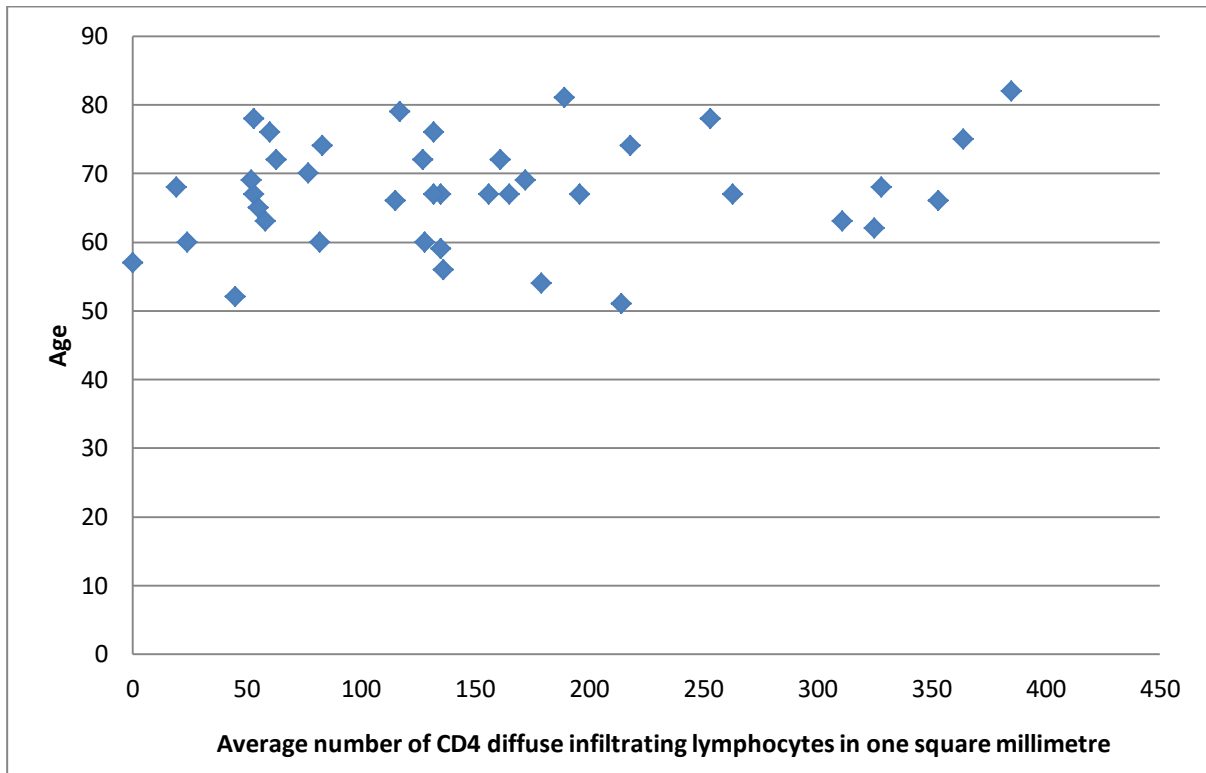
As seen above, there is no correlation between patient age and the average number of CD4 diffuse tumour-infiltrating lymphocytes in one square millimetre. The correlation coefficient (r) is 0.19 showing that there is no linear relation.

<u>CD4 lymphocytes in herds</u>

The next box plot shows the number of CD4 tumour-infiltrating lymphocytes counted in all herds from each of the 40 patients, regardless of type of cancer.
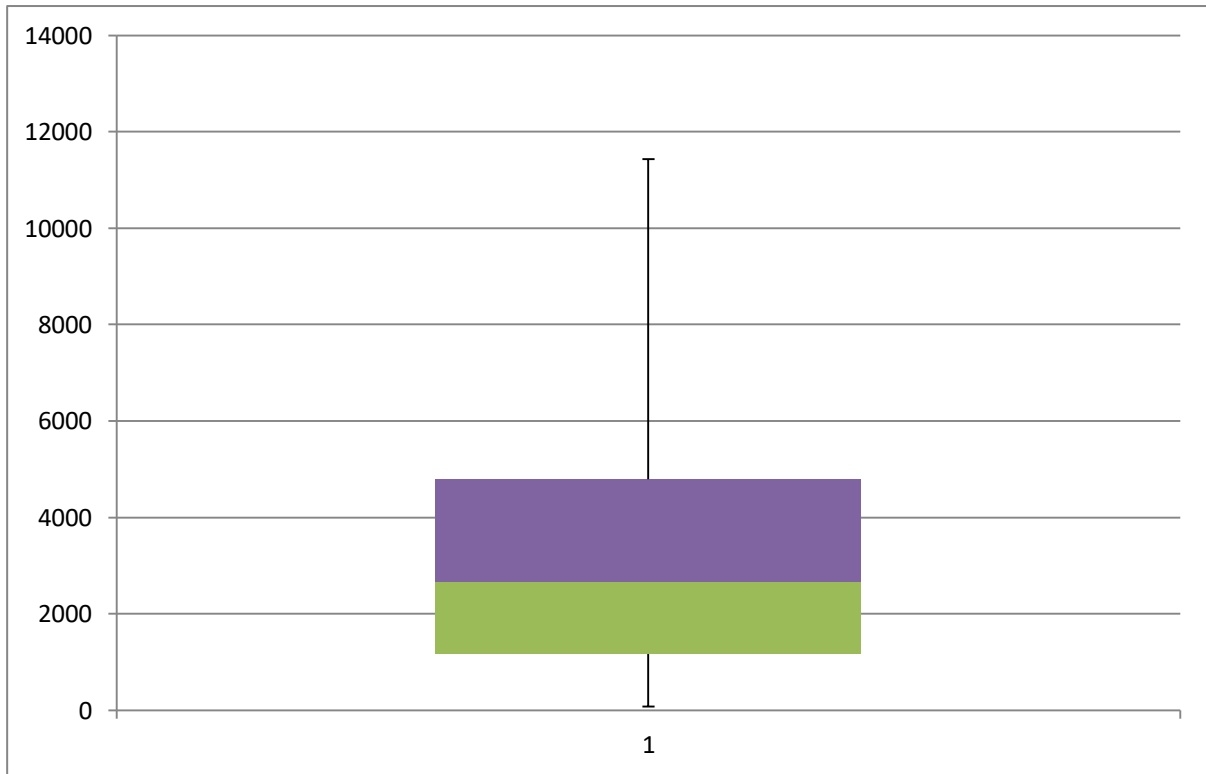

The minimum number of CD4 tumour-infiltrating lymphocytes was 71 and the maximum 11,432. The middle value was 2,657 lymphocytes.

On the following graph, the CD4 tumour-infiltrating lymphocytes counted from all herds from each patient are located on the X-axis, and the differentiation grade of the carcinomas (adenocarcinomas and squamous lung carcinomas together) on the Y-axis. Each blue point represents a patient.
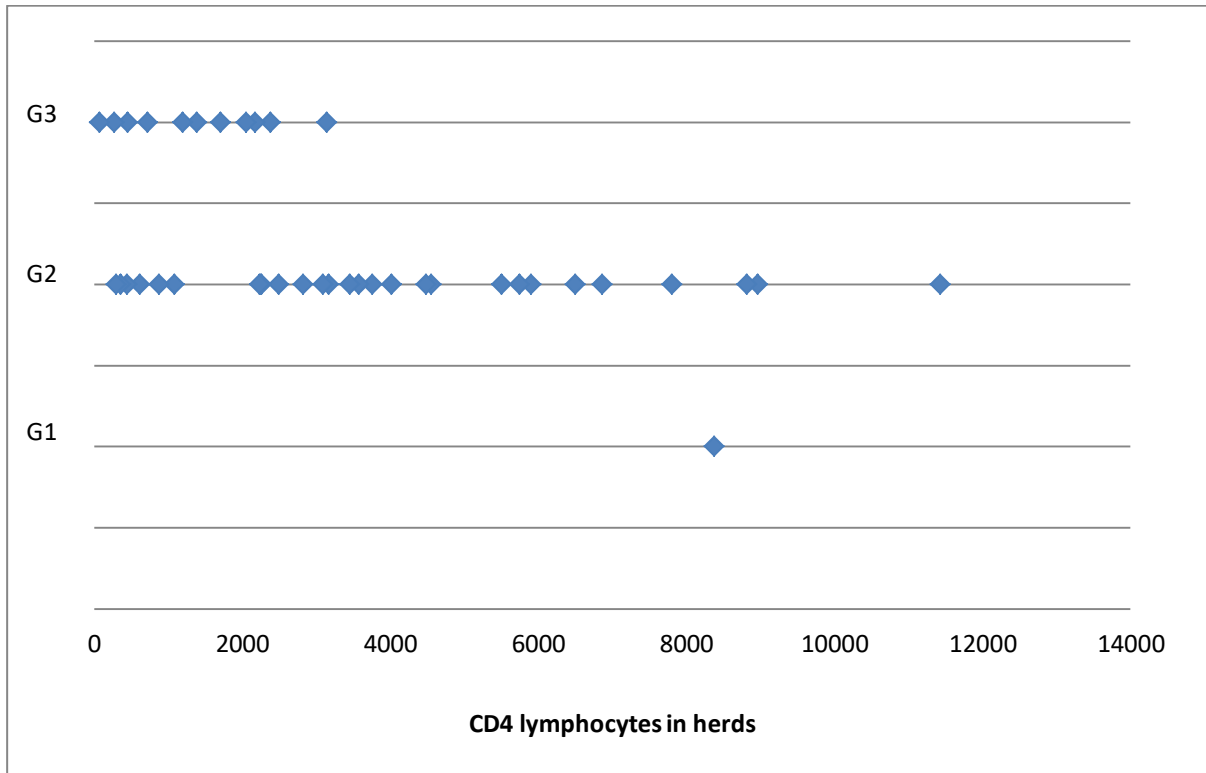

The graph shows that poorly differentiated carcinomas (G3) tend to have less CD4 lymphocytes in herds than G2 carcinomas. This result is statistically significant (p=0.0020).

The next box plot shows the difference of CD4 lymphocytes counted in all herds from each patient between G2 and G3 lung carcinomas (adenocarcinomas and squamous lung carcinomas together).
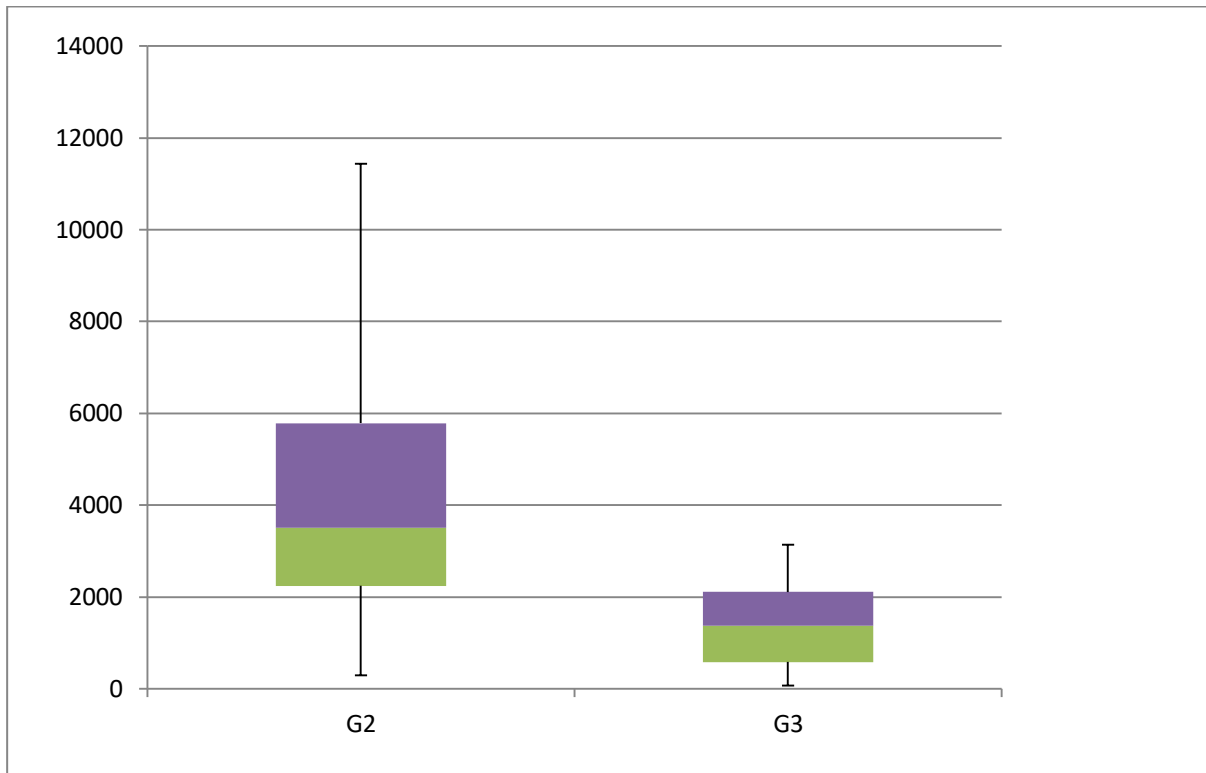

The G2 lung cancers show a minimum number of CD4 lymphocytes (in herds) of 292 and a maximum number of 11,432. On the other side, the G3 lung cancers show a minimum number of CD4 lymphocytes of 71 and a maximum of 3,144. It can be seen from this box plot comparison that the range of lymphocytes of G3 lung cancers almost coincides with the first and second quartile of the G2 lung cancers.

The following box plot shows a further analysis of CD4 lymphocytes counted in all herds from each patient between G2 and G3 lung carcinomas, separating them in two categories, squamous lung carcinomas and lung adenocarcinomas.
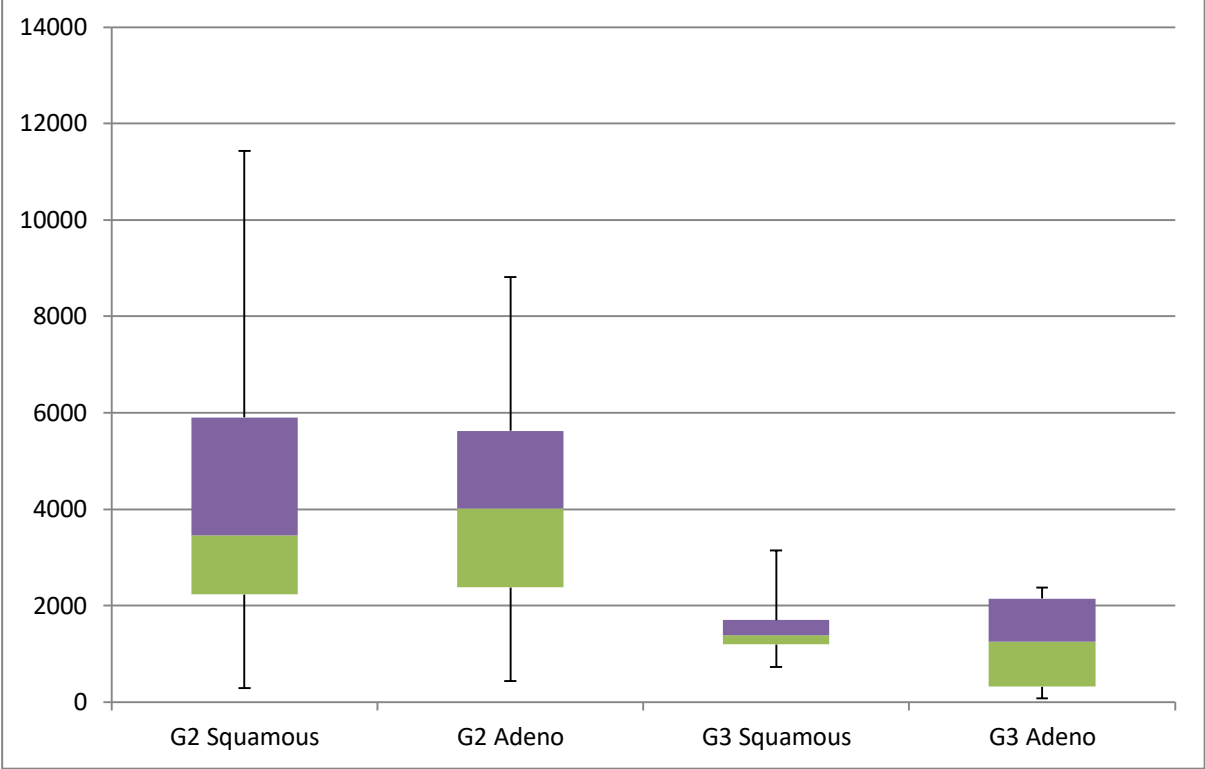

The patients with G2 squamous lung cancers have the most of CD4 lymphocytes in herds, showing a range between 292 to 11,432 lymphocytes. On the other side, the patients with G3 lung adenocarcinomas have the least CD4 lymphocytes in herds, with a range between 71 to 2,378 lymphocytes.

On the following graph, the CD4 tumour-infiltrating lymphocytes counted in all herds from each patient are located on the X-axis and the T-grading of the lung cancers on the Y-axis. Each blue point represents a patient.
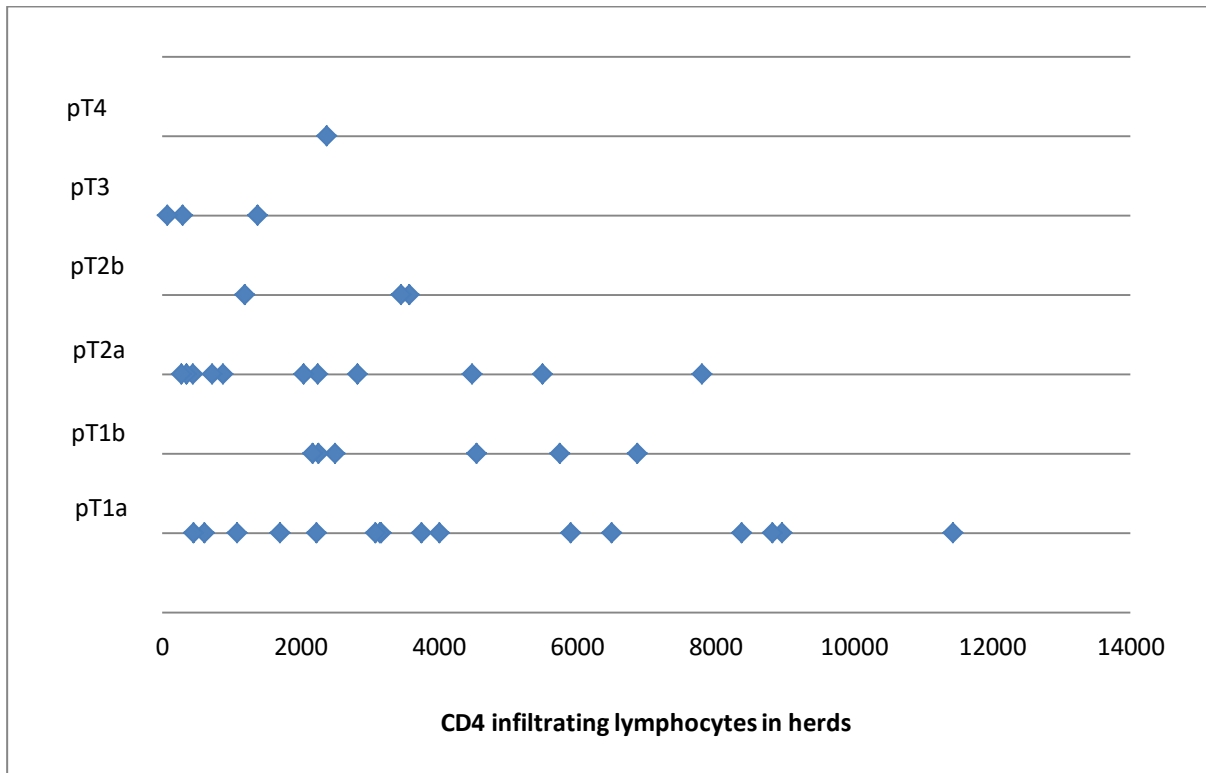
As seen above, there is no correlation between the T grading of carcinomas and the CD4 infiltrating lymphocytes in herds. The correlation coefficient (r) is -0.40085 showing that there is no linear relation.

On the last graph, the CD4 infiltrating lymphocytes counted in all herds from each patient are located on the X-axis and the age of the patients on the Y-axis. Each blue point on the graph represents a patient.
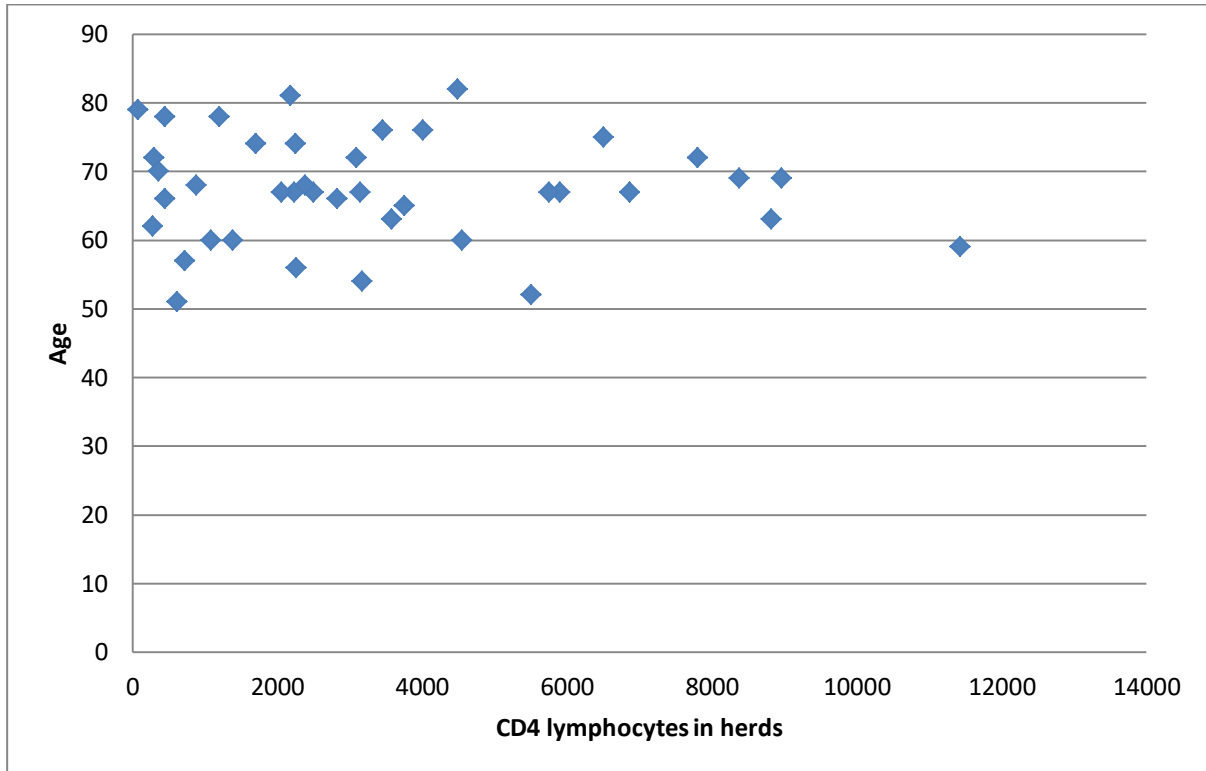
As seen above, there is no correlation between patient age and the CD4 infiltrating lymphocytes in herds. The correlation coefficient (r) is -0.07459 showing that there is no linear relation.

CD8 diffuse infiltrating lymphocytes:

The next box plot shows the average number of diffuse tumour-infiltrating CD8 lymphocytes in one square millimetre from all 40 patients, regardless of type of cancer.
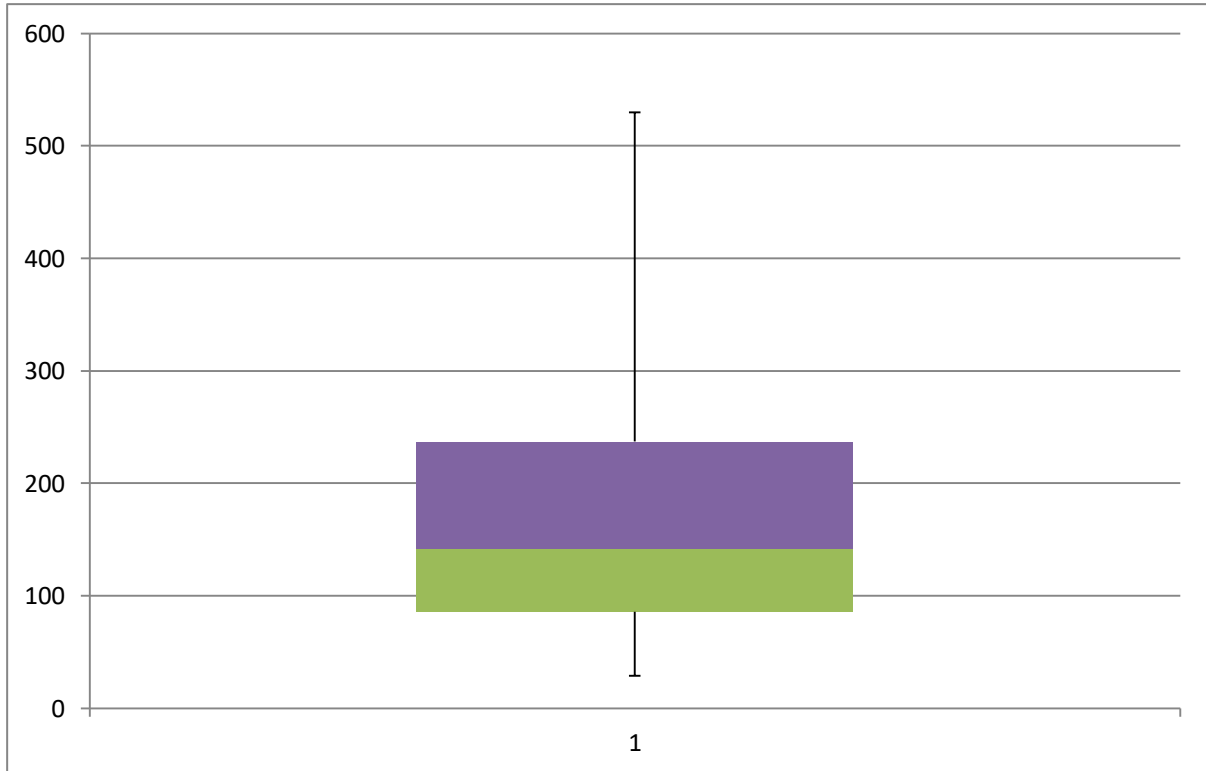

The minimum average number of CD8 tumour-infiltrating lymphocytes in one square millimetre was 29 and the maximum 530. The middle value was 142 lymphocytes.

On the following graph, the average numbers of CD8 diffuse tumour-infiltrating lymphocytes in one square millimetre are located on the X-axis and the differentiation grade of the carcinomas (adenocarcinomas and squamous lung carcinomas together) on the Y-axis. Each blue point on the graph represents a patient.

Average number of CD8 Diffuse infiltrating lymphocytes in one square millimetre

As seen above, there is no correlation between the differentiation grade of the carcinomas and the average number of CD8 diffuse tumour-infiltrating lymphocytes in one square millimetre.

On the following graph, the average numbers of CD8 diffuse tumour-infiltrating-lymphocytes in one square millimetre are located on the X-axis and the T-grading of the lung cancers on the Y-axis. Each blue point on the graph represents a patient.

Average number of CD8 Diffuse infiltrating lymphocytes in one square millimetre

As seen above, there is no correlation between the T-grading of carcinomas and the average number of CD8 diffuse tumour-infiltrating lymphocytes in one square millimetre. The correlation coefficient (r) is -0.035 showing that there is no linear relation.

On the last graph the average numbers of CD8 diffuse tumour-infiltrating lymphocytes in one square millimetre are located on the X-axis, and the age of the patients on the Y-axis. Each blue point on the graph represents a patient.

As seen above, there is no correlation between patient age and the average numbers of CD8 diffuse tumour-infiltrating lymphocytes in one square millimetre. The correlation coefficient (r) is -0.00191 showing that there is no linear relation.

CD8 lymphocytes in herds:

The next box plot shows the numbers of CD8 tumour-infiltrating lymphocytes counted in all herds from each of the 40 patients, regardless of type of cancer.
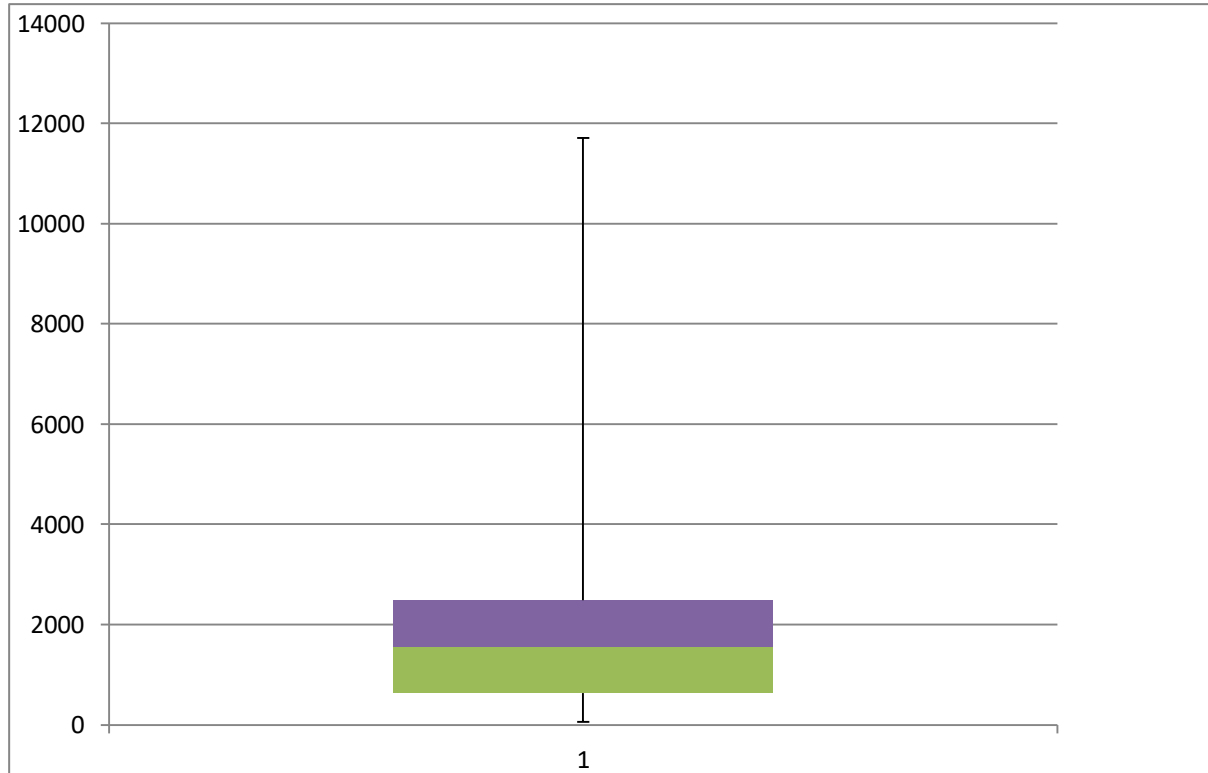

The minimum number of CD8 tumour-infiltrating lymphocytes was 57 and the maximum 11,709. The middle value was 1,555 lymphocytes.

On the following graph, the CD8 tumour-infiltrating lymphocytes counted in all herds from each patient are located on the X-axis and the differentiation grade of the carcinomas (adenocarcinomas and squamous lung carcinomas together) on the Y-axis. Each blue point on the graph represents a patient.
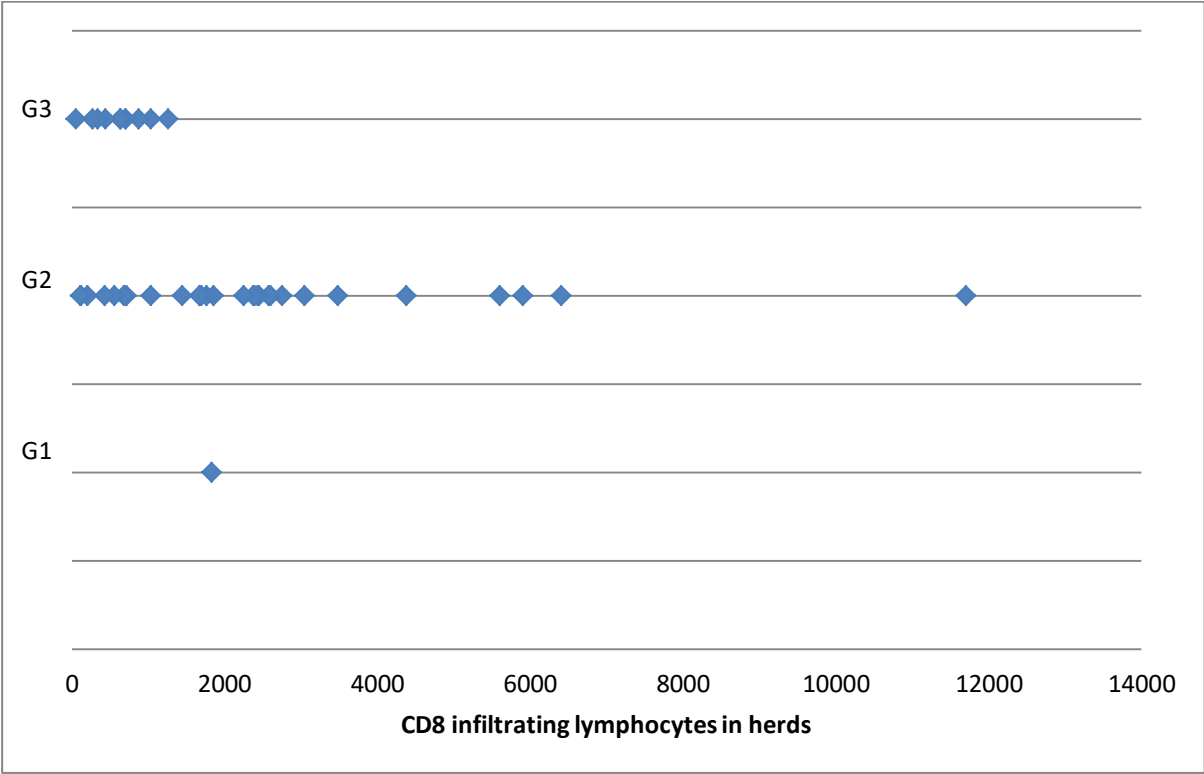

The graph shows that poorly differentiated carcinomas (G3) tend to have less CD8 Lymphocytes in herds than G2 carcinomas. This result is statistically significant (p=0. 0014).

The next box plot shows the difference of CD8 lymphocytes counted in all herds from each patient between G2 and G3 lung carcinomas.
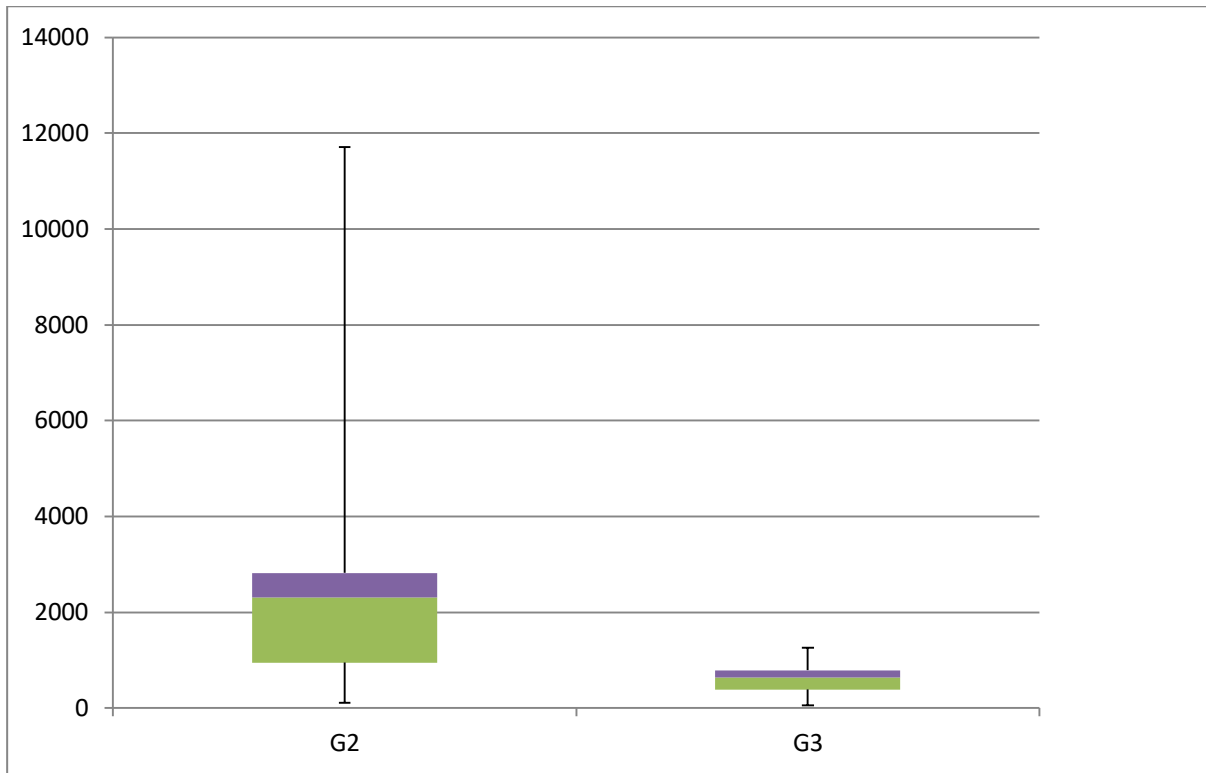

The G2 lung cancers show a minimum number of CD8 lymphocytes (in herds) of 108 and a maximum number of 11,709. On the other side, the G3 lung cancers show a minimum number of CD8 lymphocytes of 57 and a maximum of 1,262. As we see in this box plot comparison, the range of lymphocytes of G3 lung cancers almost coincides with the first and second quartile of the G2 lung cancers.

The following box plot shows a further analysis of CD8 lymphocytes counted in all herds from each patient between G2 and G3 lung carcinomas, separating them in two categories, squamous lung carcinomas and lung adenocarcinomas.
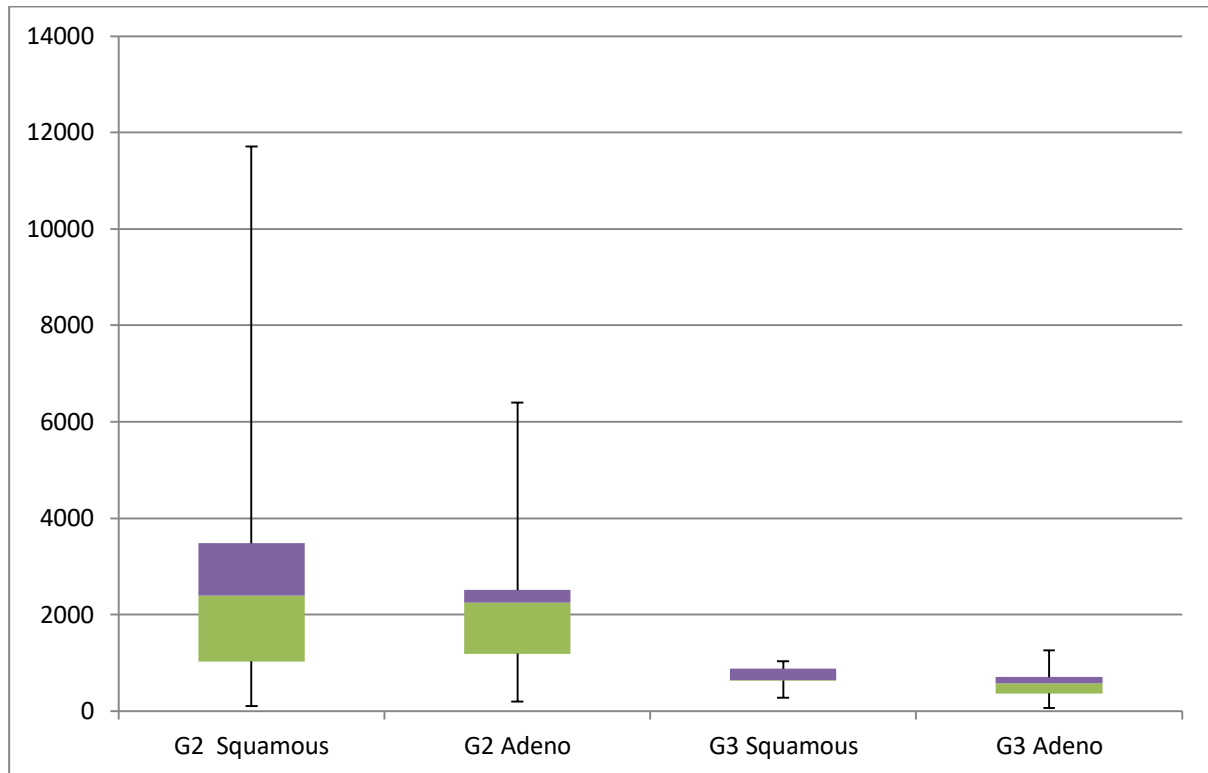

The patients with G2 squamous lung cancers have the most of CD8 lymphocytes in herds, showing a range between 108 and 11,709 lymphocytes. On the other side, the patients with G3 lung adenocarcinomas and G3 squamous lung cancers have the least CD8 lymphocytes in herds, with a range between 57 and 1,262 lymphocytes and between 269 and 1,032 lymphocytes.

On the following graph, the CD8 tumour infiltrating lymphocytes counted in all herds from each patient are located on the X-axis and the T-grading of the lung cancers on the Y-axis. Each blue point on the graph represents a patient.
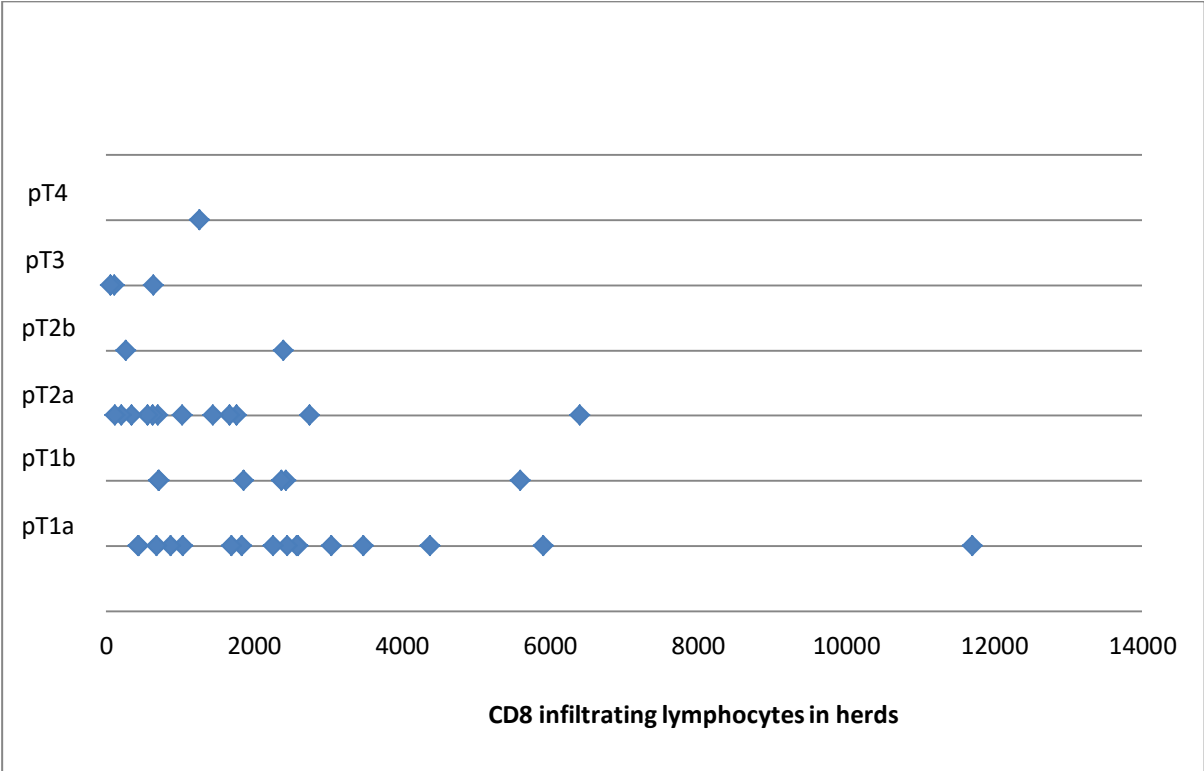
As seen above, there is no correlation between the T-grading of carcinomas and the CD8 infiltrating lymphocytes in herds. The correlation coefficient (r) is -0.34375 showing that there is no linear relation.

On the last graph, the CD8 infiltrating lymphocytes counted in all herds from each patient are located on the X-axis and the age of the patients on the Y-axis. Each blue point on the graph represents a patient.
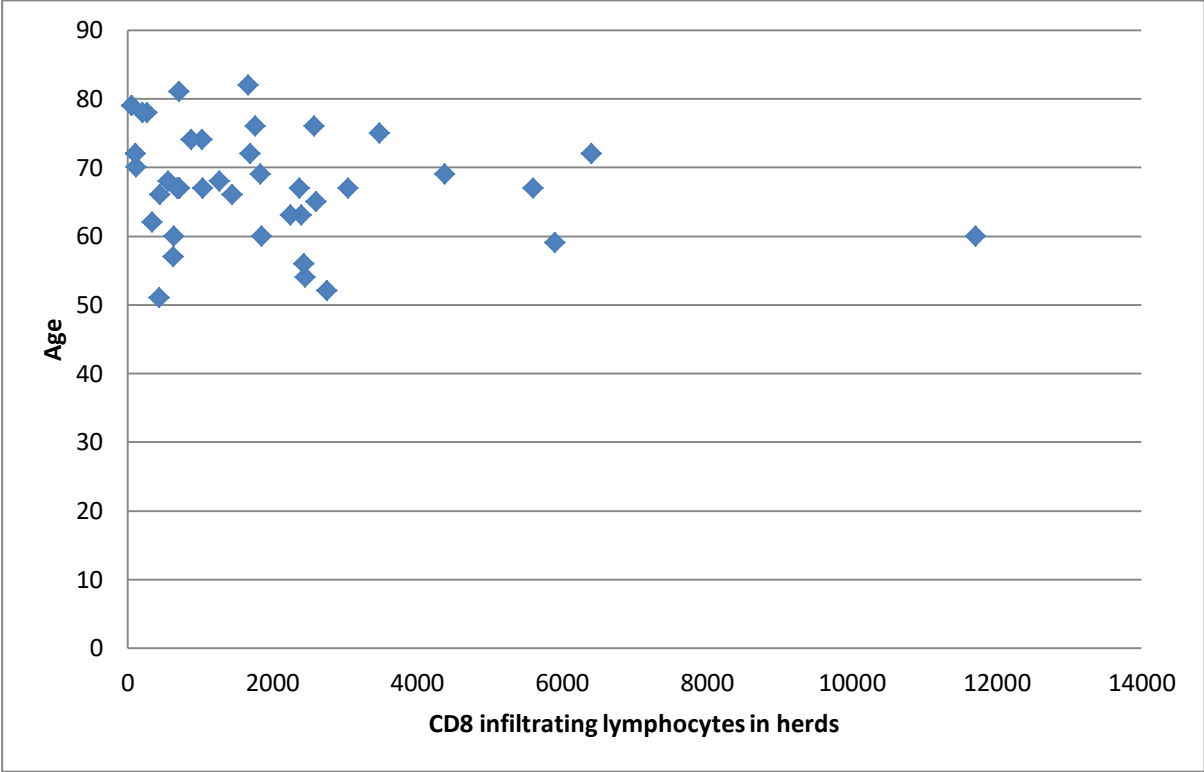
As seen above, there is no correlation between patient age and the CD8 infiltrating lymphocytes in herds. The correlation coefficient (r) is -0.21086 showing that there is no linear relation.

CD20 lymphocytes in herds:

The next box plot shows the number of CD20 tumour-infiltrating lymphocytes counted in all herds from each patient from all 40 patients, regardless of the type of cancer.
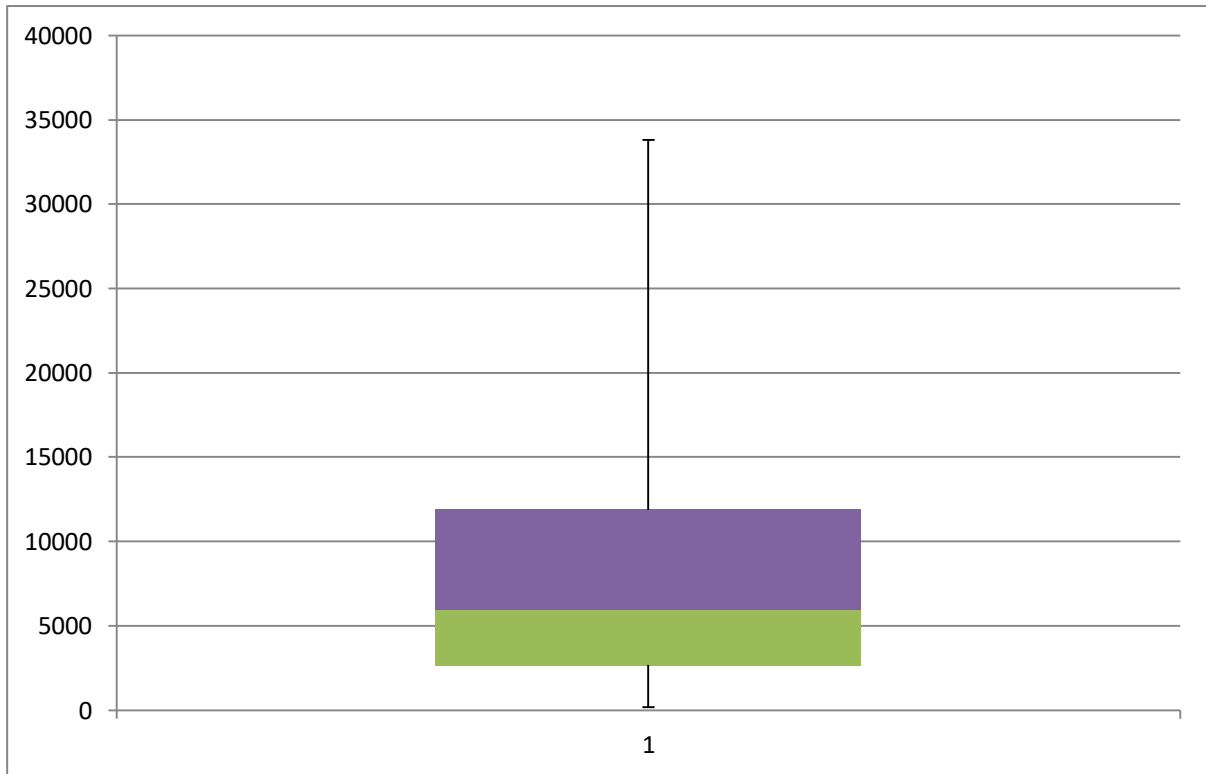
The minimum number of CD20 tumour-infiltrating lymphocytes was 164 and the maximum 33,795. The middle value was 5,942 lymphocytes.

On the following graph, the CD20 tumour-infiltrating lymphocytes counted in all herds from each patient are located on the X-axis and the differentiation grade of the carcinomas (adenocarcinomas and squamous lung carcinomas together) on the Y-axis. Each blue point on the graph represents a patient.
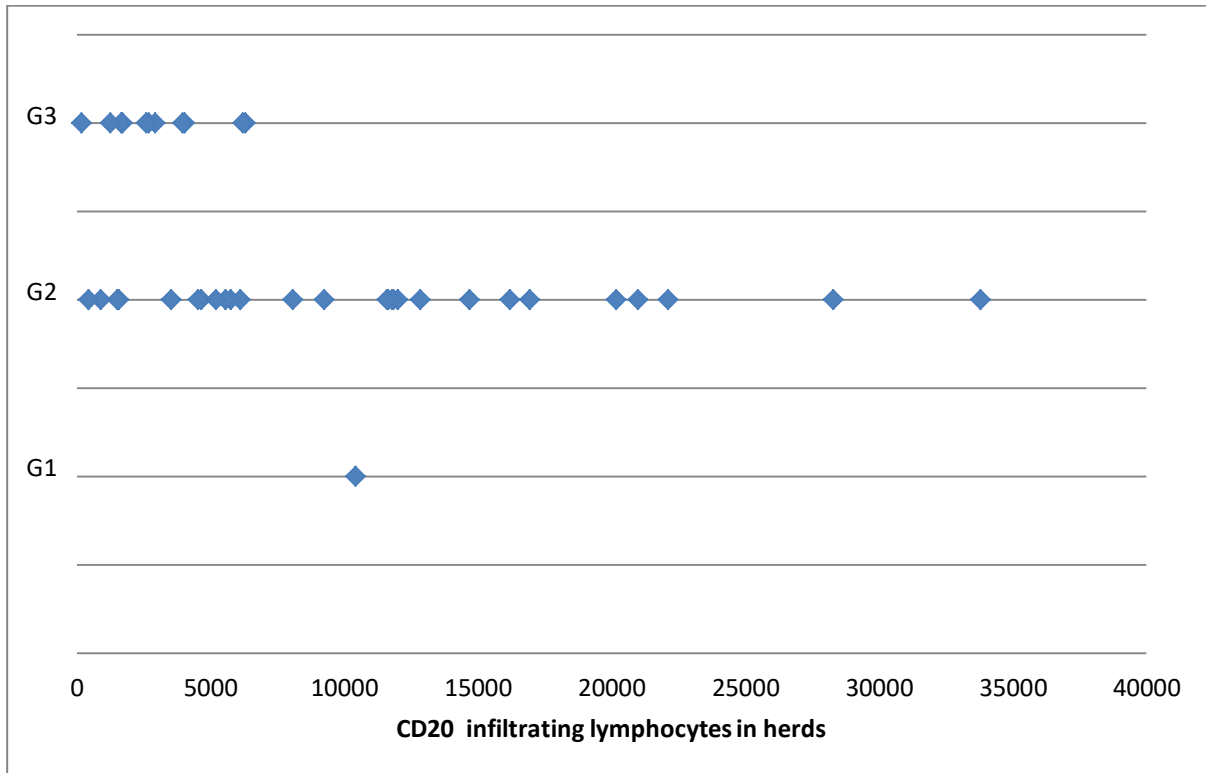
The graph shows that poorly differentiated carcinomas (G3) tend to have less CD20 lymphocytes in herds than G2 carcinomas. This result is statistically significant (p=0.0036).

The next box plot shows the difference of CD20 lymphocytes counted in all herds from each patient between G2 and G3 lung carcinomas (adenocarcinomas and squamous lung carcinomas together).
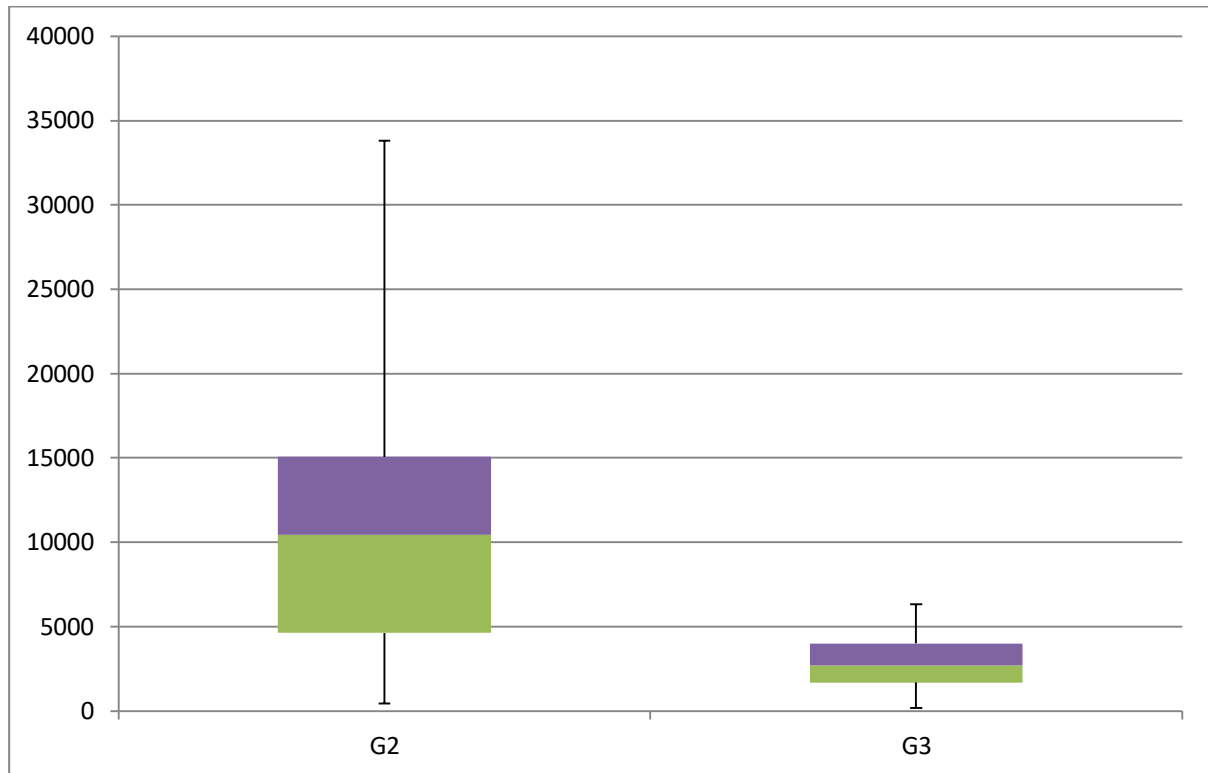
The G2 lung cancers show a minimum number of CD20 lymphocytes (in herds) of 429 and a maximum number of 33,795. On the other side, the G3 lung cancers show a minimum number of CD20 lymphocytes of 164 and a maximum of 6,318. It can be seen in this box plot comparison, that the range of lymphocytes of G3 lung cancers almost coincides with the first and second quartile of the G2 lung cancers.

The following box plot shows a further analysis of CD20 lymphocytes counted in all herds from each patient between G2 and G3 lung carcinomas, separating them in two categories, squamous lung carcinomas and lung adenocarcinomas.
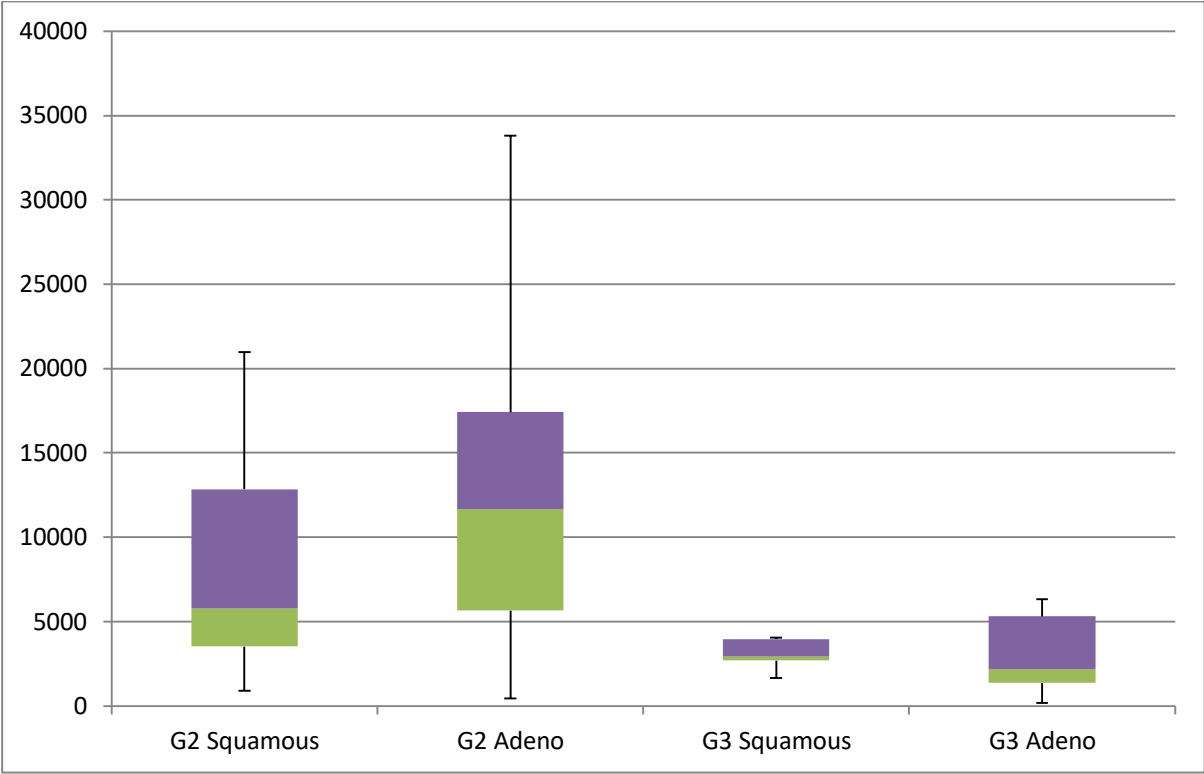
The patients with G2 lung adenocarcinoma have the most of CD20 lymphocytes in herds, showing a range between 429 and 33,795 lymphocytes. On the other side, the patients with G3 lung adenocarcinomas and G3 squamous lung cancers have the least CD20 lymphocytes in herds, with a range between 163 and 6,318 lymphocytes and between 1,668 and 4,038 lymphocytes.

On the following graph the CD20 tumour infiltrating lymphocytes counted in all herds from each patient are located on the X-axis, and the T-grading of the lung cancers on the Y-axis. Each blue point on the graph represents a patient.
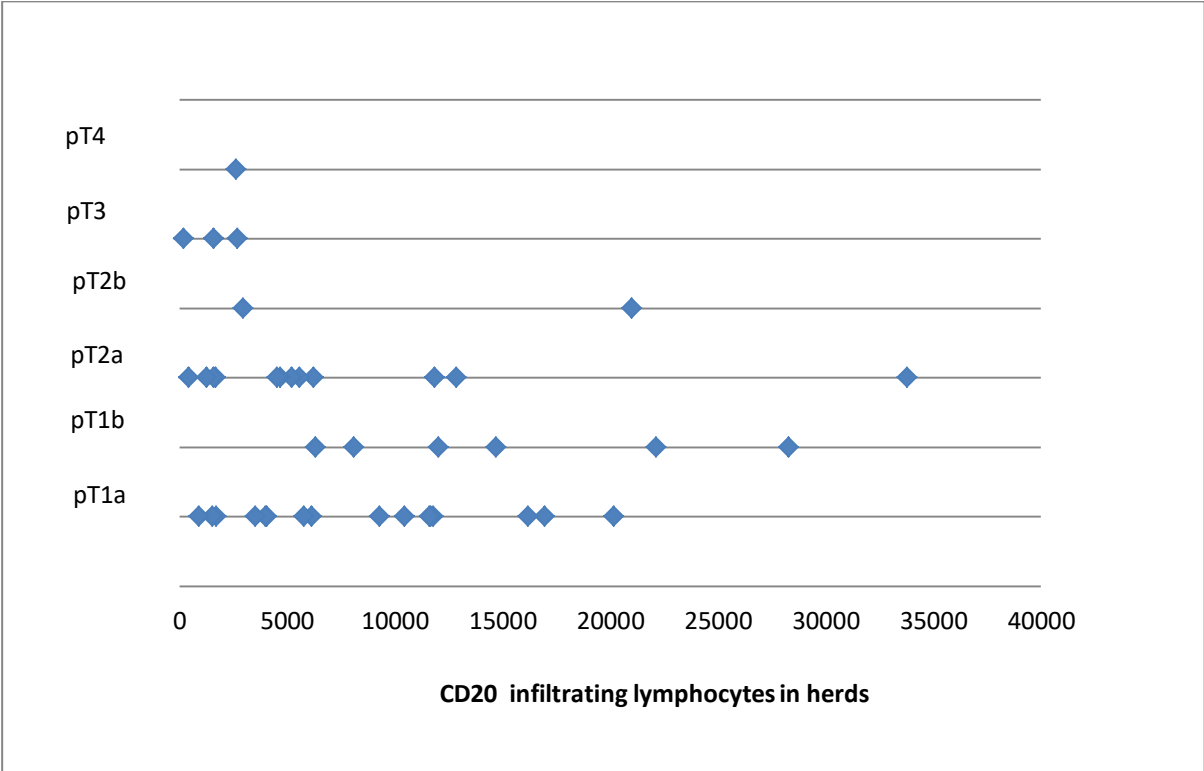
As seen above, there is no correlation between the T-grading of carcinomas and the CD20 infiltrating lymphocytes in herds. The correlation coefficient (r) is -0.20328 showing that there is no linear relation.

On the last graph, the CD20 infiltrating lymphocytes counted in all herds from each patient are located on the X-axis and the age of the Patients on the Y-axis. Each blue point on the graph represents a patient.
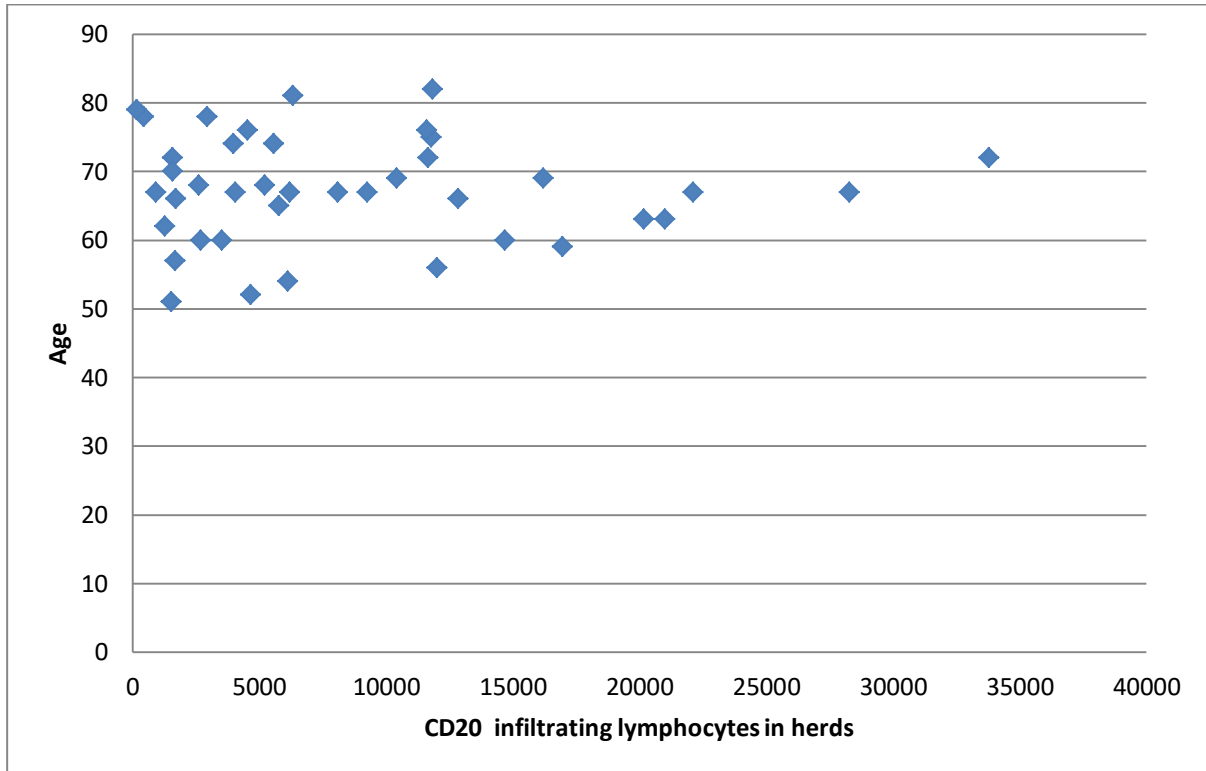
As seen above, there is no correlation between the patient age and the CD20 infiltrating lymphocytes in herds. The correlation coefficient (r) is -0.01176 showing that there is no linear relation.

PD1 and diffuse infiltrating lymphocytes:

On the following graph, the percentage of PD-1 positive diffuse infiltrating lymphocytes is located on the X-axis and the T-grading of the lung cancers on the Y-axis.
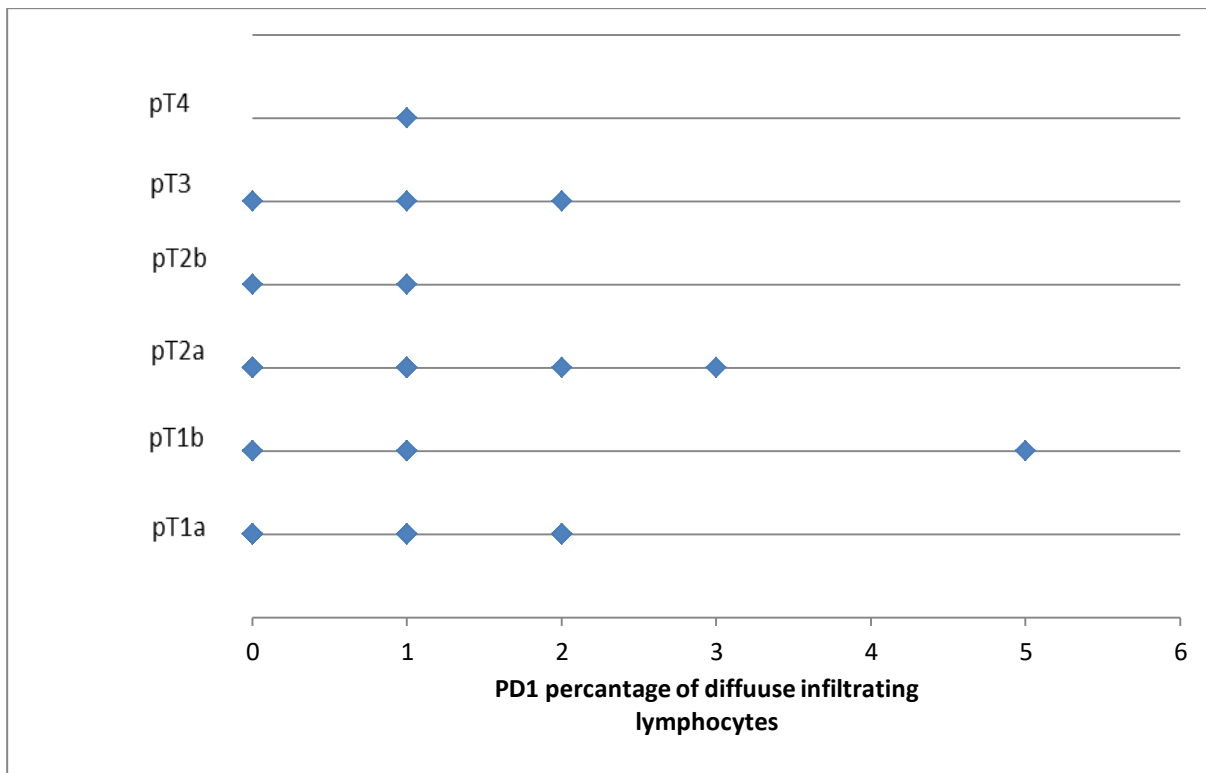
As seen above, there is no correlation between T-grading and the percentage of PD-1 positive lymphocytes in herds. The correlation coefficient (r) is -0.00625 showing that there is no linear relation.

The next box plot shows the PD-1 percentage of diffuse infiltrating lymphocytes from all 40 patients, regardless of the type of cancer.
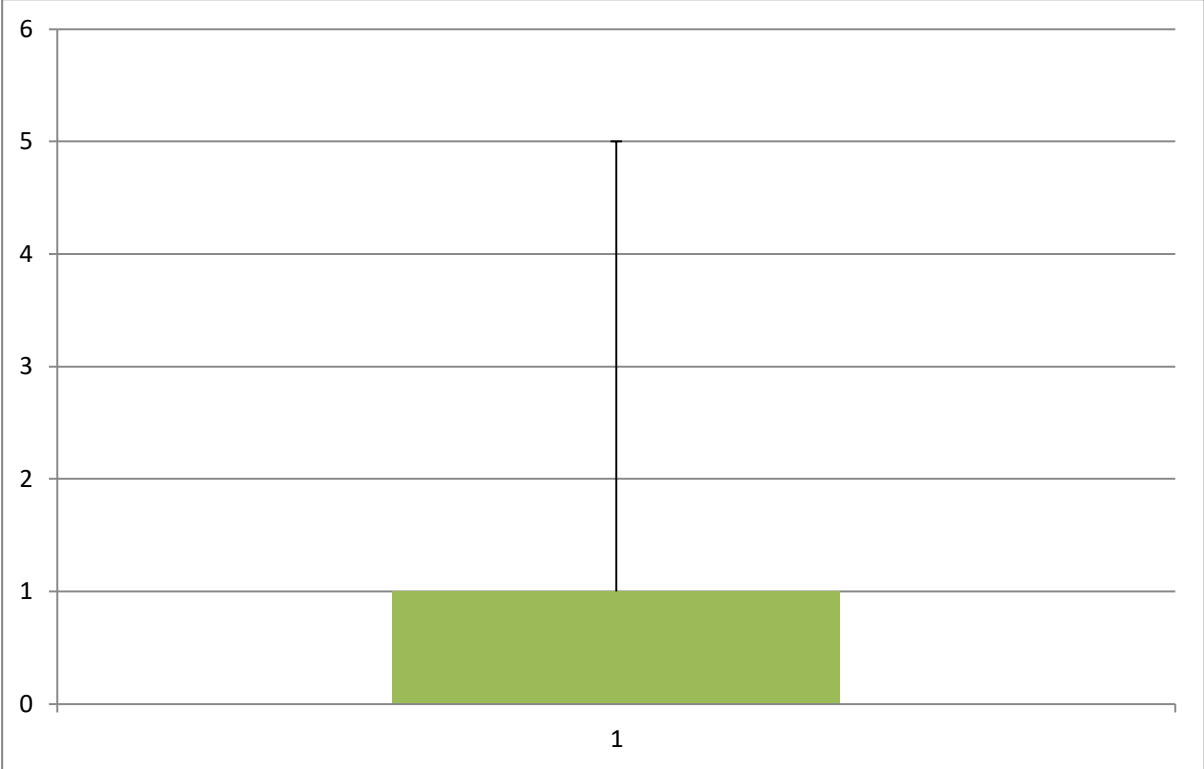
The minimum is 1% and the maximum 5%.

On the following graph, all the diffuse lymphocytes (CD3, CD4, and CD8) of every patient are located on the X-axis and the percentage of PD-1 positive diffuse lymphocytes on the Y-axis.
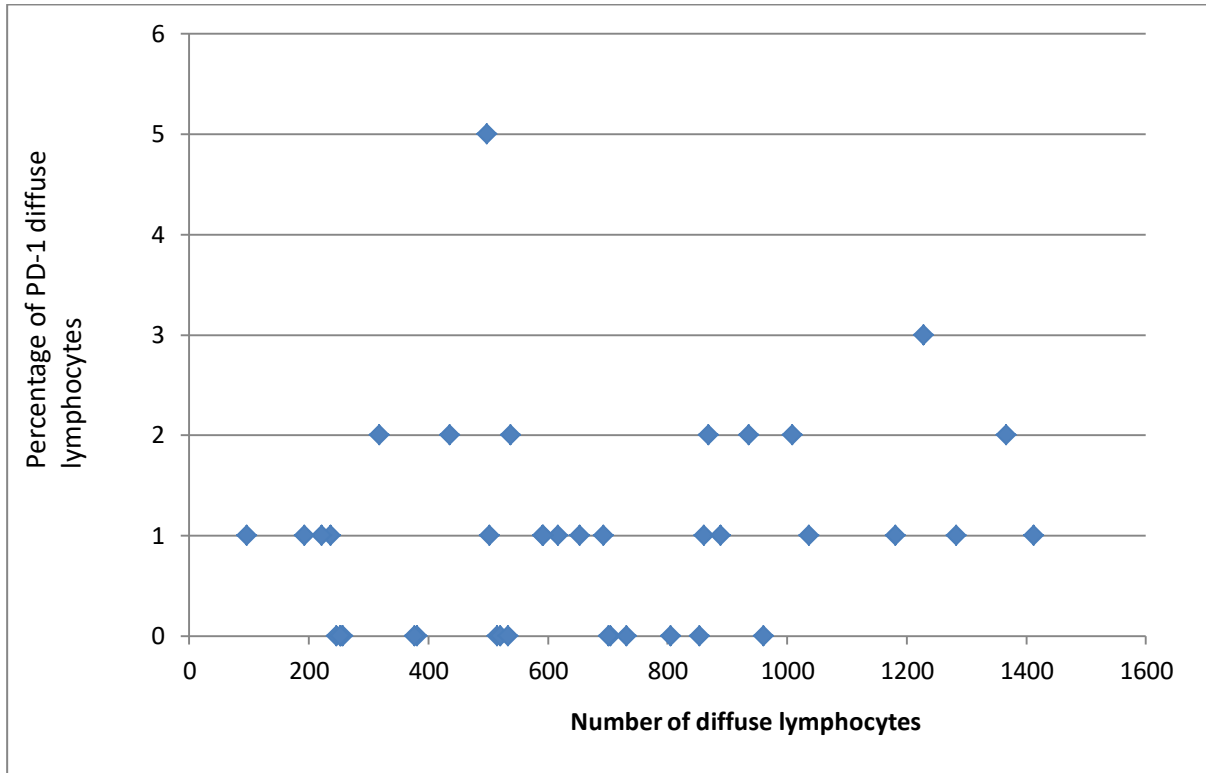
As seen above, there is no correlation between the number of the diffuse lymphocytes and the percentage of PD-1 positive diffuse lymphocytes. The correlation coefficient (r) is -0.223569 showing that there is no linear relation.

PD-1 and infiltrating lymphocytes in herds:

On the following graph, the percentage of PD-1 lymphocytes in herds is located on the X-axis and the T grading of the lung cancers on the Y-axis. Each blue point on the graph represents a patient.
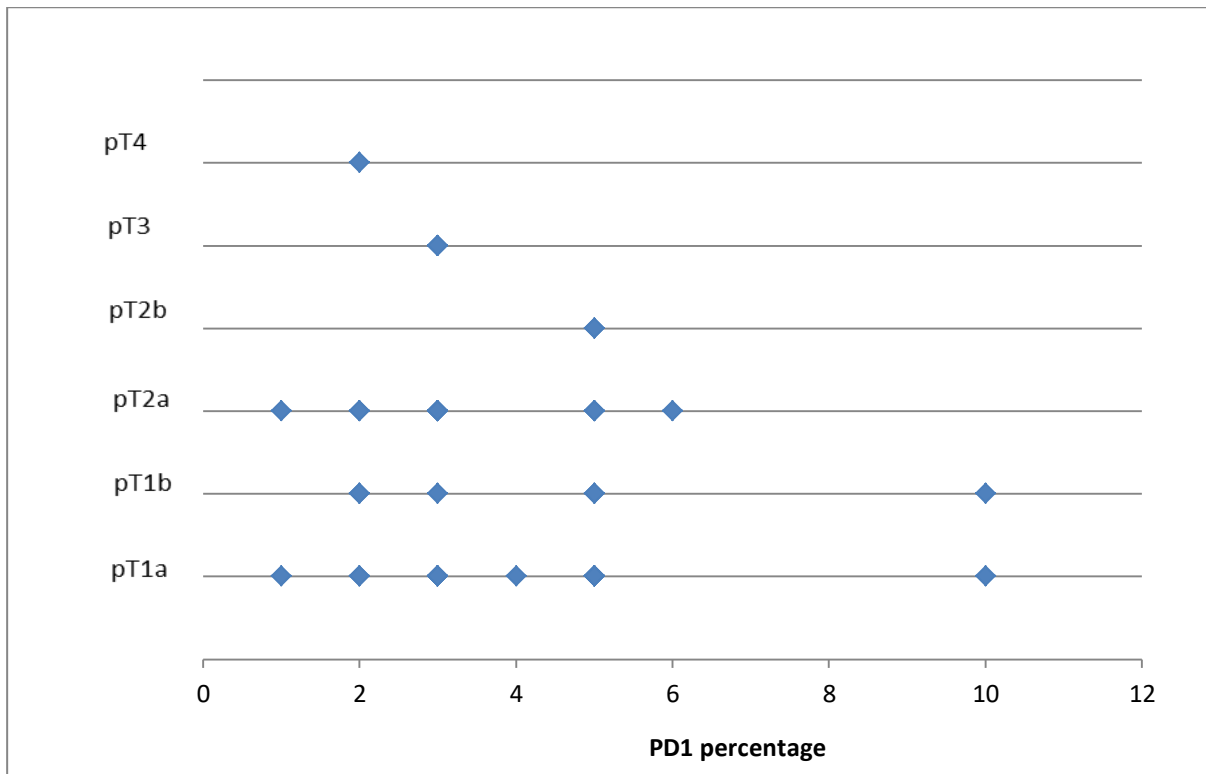
As seen above, there is no correlation between T-grading and the percentage of PD-1 positive lymphocytes in herds. The correlation coefficient (r) is -0.16862 showing that there is no linear relation.

The next box plot shows the PD-1 percentage of lymphocytes in herds from all 40 patients, regardless of the type of cancer.
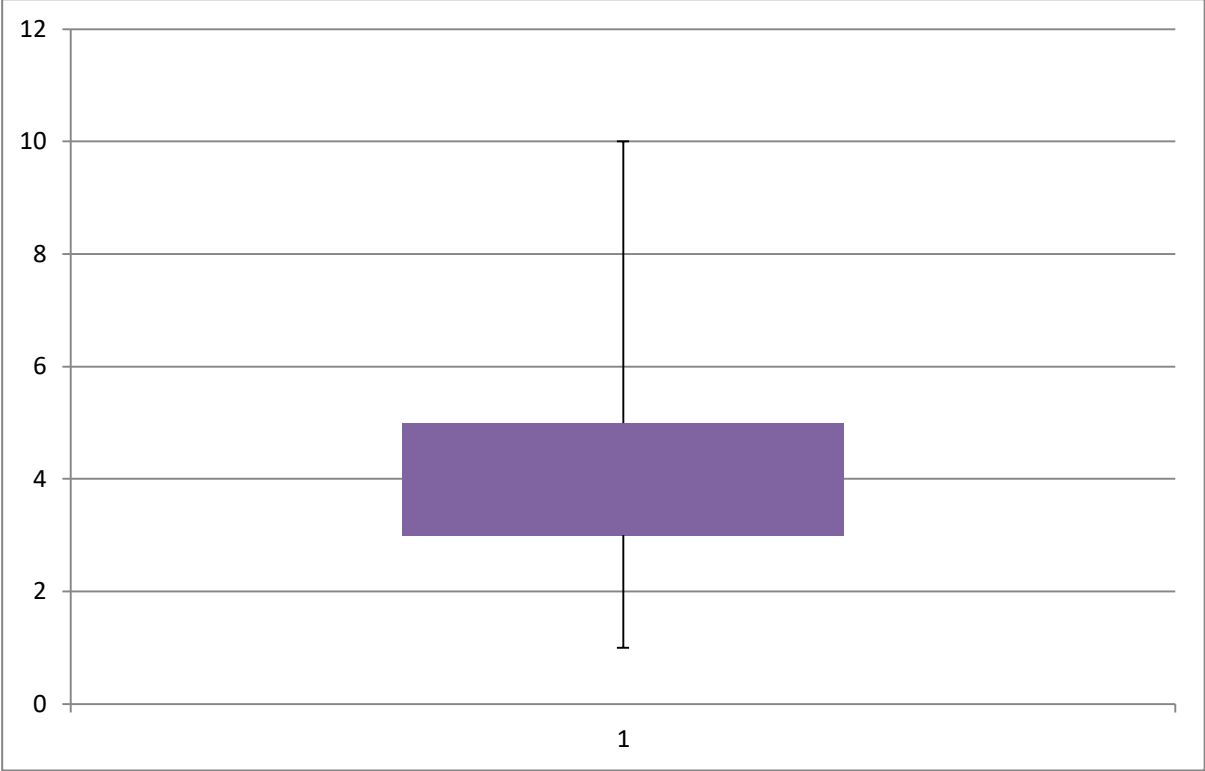
The minimum is 1% and the maximum 10%. The middle value is 3%.

The next box plot shows the difference of PD-1 percentage of lymphocytes in herds between G2 and G3 lung carcinomas.
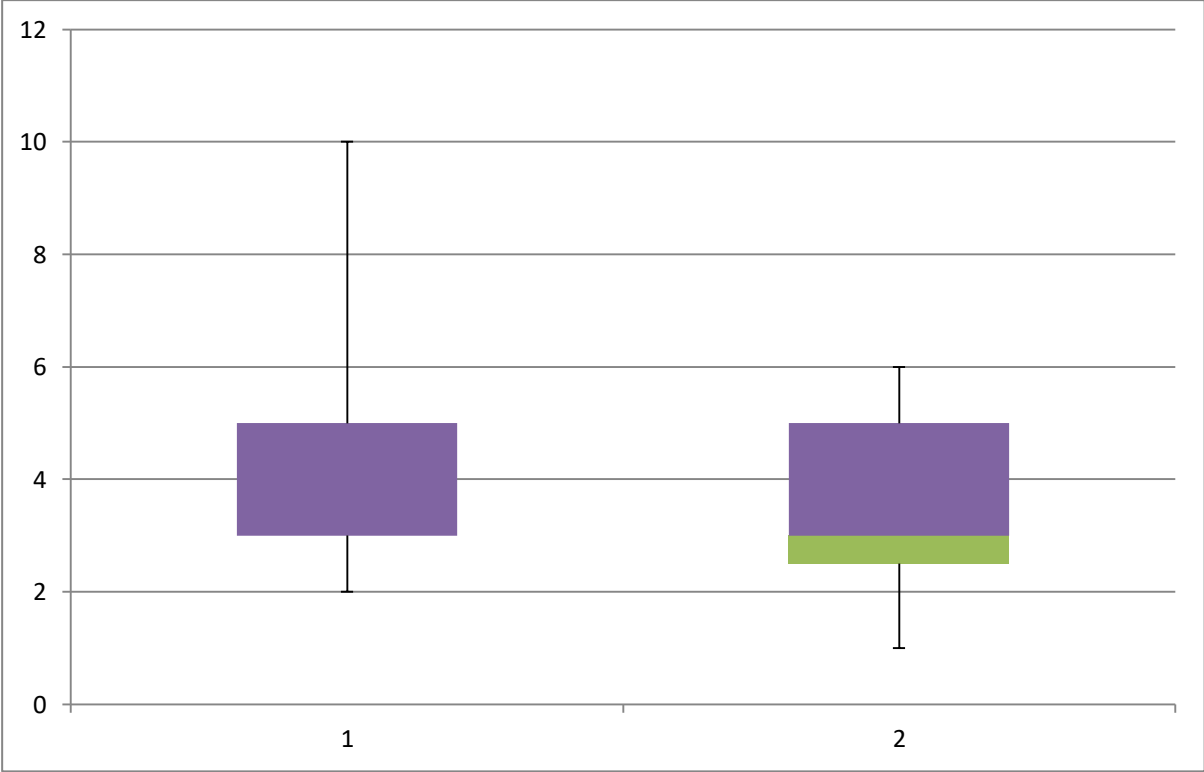
It can be seen in this box plot that the G2 lung cancer has a minimum of 2% PD-1 and a maximum of 10% while G3 lung cancers have a minimum of 1% and maximum of 6% PD-1.

The next box plot shows the difference of PD-1 percentage of lymphocytes in herds between G2 and G3 lung carcinomas, separating them in two categories, squamous lung carcinomas and lung adenocarcinomas.
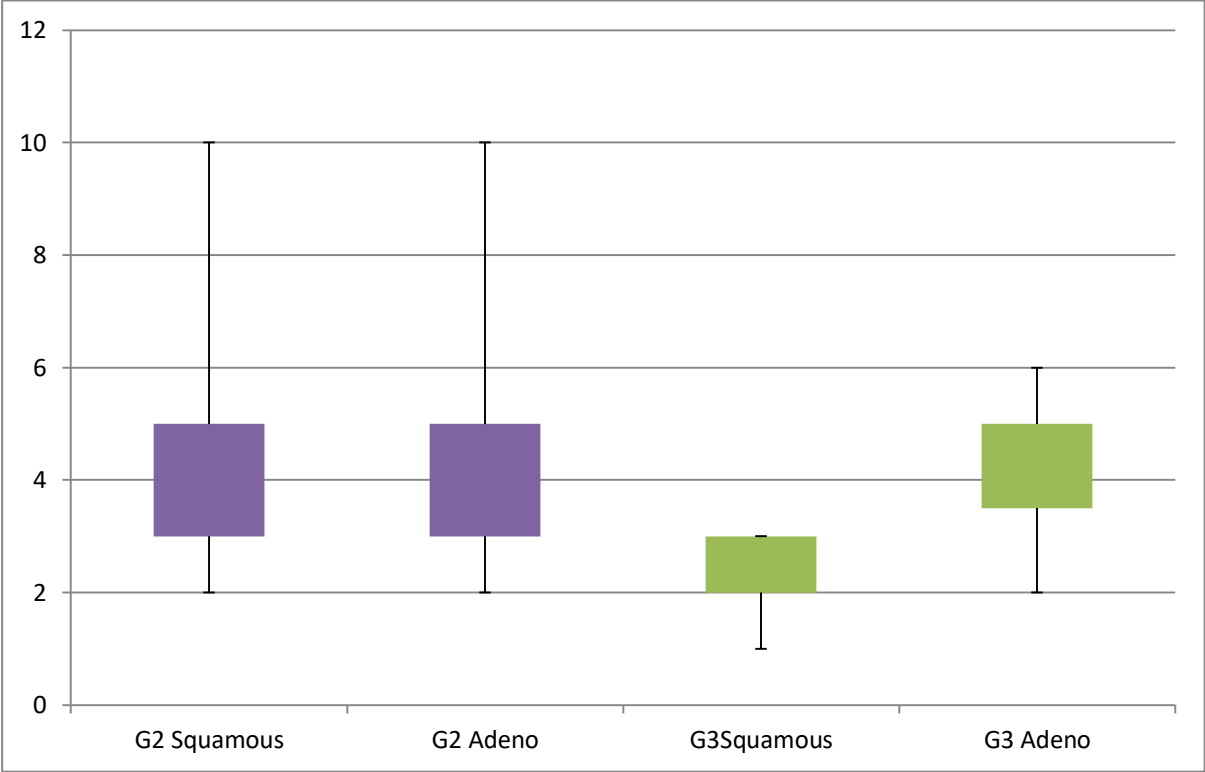
On the following graph all lymphocytes in all herds (CD3, CD4, CD8 and CD20) of each patient are located on the X-axis and the percentage of PD-1 lymphocytes in herds on the Y-axis. Each blue point on the graph represents a patient.
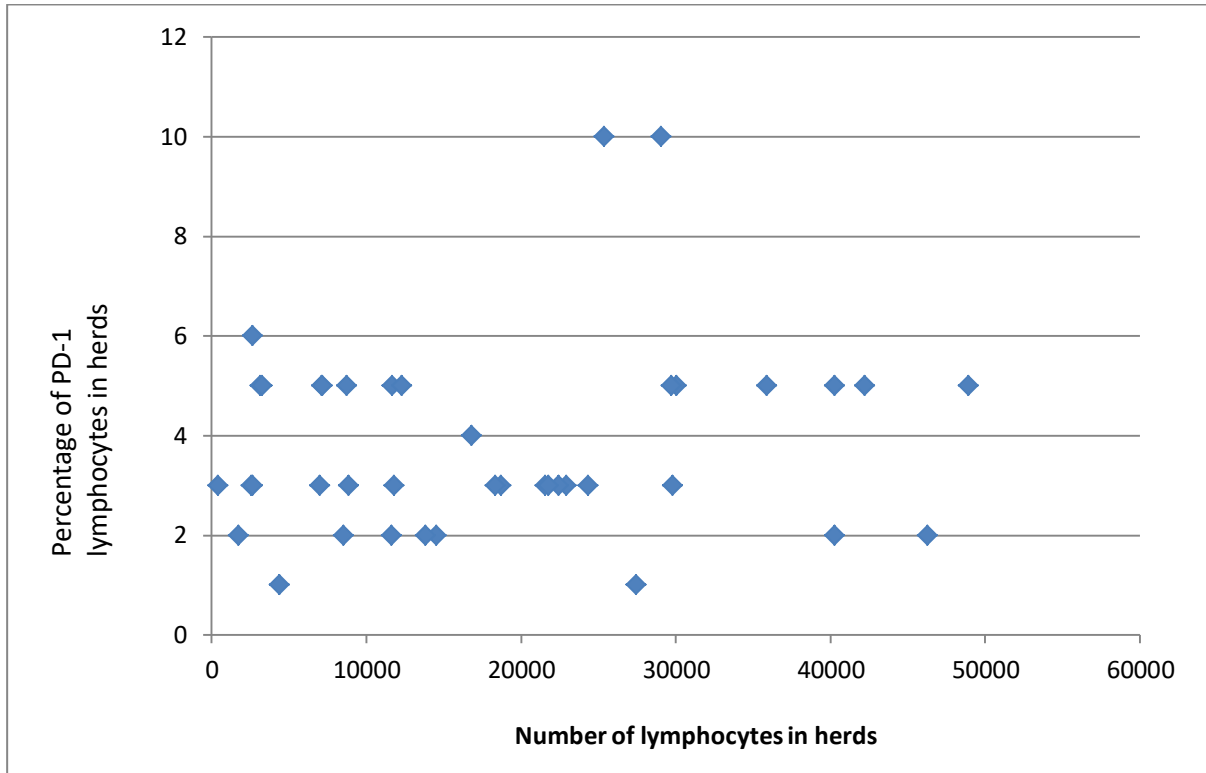
As seen above, there is no correlation between the number of lymphocytes in herds and the percentage of PD-1 positive lymphocytes in herds. The correlation coefficient (r) is – 0.154458 showing that there is no linear relation.

Discussion

Despite new operation techniques and therapies, lung cancer remains among the leading causes of death worldwide today. Squamous cell carcinoma and adenocarcinoma of the lung are the most common types of non-small cell lung carcinoma. Generally, all malignant tumours have an environment containing fibroblasts, endothelial cells, and other structural components and infiltrating immune cells. Tumour-infiltrating immune cells and especially the tumour infiltrating lymphocytes (TILs) are important in anticancer immunosurveillance and they have a differing prognostic value among various carcinomas. In recent years, many studies have shown how important tumour-infiltrating lymphocytes are for clinical outcome and therapy. Some studies have gone even further and proposed an additional "TNM" staging of TILs, for example the study: TNM Staging in Colorectal Cancer: T is for T-Cell and M is for Memory (Broussard et al., 2011).

The sample for this study contains 40 patients with non-small cell lung cancer of which 18 are patients with squamous cell lung carcinomas and 22 patients with lung adenocarcinomas. The histological material comes from the archive of the Institute of Pathology of the University of Gießen. The goal of this study is to determine the type of tumour-infiltrating lymphocytes, the infiltrating pattern of the tumour–infiltrating lymphocytes and to find out if there is a correlation between the age of patients, the T-stage and the differentiation of cancer with the numbers of TILs. The correlation between tumour-infiltrating lymphocytes, the T-stage and the differentiation of cancer with the expression of PD-1 was also studied.

CD3, CD4, CD8 and CD20 tumour-infiltrating lymphocytes

Histologically, two variations of infiltrating patterns of TILs were observed, the diffuse tumour-infiltrating lymphocytes and the tumour-infiltrating lymphocytes in herds / small clusters. The CD3, CD4 and CD8 TILs showed both types of patterns whereas the CD20 TILs showed the pattern almost exclusively in herds / small clusters. Because of this observation, the tumour-infiltrating lymphocytes were divided into these two categories and further analysed.

<u>CD3, CD4, CD8 and CD20 tumour infiltrating lymphocytes diffuse pattern</u>

The average numbers of TILs in one square millimetre in a diffuse pattern from all 40 patients shows a predomination of CD3 TILs (a minimum average number of 48 TILs and a maximum average number of 918 TILs in one square millimetre), followed by CD8 TILs (a minimum average number of 29 TILs and maximum average number of 530 TILs in one square millimetre) and CD4 TILs (a minimum average number of 0 and a maximum average number of 385 TILs in one square millimetre).

There was no correlation between the average numbers of diffuse tumour-infiltrating lymphocytes and differentiation grade of the carcinomas.

Furthermore, no correlation was found between the average numbers of diffuse tumour-infiltrating lymphocytes in one square millimetre and the T-stage of the carcinomas. The correlation coefficient (r) between the average numbers in one square millimetre of CD3 diffuse tumour-infiltrating lymphocytes and the T-stage is 0.007, between the average numbers in one square millimetre of CD4 diffuse tumour-infiltrating lymphocytes and the T-stage is -0,035 and between the average numbers in one square millimetre of CD8 diffuse tumour-infiltrating lymphocytes and the T-stage is -0.035.

The age of the patients and the average number in one square millimetre of diffuse tumour-infiltrating lymphocytes also did not show any correlation. The correlation coefficient (r) between the average numbers in one square millimetre of CD3 diffuse tumour-infiltrating lymphocytes and the age of the patients is -0.093, between the average numbers in one square millimetre of CD4 diffuse tumour-infiltrating lymphocytes and the age of the patients is 0.19 and between the average numbers in one square millimetre of CD8 diffuse tumour-infiltrating lymphocytes and the age of the patients is -0.00191. These results are consistent with the study of Schalper KA et al. where no consistent association between the level of TIL subtypes and age or tumour size was found (Schalper et al., 2015).

CD3, CD4, CD8 and CD20 tumour-infiltrating lymphocytes in herds / clusters

All TILs found in every herd / clusters of stains CD3, CD4, CD8 and CD20 for every patient were counted individually. The TILs in herds from all 40 patients show that CD20 TILs in herds are predominant (a minimum of 164 TILs and a maximum of 33,795 TILs), followed by CD3 TILs (a minimum of 124 TILS and a maximum of 14,622 TILs), followed by CD8 TILs (a minimum of 57 TILs and a maximum of 11,709 TILs) and finally the CD4 TILs (a minimum of 71 TILs and a maximum of 11,432 TILs).

No correlation was found between tumour-infiltrating lymphocytes in herds and patient age. The correlation coefficient (r) between the CD3 tumour-infiltrating lymphocytes in herds and the age of the patients is -0.136260224, between the CD4 tumour-infiltrating lymphocytes in herds and the age of the patients is -0.07459, between the CD8 tumour-infiltrating lymphocytes in herds and the age of the patients is -0.21086 and between the CD20 tumour-infiltrating lymphocytes in herds and the age of the patients is -0.01176.

Additionally, there is no correlation between the tumour-infiltrating lymphocytes in herds and the carcinoma's T-stage / size. The correlation coefficient (r) between CD3 TILs in herds and the T-stage is -0.36238, between CD4 TILs in herds and the T-stage is -0.40085, between CD8 TILs in herds and the T-stage is -0.34375 and between CD20 TILs in herds and the T-stage is -0.20328.

The results of the comparison between the cancer differentiation and the tumour-infiltrating lymphocytes in herds showed that poorly differentiated carcinomas (G3) tend to have fewer tumour-infiltrating lymphocytes in herds than middle differentiated carcinomas (G2). These results are statistically significant.

The graphic of CD3 TILs counted from all herds from every patient and G2/G3 carcinomas (adenocarcinomas and squamous lung carcinomas together) shows a p-value of 0.0012.
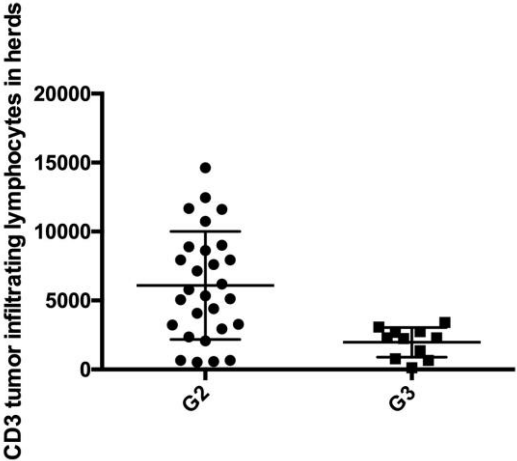
The graphic of CD4 TILs counted from all herds from each patient and G2/G3 carcinomas (adenocarcinomas and squamous lung carcinomas together) shows a p-value of 0.0020.
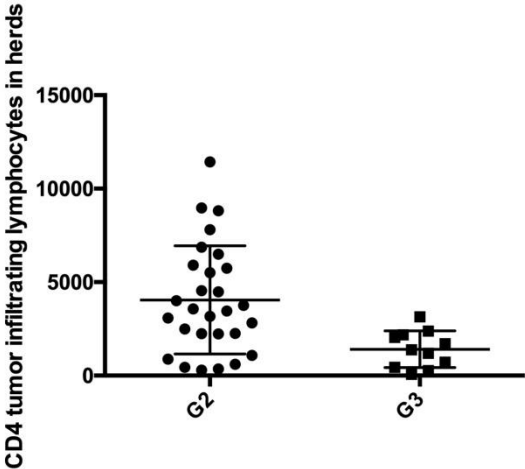
The graphic of CD8 TILs counted from all herds from each patient and G2/G3 carcinomas (adenocarcinomas and squamous lung carcinomas together) shows a p-value of 0.0014.
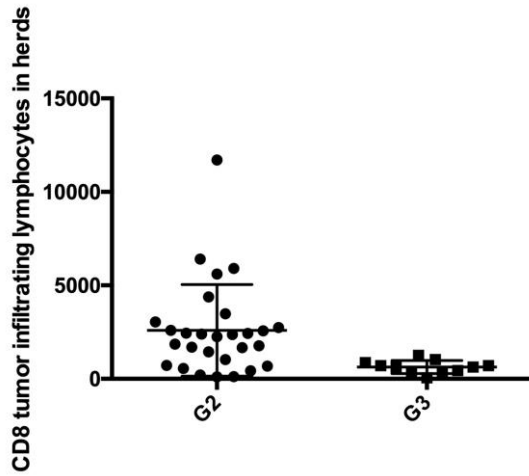
The graphic of CD20 TILs counted from all herds from each patient and G2/G3 carcinomas (adenocarcinomas and squamous lung carcinomas together) shows a p-value of 0.0036.
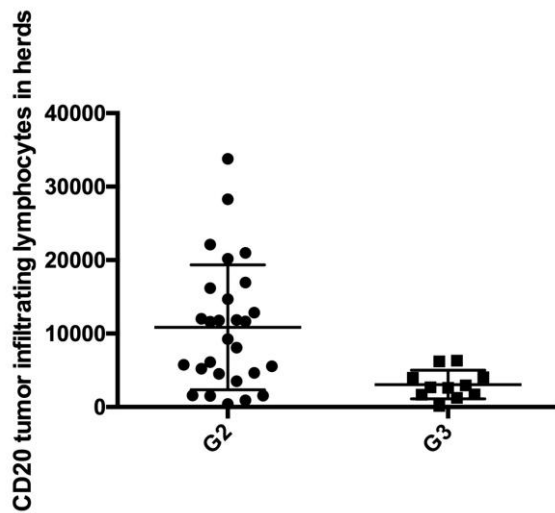
PD-1 and diffuse infiltrating lymphocytes and lymphocytes in herds:

As demonstrated above, there is no correlation between the number of the diffuse lymphocytes and the percentage of PD-1 positive diffuse lymphocytes or between the number of lymphocytes in herds and the percentage of PD-1 positive lymphocytes. The percentage of PD-1 positive diffuse lymphocytes is between 0% and 5% and the percentage of PD-1 positive lymphocytes in herds is between 1% and 10%. This shows a low percentage / low levels of PD-1 and thus a positive immune response in the tumour and a large number of tumour-infiltrating lymphocytes.

Summary

Lung cancer is the most frequent and one of the deadliest types of cancer. Lung adenocarcinoma ranks as the number one type of major lung cancer while squamous cell lung carcinoma is less common than adenocarcinoma. All lung carcinomas are strongly associated with tobacco smoking, the risk being the highest for squamous cell carcinoma, followed by small cell carcinoma and adenocarcinoma. Worldwide, more than 1.1 million deaths annually are due to lung cancer. Tumour-infiltrating lymphocytes are the immune reaction of human`s immune system to a tumour. They are white blood cells that have left the blood system with one goal, to find, infiltrate and kill the tumour cells.

The goal of this study was to determine the type of tumour-infiltrating lymphocytes, map them and show which types of lymphocytes predominate in the immune response. In the end, an attempt was made to find correlations between the obtained results. Furthermore, the tumour-infiltrating lymphocytes were stained to find the percentage of expression of PD-1 surface protein.

Observations revealed two types of infiltrating patterns of the tumour-infiltrating lymphocytes: the diffuse pattern and the TILs in herds. This differentiation was also critical for counting TILs in these two groups using two different methods.

The counting of the average number of TILs in one square millimetre in a diffuse pattern from all 40 patients shows a predomination of CD3 TILs, followed by CD8 and CD4 TILs. CD20 TILs were almost absent in the diffuse pattern. Counting TILs in herds from all 40 patients show that CD20 TILs were the most common in herds were, followed by CD3 TILs, CD8 TILs and finally by CD4 TILs.

The results show no correlation between TILs (diffuse or in herds) and the age of the patients or the tumour stage. There was also no correlation between the average number in one square millimetre of diffuse tumour-infiltrating lymphocytes and the differentiation grade of the carcinomas. There was no correlation between the number of diffuse lymphocytes and the percentage of PD-1 positive diffuse lymphocytes or between the number of lymphocytes in herds and the percentage of PD-1 positive lymphocytes. An important observation was the comparison between the cancer differentiation and tumour-infiltrating lymphocytes in herds. In this respect, it has been shown that poorly differentiated carcinomas (G3) tend to have fewer tumour-infiltrating lymphocytes in herds than middle differentiated carcinomas (G2) in herds. These results are statistically significant. This result can be further discussed in combination with the more aggressive behaviour and poor prognosis of poorly differentiated carcinomas. Therefore, an extension of the results of this study may be a subject of further discussion that poorly differentiated carcinomas tend to have a negative immune response / fewer TILs and thus exhibit much more aggressive behaviour. A possible theory could be that poorly differentiated carcinomas have developed a better immune escape mechanism than middle differentiated carcinomas. Identifying the actual reason and the mechanism that leads to a reduced number of TILs in herds of poorly differentiated adenocarcinomas and squamous lung carcinomas was not the goal, however. The importance of TILs in many malignancies is not just a theory but a fact. Many studies have shown the role and importance of TILs for the prognosis of patients with malignancies. As a result, revolutionary therapies called checkpoint inhibitors have been developed to improve the immunoreaction of patients against malignancies. The observation in this study that TILs found in herds are less numerous in poorly differentiated adenocarcinomas and squamous lung carcinomas may be important for planning future therapies and a subject for future studies. The importance of the immunoreaction (TILs) against malignancies raises the question of creating an immune score (similar to the TNM score) as discussed by Broussard E K et Al (Broussard et al.,2011) for patients with colorectal cancers. Similarly, if in the future a prognostic immune score for patients with lung cancers were to become a subject of serious discussion, then the results of this study may offer some insight.

Zusammenfassung

Lungenkrebs ist die häufigste und eine der tödlichsten Krebsarten. Das Lungenadenokarzinom gilt als die häufigste Form von Lungenkrebs, während das Plattenepithelkarzinom seltener vorkommt als das Adenokarzinom. Alle Lungenkarzinome sind stark auf das Tabakrauchen zurückzuführen, wobei das Risiko für Plattenepithelkarzinome am größten ist, gefolgt von Kleinzellkarzinomen und Adenokarzinomen. Weltweit sind jährlich mehr als 1,1 Millionen Todesfälle auf Lungenkrebs zurückzuführen. Die tumorinfiltrierenden Lymphozyten sind die Immunreaktion des menschlichen Immunsystems auf einen Tumor. Es sind weiße Blutkörperchen, die das Blutsystem mit dem Ziel verlassen haben, die Tumorzellen zu finden, zu infiltrieren und abzutöten.

Ziel dieser Doktorarbeit war es, die Art der tumorinfiltrierenden Lymphozyten zu bestimmen, sie zu kartieren und zu zeigen, welche Lymphozytentypen in der Immunantwort dominieren. Am Ende wurde versucht, Zusammenhänge zwischen den gesammelten Informationen zu finden. Darüber hinaus wurden die tumorinfiltrierenden Lymphozyten gefärbt, um den prozentualen Anteil der Expression von PD-1-Oberflächenprotein zu finden.

Bei der Untersuchung wurden zwei Arten von infiltrierenden Mustern der tumorinfiltrierenden Lymphozyten aufgezeigt: das diffuse Muster und die TILs in den Herden. Diese Differenzierung war auch entscheidend für die Zählung der TILs in diesen beiden Gruppen mit zwei verschiedenen Methoden.

Die Zählung der durchschnittlichen Anzahl von TILs in einem Quadratmillimeter von allen 40 Patienten zeigt eine Prädominanz der CD3-TILs, gefolgt von den TILs CD8 und CD4. Die CD20 TILs waren im diffusen Muster fast nicht vorhanden. Die Zählung der TILs in den Herden von allen 40 Patienten zeigt, dass CD20 TILs in den Herden am häufigsten aufgekommen sind, gefolgt von CD3 TILs, CD8 TILs und schließlich CD4 TILs.

Die Ergebnisse zeigen keinen Zusammenhang zwischen TILs (diffuser Muster oder in Herds) und dem Alter der Patienten oder dem Tumorstadium. Es gab auch keine Korrelation zwischen der durchschnittlichen Nummer der diffusen tumorinfiltrierenden Lymphozyten in einem Quadratmillimeter und dem Differenzierungsgrad der

Karzinome. Es gibt keinen Zusammenhang zwischen der Anzahl der diffusen Lymphozyten und dem Prozentsatz der PD1-positiven diffusen Lymphozyten oder zwischen der Anzahl der Lymphozyten in den Herden und dem Prozentsatz der PD1-positiven Lymphozyten. Eine wichtige Beobachtung dieser Doktorarbeit war der Vergleich zwischen der Krebsdifferenzierung und den tumorinfiltrierenden Lymphozyten in Herden. In diesem Zusammenhang konnte gezeigt werden, dass schlecht differenzierte Karzinome (G3) tendenziell weniger tumorinfiltrierende Lymphozyten in Herden haben als mittel differenzierte Karzinome (G2) in Herden. Diese Ergebnisse sind statistisch signifikant. Dieses Ergebnis kann in Kombination mit dem aggressiveren Verhalten und der schlechten Prognose von schlecht differenzierten Karzinomen weiter diskutiert werden. Eine Erweiterung der Ergebnisse dieser Doktorarbeit kann daher in einer Diskussion vertieft werden, dass schlecht differenzierte Karzinome tendenziell eine negative Immunantwort / weniger TILs und damit ein aggressiveres Verhalten haben. Eine mögliche Theorie kann sein, dass schlecht differenzierte Karzinome einen besseren Tumorfluchtmechanismus entwickelt haben als mitteldifferenzierte Karzinome. Das Ziel war nicht den tatsächlichen Grund und den Mechanismus zu identifizieren, der zu einer verringerten Anzahl von TILs in Herden von schlecht differenzierten Adenokarzinomen und Plattenepithelkarzinomen führt. Die Bedeutung von TILs bei vielen malignen Erkrankungen ist nicht nur eine Theorie, sondern eine Tatsache. Viele Studien haben die Rolle und Bedeutung von TILs für die Prognose von Patienten mit malignen Erkrankungen gezeigt. Infolgedessen wurden revolutionäre Therapien entwickelt, die als Checkpoint-Inhibitoren bezeichnet werden, um die Immunreaktion von Patienten gegen maligne Erkrankungen zu verbessern. Die Beobachtung in dieser Studie, dass die TILs in Herden bei schlecht differenzierten Adenokarzinomen und Plattenepithelkarzinomen weniger sind, kann für die Planung zukünftiger Therapien wichtig und ein Thema für zukünftige Studien sein. Aufgrund der Wichtigkeit der Immunreaktion (TILs) gegen maligne Erkrankungen stellte sich die Frage, ob ein Immun-Score (ähnlich dem TNM-Score) erstellt werden sollte, wie von Broussard E K et Al (Broussard et al.,2011) für Patienten mit Darmkrebs diskutiert wurde. In ähnlicher Weise können die Ergebnisse dieser Studie berücksichtigt werden, wenn in Zukunft ein prognostischer Immun-Score für Patienten mit Lungenkrebs diskutiert wird.

Alsaab, H. O., Sau, S., Alzhrani, R., Tatiparti, K., Bhise, K., Kashaw, S. K., & Iyer, A. K. (2017). PD-1 and PD-L1 checkpoint signaling inhibition for cancer immunotherapy: mechanism, combinations, and clinical outcome. *Frontiers in Pharmacology*.

Berger, M. S., & Prados, M. D. (2005). Textbook of Neuro-Oncology. In *Textbook of Neuro-Oncology* (pp. 88–89).

Broussard, E. K., & Disis, M. L. (2011). TNM Staging in Colorectal Cancer: T Is for T Cell and M Is for Memory. *Journal of Clinical Oncology*.

Fraire, A. E., Cagle, P. T., Irwin, R. S., Mody, D. R., & Allen, T. C. (2010). Atlas of Pulmonary Disease Atlas of Neoplastic Pulmonary Disease. In *Atlas of Pulmonary Disease Atlas of Neoplastic Pulmonary Disease* (p. 145). Springer New York Dordrecht Heidelberg London.

Hanahan, D., & Weinberg, R. A. (2011). Hallmarks of cancer: The next generation. *Cell*.

Hecker, L., Thannickal, V. J., & Phan, S. H. (2009). Basic Concepts of Molecular Pathology. In *Basic Concepts of Molecular Pathology* (pp. 140–142).

Hida, A. I., Sagara, Y., Yotsumoto, D., Kanemitsu, S., Kawano, J., Baba, S., … Ohi, Y. (2016). Prognostic and predictive impacts of tumor-infiltrating lymphocytes differ between Triple-negative and HER2-positive breast cancers treated with standard systemic therapies. *Breast Cancer Research and Treatment*.

Ingold Heppner, B., Loibl, S., & Denkert, C. (2016). Tumor-Infiltrating Lymphocytes: A Promising Biomarker in Breast Cancer. *Breast Care*.

Jin, H. T., Ahmed, R., & Okazaki, T. (2011). Role of PD-1 in regulating T-cell immunity. *Current Topics in Microbiology and Immunology*.

Jun, S.-Y., Park, E. S., Lee, J. J., Chang, H.-K., Jung, E. S., Oh, Y.-H., & Hong, S.-M. (2019). Prognostic Significance of Stromal and Intraepithelial Tumor-Infiltrating Lymphocytes in Small Intestinal Adenocarcinoma. *American Journal of Clinical Pathology*.

McGurk, S. (2013). Junqueira's Basic Histology Text and Atlas – 13th edition Mescher Anthony L Junqueira's Basic Histology Text and Atlas. *Nursing Standard*, 343–345.

Mihm, M. C., & Mule, J. J. (2015). Reflections on the Histopathology of Tumor-Infiltrating Lymphocytes in Melanoma and the Host Immune Response. *Cancer Immunology Research*.

Moran, C. A., & Suster, S. (2010). Tumors and tumor-like conditions of the lung and pleura. In *Tumors and Tumor-like Conditions of the Lung and Pleura* (pp. 52–72).

Νίκη Ι.Αγνάντη, Β. Μαλάμου-Μήτση, Δ. Στεφάνου, Μ. Μ. (2005). Γενική Παθολογία και Παθολογική Ανατομική. In *Γενική Παθολογία και Παθολογική Ανατομική* (pp. 104–131).

Paulsen, F., & Waschke, J. (2010). *Sobotta, Atlas der Anatomie des Menschen Band 2 : Innere Organe. Atlas der Anatomie des Menschen*.

Preiß, Honecker, Claßen, D. (2017). Interdisziplinäre Empfehlungen zur Therapie 2016/17 (pp. 120–127).

Radvanyi, L. G. (2015). Tumor-infiltrating lymphocyte therapy: Addressing prevailing Questions

Rekhtman, N., & Bishop, J. A. (2011). Quick Reference Handbook for Surgical Pathologists (pp. 60–63).

Schalper, K. A., Brown, J., Carvajal-Hausdorf, D., McLaughlin, J., Velcheti, V., Syrigos, K. N., … Rimm, D. L. (2015). Objective measurement and clinical significance of TILs in non-small cell lung cancer. *Journal of the National Cancer Institute*.

Serhan, C. N., Ward, P. a., Arbor, A., & Gilroy, D. W. (2010). Fundamentals of inflammations (pp. 108–125).

Travis, W. D., Brambilla, E., Nicholson, A. G., Yatabe, Y., Austin, J. H. M., Beasley, M. B., … WHO Panel. (2015). WHO Classification of Tumours of the Lung, Pleura, Thymus and Heart. *J Thorac Oncol*.

W.Böcker, H.Denk, Ph. U. Heitz, H. M. (2008). Pathologie. In *Pathologie* (p. 639).

William B. Coleman, & Gregory J. Tsongalis. (2009). Essential concepts in molecular pathology. In *Essential concepts in molecular pathology* (pp. 207–210).

.

Erklärung zur Dissertation

„Hiermit erkläre ich, dass ich die vorliegende Arbeit selbständig und ohne unzulässige Hilfe oder Benutzung anderer als der angegebenen Hilfsmittel angefertigt habe. Alle Textstellen, die wörtlich oder sinngemäß aus veröffentlichten oder nichtveröffentlichten Schriften entnommen sind, und alle Angaben, die auf mündlichen Auskünften beruhen, sind als solche kenntlich gemacht. Bei den von mir durchgefürten und in der Dissertation erwähnten Untersuchungen habe ich die Grundsätze guter wissenschaftlicher Praxis, wie sie in der „Satzung der Justus-Liebig-Universität Gießen zur Sicherung guter wissenschaftlicher Praxis „niedergelegt sind, eingehalten sowie ethische, datenschutzrechtliche und tierschutzrechtliche Grundsätze befolgt. Ich versichere, dass Dritte von mir weder unmittelbar noch mittelbar geldwerte Leistungen für Arbeiten erhalten haben, die im Zusammenhang mit dem Inhalt der vorgelegten Dissertation stehen, oder habe diese nachstehend spezifiziert. Die vorgelegte Arbeit wurde weder im Inland noch im Ausland in gleicher oder ähnlicher Form einer anderen Prüfungsbehörde zum Zweck einer Promotion oder eines anderen Prüfungsverfahrens vorgelegt. Alles aus anderen Quellen und von anderen Personen übernommene Material, das in der Arbeit verwendet wurde oder auf das direkt Bezug genommen wird, wurde als solches kenntlich gemacht. Insbesondere wurden alle Personen genannt, die direkt und indirekt an der Entstehung der vorliegenden Arbeit beteiligt waren. Mit der Überprüfung meiner Arbeit durch eine Plagiatserkennungssoftware bzw. ein internetbasiertes Softwareprogramm erkläre ich mich einverstanden"

_____   _____

Ort,Datum   Unterschrift